



uOttawa

L'Université canadienne
Canada's university

FACULTÉ DES ÉTUDES SUPÉRIEURES
ET POSTDOCTORALES



FACULTY OF GRADUATE AND
POSTDOCTORAL STUDIES

Victoria Kostina

AUTEUR DE LA THÈSE / AUTHOR OF THESIS

M.A.Sc. (Electrical Engineering)

GRADE / DEGRÉ

School of Information Technology and Engineering

FACULTÉ, ÉCOLE, DÉPARTEMENT / FACULTY, SCHOOL, DEPARTMENT

Optimization and Performance Analysis of the V-BLAST Algorithm

TITRE DE LA THÈSE / TITLE OF THESIS

S. Loyka

DIRECTEUR (DIRECTRICE) DE LA THÈSE / THESIS SUPERVISOR

CO-DIRECTEUR (CO-DIRECTRICE) DE LA THÈSE / THESIS CO-SUPERVISOR

EXAMINATEURS (EXAMINATRICES) DE LA THÈSE / THESIS EXAMINERS

C. D'Amours

D. Falconer

Gary W. Slater

Le Doyen de la Faculté des études supérieures et postdoctorales / Dean of the Faculty of Graduate and Postdoctoral Studies

Optimization and Performance Analysis of the V-BLAST Algorithm

Victoria Kostina

Thesis submitted to the Faculty of Graduate and Postdoctoral Studies

In partial fulfillment of the requirements for the MSc degree in Electrical Engineering

School of Information Technology and Engineering

Faculty of Engineering

University of Ottawa

2006



Library and
Archives Canada

Bibliothèque et
Archives Canada

Published Heritage
Branch

Direction du
Patrimoine de l'édition

395 Wellington Street
Ottawa ON K1A 0N4
Canada

395, rue Wellington
Ottawa ON K1A 0N4
Canada

Your file *Votre référence*
ISBN: 978-0-494-25795-1
Our file *Notre référence*
ISBN: 978-0-494-25795-1

NOTICE:

The author has granted a non-exclusive license allowing Library and Archives Canada to reproduce, publish, archive, preserve, conserve, communicate to the public by telecommunication or on the Internet, loan, distribute and sell theses worldwide, for commercial or non-commercial purposes, in microform, paper, electronic and/or any other formats.

The author retains copyright ownership and moral rights in this thesis. Neither the thesis nor substantial extracts from it may be printed or otherwise reproduced without the author's permission.

AVIS:

L'auteur a accordé une licence non exclusive permettant à la Bibliothèque et Archives Canada de reproduire, publier, archiver, sauvegarder, conserver, transmettre au public par télécommunication ou par l'Internet, prêter, distribuer et vendre des thèses partout dans le monde, à des fins commerciales ou autres, sur support microforme, papier, électronique et/ou autres formats.

L'auteur conserve la propriété du droit d'auteur et des droits moraux qui protègent cette thèse. Ni la thèse ni des extraits substantiels de celle-ci ne doivent être imprimés ou autrement reproduits sans son autorisation.

In compliance with the Canadian Privacy Act some supporting forms may have been removed from this thesis.

Conformément à la loi canadienne sur la protection de la vie privée, quelques formulaires secondaires ont été enlevés de cette thèse.

While these forms may be included in the document page count, their removal does not represent any loss of content from the thesis.

Bien que ces formulaires aient inclus dans la pagination, il n'y aura aucun contenu manquant.


Canada

Abstract

Complexity-performance tradeoff in different implementations of the V-BLAST algorithm is discussed. Low-complexity alternatives to the optimal ordering procedure, such as ordering at 1st step, adaptive power allocation and pre-set non-uniform power allocation are proposed. A unified analytical framework for the optimum power allocation in the V-BLAST algorithm is presented. Comparative performance analysis of the optimum power allocation based on various optimization criteria (average and instantaneous block and total error rates) is given. Uniqueness of the optimum power allocation is proven for several scenarios. Compact closed-form approximations for the optimum power allocation and for the optimized error rates are derived. The SNR gain of optimization is rigorously defined and analyzed using analytical tools, including lower and upper bounds, high and low SNR approximations. The gain is upper bounded by the number of transmitters, for any modulation format and type of fading channel. While the average optimization is less complex than the instantaneous one, its performance is almost as good at high SNR. A measure of robustness of the optimized algorithm is introduced and evaluated. The optimized algorithm is shown to be robust to perturbations in individual and total transmit powers.

Table of Contents

1.	INTRODUCTION	1
1.1.	MOTIVATION OF THIS RESEARCH.....	1
1.2.	CONTRIBUTION OF THE THESIS	2
1.3.	ORGANIZATION OF THE THESIS.....	3
2.	LITERATURE REVIEW	5
2.1.	MIMO CHANNEL MODELING AND CAPACITY	7
2.2.	SPACE-TIME CODING	8
2.3.	SIGNAL PROCESSING AT THE MIMO RECEIVER: V-BLAST	9
2.4.	SUMMARY	15
3.	V-BLAST ALGORITHM AND ITS CHALLENGES	16
3.1.	WHY V-BLAST? ALTERNATIVE RECEIVER ARCHITECTURES.....	16
3.2.	BASIC V-BLAST ALGORITHM	18
3.3.	COMPLEXITY-PERFORMANCE TRADEOFF IN DIFFERENT IMPLEMENTATIONS OF V-BLAST.....	20
3.4.	ZF-V-BLAST WITH ORDERING AT 1 ST STEP	21
3.5.	UNORDERED V-BLAST WITH OPTIMUM POWER ALLOCATION.....	24
3.6.	SUMMARY	25
4.	ERROR RATES.....	26
4.1.	BLOCK ERROR RATE.....	26
4.2.	TOTAL BIT ERROR RATE.....	27
4.3.	AVERAGE ERROR RATES IN HIGH SNR REGION	32
4.4.	SUMMARY	33
5.	OPTIMUM POWER ALLOCATION.....	34
5.1.	UNIQUENESS OF THE SOLUTION.....	34

5.2.	INSTANTANEOUS POWER ALLOCATION.....	38
5.3.	OPTIMUM POWER ALLOCATION USING THE AVERAGE BLER.....	41
5.4.	OPTIMUM POWER ALLOCATION USING THE AVERAGE TBER.....	46
5.5.	INSTANTANEOUS VS. AVERAGE POWER ALLOCATION	50
5.6.	SUMMARY	52
6.	ROBUSTNESS OF THE OPTIMUM POWER ALLOCATION.....	53
6.1.	LOCAL ROBUSTNESS.....	54
6.2.	V-BLAST WITH PRE-SET POWER ALLOCATION.....	60
6.3.	GLOBAL ROBUSTNESS.....	61
6.4.	SUMMARY	63
7.	SNR GAIN OF OPTIMUM POWER ALLOCATION	64
7.1.	BLER SNR GAIN OF THE OPTIMUM POWER ALLOCATION	66
7.2.	TBER SNR GAIN OF THE OPTIMUM POWER ALLOCATION	69
7.3.	EXAMPLES AND COMPARISONS	73
7.4.	SUMMARY	79
8.	CONCLUSION.....	80
8.1.	SUMMARY OF THE THESIS	80
8.2.	FUTURE RESEARCH.....	82
9.	REFERENCES	83
9.1.	OVERVIEWS AND HANDBOOKS	83
9.2.	MIMO CHANNELS/CAPACITY	84
9.3.	SPACE-TIME CODES.....	85
9.4.	V-BLAST	86
	APPENDIX A. MATHEMATICAL DERIVATIONS	90
A.1.	CLOSED-FORM EXPRESSIONS FOR OPTIMUM POWER ALLOCATION.....	90
A.2.	THE GAIN OF OPTIMIZATION FOR SMALL SNR.....	91

A.3.	THE GAIN OF OPTIMIZATION FOR HIGH SNR	94
A.4.	PROOF OF THEOREM 7.4.....	96
APPENDIX B. MATLAB CODE.....		97
B.1.	AUXILIARY FUNCTIONS	97
B.2.	ANALYTICAL AVERAGE AND INSTANTANEOUS ERROR RATES FOR ARBITRARY POWER ALLOCATION.....	98
B.3.	OPTIMIZATION BASED ON VARIOUS CRITERIA	101
B.4.	ERROR RATES THROUGH MONTE-CARLO SIMULATIONS.....	106

List of Figures

Fig. 2-1. Basic MIMO scheme.....	6
Fig. 2-2. Number of MIMO publications for the last decade	7
Fig. 2-3. Number of V-BLAST publications for the last decade	10
Fig. 2-4. V-BLAST with optimum power allocation	13
Fig. 3-1. TBER for ZF and MMSE V-BLAST, with and without optimal ordering, $n=m=3$, number of Monte Carlo simulations gradually increasing with SNR up to 10^8 , BPSK modulation, Rayleigh fading	21
Fig. 3-2. TBER for ZF-V-BLAST with 1 st step ordering and with optimal ordering, $n=m=3$, BPSK modulation, Rayleigh fading.....	23
Fig. 4-1. TBER for 3×3 ZF-V-BLAST, analytical and simulated, number of Monte Carlo simulations gradually increasing with SNR up to $5 \cdot 10^6$, BPSK modulation, Rayleigh channel.	31
Fig. 4-2. Exact and approximate analytical instantaneous TBER compared to simulations, 3×3 ZF-V-BLAST with non-uniform power allocation given by (5.7), number of Monte-Carlo simulations 10^6 , BPSK modulation	31
Fig. 5-1. Two-dimensional illustration of Theorem 2 geometry.....	35
Fig. 5-2. Normalized closed-form second derivative (i.e. P_{ei}''/P_{ei}) of M-ary FSK SER in AWGN channel, $M=50$	36
Fig. 5-3. Instantaneous TBER (for two different channel realizations) versus α_1 for for 2×2 ZF-V-BLAST, BPSK modulation, SNR = 10 dB.	38
Fig. 5-4. TBER of 2×2 instantaneously optimized MMSE-V-BLAST with BPSK modulation.....	39
Fig. 5-5. SNR Gain for various starting points for numerical optimization, 2×2 ZF-V- BLAST, BPSK modulation.	41
Fig. 5-6. Closed-form power allocation by (5.7) and (5.9) with b_i given by (5.8), 2×2 ZF- V-BLAST with BPSK modulation.	45
Fig. 5-7. SNR Gain of optimization by BLER using closed-form power allocation (5.8) and (5.9) with b_i given by (5.8), 2×2 ZF-V-BLAST, BPSK modulation.	45
Fig. 5-8. Closed-form power allocation by (5.7) and (5.9) with b_i given by (5.17), 2×2 ZF- V-BLAST with BPSK modulation.	48
Fig. 5-9. SNR Gain of optimization by TBER using closed-form power allocation (5.8) and (5.9) with b_i given by (5.17), 2×2 ZF-V-BLAST, BPSK modulation.	48
Fig. 5-10. Optimum power allocation for 2×2 ZF-V-BLAST with BPSK modulation for various optimization strategies.	49

Fig. 5-11. Optimum power allocation for 3x3 ZF-V-BLAST with BPSK modulation for various optimization strategies.	49
Fig. 5-12. TBER of 2x2 ZF-V-BLAST with BPSK modulation for various optimization strategies.....	51
Fig. 5-13. TBER of 3x3 ZF-V-BLAST with BPSK modulation for various optimization strategies.....	51
Fig. 6-1. The robustness measure of the BLER-based optimization with respect to the variations in $\alpha_1 \dots \alpha_m$, exact and approximate, versus SNR for 3x3 ZF-V-BLAST, BPSK modulation, $\Delta u/u = 10\%$	56
Fig. 6-2. The robustness measure of the TBER-based optimization with respect to the variations in $\alpha_1 \dots \alpha_m$, exact and approximate, versus SNR for 2x2 ZF-V-BLAST, BPSK modulation, $\Delta u/u = 20\%$	57
Fig. 6-3. Average TBER versus α_1 for 2x2 ZF-V-BLAST with BPSK modulation.	58
Fig. 6-4. Average TBER versus α_1, α_2 for 3x3 ZF-V-BLAST with BPSK modulation...	58
Fig. 6-5. Average BLER versus α_1 for 2x2 ZF-V-BLAST with BPSK modulation.	59
Fig. 6-6. Average BLER versus α_1, α_2 for 3x3 ZF-V-BLAST with BPSK modulation...	59
Fig. 6-7. TBER of 3x3 ZF-V-BLAST with BPSK modulation for fixed power allocation.	61
Fig. 6-8. The Lagrange multiplier for the BLER-based optimization versus SNR for 3x3 ZF-V-BLAST.	63
Fig. 7-1. Definition of the SNR gain.	65
Fig. 7-2. Empirical PDF of instantaneous α_1^{opt} for 2x2 ZF V-BLAST, BPSK modulation, Rayleigh channel, SNR = 20dB, number of trials 10^4	71
Fig. 7-3. Average BLER SNR gain vs. SNR for 2x2 ZF-V-BLAST with BPSK modulation.....	75
Fig. 7-4. Average TBER SNR gain vs. SNR for 2x2 ZF-V-BLAST with BPSK modulation.....	75
Fig. 7-5. Optimum power allocation at low SNR for average BLER-based optimization, 3x3 ZF-V-BLAST with BPSK modulation.....	77
Fig. 7-6. Average BLER at low SNR for unoptimized 2x2 ZF-V-BLAST with BPSK modulation, exact and approximate by (7.21).....	77
Fig. 7-7. Average BLER SNR gain at low SNR for 2x2 ZF-V-BLAST with BPSK modulation.....	78
Fig. 7-8. Average TBER SNR gain at low SNR for 2x2 ZF-V-BLAST with BPSK modulation.....	78

List of Acronyms

Acronym	Meaning
BER	bit error rate
BFSK	binary frequency shift keying
BPSK	binary phase shift keying
CSI	channel state information
IEEE	Institute of Electrical and Electronics Engineers, Inc.
ML	maximum likelihood
MIMO	multiple-input multiple-output
MMSE	minimum mean-square error
M-PSK	M-ary phase shift keying
NLOS	non line of sight
OOK	on-off keying
PDF	probability density function
QoS	quality of service
QAM	quadrature amplitude modulation
QPSK	quadrature phase shift keying
Rx	receive
SER	symbol error rate
SQP	sequential quadratic programming
SISO	single-input single-output
SNR	signal to noise ratio
SNIR	signal to noise plus interference ratio
STTC	space-time trellis code
STC	space-time code
Tx	transmit
TBER	total bit error rate
V-BLAST	Vertical Bell Laboratories Layered Space-Time
WLAN	wireless local area network
WWAN	wireless wide area network
ZF	zero-forcing

List of Symbols and Notations

Notation	Meaning
T	transposition
+	conjugate transposition
$ \mathbf{a} $	Euclidean norm of the vector \mathbf{a}
a_i	i -th component of vector $\mathbf{a} = [a_1, a_2, \dots, a_m]^T$
\mathbf{a}_i or $(\mathbf{A})_i$	i -th column of matrix $\mathbf{A} = [\mathbf{a}_1, \mathbf{a}_2, \dots, \mathbf{a}_m]$

Symbol	Meaning	First appearance
m	number of transmit antennas	Section 2.1
n	number of receive antennas	Section 2.1
$\mathbf{s} = [s_1, s_2, \dots, s_m]^T$	Tx vector	(3.1)
$\mathbf{r} = [r_1, r_2, \dots, r_m]^T$	Rx vector	(3.1)
$\mathbf{H} = [\mathbf{h}_1, \mathbf{h}_2, \dots, \mathbf{h}_m]$	MIMO channel matrix, \mathbf{h}_i denotes i -th column of \mathbf{H}	(3.1)
$\xi \sim \mathcal{CN}(0, \sigma_0^2 \mathbf{I})$	noise vector	(3.1)
σ_0^2	noise power	(3.1)
$\gamma_0 = 1/\sigma_0^2$	average per-channel SNR for unoptimized V-BLAST	(4.3)
$\hat{\mathbf{s}}$	decision variable	(3.4)
$e_j = \hat{s}_j - s_j$	demodulation error at step j , for BPSK $e_j \in \{0, \pm 2\}$	(3.9)
$\mathbf{E}_{i-1} = [e_1, e_2, \dots, e_{i-1}]$	error vector at step i ,	(4.5)
\mathbf{w}_i	nulling vectors	(3.9)
$\boldsymbol{\alpha} = [\alpha_1, \dots, \alpha_m]$	power allocation vector	(3.13)
$\mathbf{A} = \text{diag}(\sqrt{\alpha_1}, \dots, \sqrt{\alpha_m})$	precoder matrix for power allocation	(3.13)
$\mathbf{A}_{i-1} = \text{diag}(\sqrt{\alpha_1}, \dots, \sqrt{\alpha_{i-1}})$	truncated precoder matrix for power allocation	(4.8)

$\gamma_i^{eff} = \frac{\alpha_i}{ \mathbf{E}_{i-1}\mathbf{A}_{i-1} ^2 + \sigma_0^2}$	the “effective step SNR”, which includes propagating errors from the past decisions as interference	(4.8)
$\bar{P}_{(n)}^{MRC}$	average BER with n -th order MRC	(4.3)
$P_{ei} = P_e(\gamma_i)$	conditional (on no errors at previous steps) error rate at step i	(4.1)
$P_{ui} = \sum_{\mathbf{E}_{i-1}} P_{ei \mathbf{E}_{i-1}} P_{\mathbf{E}_{i-1}}$	unconditional error rate at step i	(4.4)
$P_{ei \mathbf{E}_{i-1}} = P_{ei \mathbf{E}_{i-1}}(\gamma_i)$	probability of error at i -th step conditioned on the error vector \mathbf{E}_{i-1}	(4.5)
$P_{\mathbf{E}_{i-1}} = P_{\mathbf{E}_{i-1}}(\gamma_1 \dots \gamma_{i-1})$	the probability that error vector \mathbf{E}_{i-1} occurs	(4.5)
$P_B = 1 - \prod_{i=1}^m (1 - P_{ei})$	BLER (probability of having at least one error at the detected Tx vector)	(4.1)
$P_{et} = \frac{1}{m} \sum_{i=1}^m P_{ui}$	TBER (the error rate at the single output stream, to which all the sub-streams are merged)	(4.4)
$\delta = \left \frac{\Delta \bar{P} / \bar{P}}{\Delta u / u} \right $	the measure of robustness of system described by function P to system parameter u	(6.1)
G	the SNR gain found from $P(\alpha_1^{opt}, \dots, \alpha_m^{opt}) = P(\alpha, \dots, \alpha)$, $G = \alpha$	(7.1)

Acknowledgements

I would like to thank my research supervisor Dr. S. Loyka for his support and guidance.

1. Introduction

1.1. MOTIVATION OF THIS RESEARCH

Discovery of multiple-input-multiple-output (MIMO) wireless in 1995 was the most significant breakthrough in the field of communications since 1948, when Shannon founded information theory. It induced a true paradigm shift in wireless communication by turning the multipath propagation, traditionally an enemy of wireless transmission, into its ally. This has opened up plentiful opportunities and spawned numerous research activities.

MIMO offers tremendous spectral efficiencies compared to traditional systems. However, since the area is relatively new, there is still much work left to practically achieve those appealing horizons. The Vertical Bell Laboratories Layered Space-Time (V-BLAST) algorithm [37] has attracted significant attention in recent years as a signal processing strategy in the MIMO receiver due to its relative simplicity and also the ability to achieve, under certain conditions, the full MIMO capacity. Unfortunately, the algorithm has a few drawbacks as well. Its computational complexity is still high for many applications, and also its error rate performance is degraded by the effect of error propagation.

This work addresses these issues by considering an optimum transmit power allocation to improve the V-BLAST error rate performance using various optimization criteria from a unified perspective. The optimum power allocation is considered as a low complexity alternative to the computationally-demanding optimal ordering procedure of the V-BLAST algorithm. The power-optimized V-BLAST without optimal ordering and V-BLAST with optimal ordering demonstrate the same error rate performance at high SNR.

Although there have been some attempts to incorporate power allocation into the V-BLAST algorithm, they either require heavy feedback and numerical optimization, or provide analytical solutions so involved that it is hard to gain physical insight within the framework presented. None of the previous works gave comprehensive study on the impact of optimization criterion chosen, qualified analytically the gain of power allocation, or analyzed the robustness properties of the V-BLAST with adaptive power allocation. This thesis adopts systematic approach to comparative study of the power-optimized V-BLAST based on various optimization criteria and develops an analytical framework to quantify the gain of optimization.

1.2. CONTRIBUTION OF THE THESIS

The major contributions of the thesis are:

- Low complexity V-BLAST modifications such as V-BLAST with ordering at 1st step (section 3.4), V-BLAST with adaptive power allocation (section 3.5) and V-BLAST with pre-set power allocation (section 6.2);
- unifying analytical framework for optimization and performance analysis of the unordered V-BLAST with adaptive power allocation (Chapter 4);
- comparative study of various power-optimization strategies (section 5.5);
- investigation of the uniqueness of the optimum power allocation for different scenarios (section 5.1);
- compact closed-form approximations of the optimum power allocation (sections 5.3 and 5.4);
- compact closed-form approximations of the average error rates of the optimized V-BLAST (section 6.1);

- rigorous definition and analysis of the SNR gain of optimization, including lower- and upper-bounds as well as closed-form approximate expressions (Chapter 7);
- definition and analysis of a robustness measure of the power-optimized V-BLAST (Chapter 6).

The findings of this thesis have been presented in the following publications:

[1] V. Kostina, S. Loyka, On Optimum Power Allocation for the V-BLAST, *IEEE Trans. Comm.*, submitted, Sep. 2006

[2] V. Kostina, S. Loyka, On Optimization of the V-BLAST algorithm, *IEEE International Zurich Seminar on Communications 2006*, ETH Zurich, Switzerland, pp. 110 – 113, Feb. 2006

[3] V. Kostina, S. Loyka, Transmit Power Allocation for the V-BLAST Algorithm, *23rd Queen's Biennial Symposium on Communications*, Kingston, ON, Canada, pp. 165 – 168, May 2006

[4] S. Loyka, V. Kostina, F. Gagnon, On Convexity/Concavity Properties of Error Rates of the ML Detector and Their Applications, *IEEE Trans. Information Theory*, submitted, Jul. 2006

1.3. ORGANIZATION OF THE THESIS

The thesis is organized as follows. Chapter 2 indicates current trends in the rapidly developing MIMO research area and elaborates on previous studies of power allocation for the V-BLAST algorithm, drawing a distinction with the present work. Chapter 3 particularizes the V-BLAST algorithm and proposes V-BLAST with ordering at 1st step and V-BLAST with optimum power allocation as low-complexity alternatives to the optimal ordering procedure. The rest of the thesis is analytical analysis of the V-BLAST with optimum power allocation. Chapter 4 gives a brief review of the relevant error rate

expressions [54][56] and also presents some additional results, which facilitate the optimization and the performance analysis. Chapter 5 states and solves the optimum power allocation problem for various optimization criteria (TBER/BLER, average/instantaneous) and proves the uniqueness of the solution for the BLER-based optimization for a variety of modulation formats. Chapter 6 introduces and studies a robustness measure of the optimized algorithm. Chapter 7 analyses the SNR gain of the optimization defined in several ways. Finally, Chapter 8 concludes the thesis.

2. Literature Review

High data rate wireless link, which offers good quality of service (QoS), is of interest in emerging wireless local area networks (WLANs), as well as outdoor wireless wide area networks (WWANs) and cellular systems.

Designing such a link in non-line-of-sight (NLOS) environments represents a significant engineering challenge. To increase the maximum data rate which can be transmitted via a channel (i.e. channel capacity), one can, in principle, either increase the bandwidth (measured in Hz), or spectral efficiency (measured in b/s/Hz).

An increase of bandwidth is an extremely unattractive and costly solution because of the scarcity of available radio spectrum. The maximum achievable spectral efficiency, on the other hand, is limited by transmit (Tx) power and receive signal-to-noise ratio (SNR), so increasing the Tx power might be another way to boost the capacity. However this solution is also inadequate. Firstly, the transmit power in a terminal used by or located near human beings is limited to less than 1 Watt due to bio-hazard considerations. Secondly, the average SNR in NLOS environments is greatly reduced by fading, which causes fluctuations in signal level. Lastly, the signal-to-noise-and-interference-ratio (SINR) in cellular systems is capped due to the presence of co-channel interference.

Due to these factors, achieving higher data rates for power and bandwidth limited systems is a challenging task. Fortunately, another domain can be exploited to increase the channel capacity: space. Use of multiple antennas at transmitter and receiver allows to take advantage of the spatial dimension in wireless transmission (Fig. 2-1). This is based on the premise that in rich scattering environment, the signals from each individual transmit antenna appear highly uncorrelated at each of the receive antennas. The received mix of signals can be processed in such a way as to improve the QoS (the bit-error-rate or BER) or the data rate.

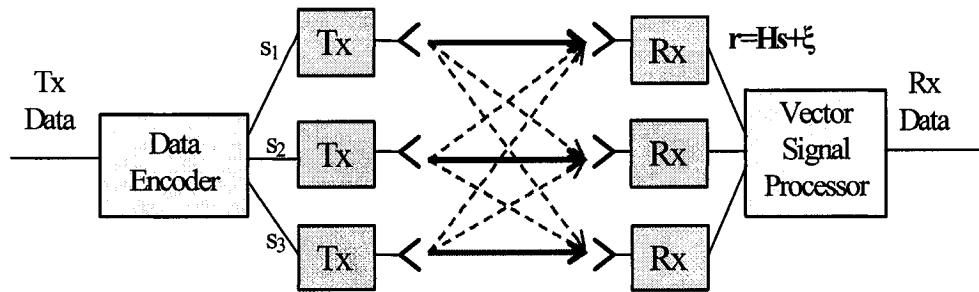


Fig. 2-1. Basic MIMO scheme

Multiple-input multiple-output (MIMO) wireless systems were discovered in 1995-1996 by Foschini [37] and Telatar [18]. Their pioneering works predicted remarkable spectral efficiencies of MIMO systems. They demonstrated that MIMO, when compared to traditional single-input single-output (SISO) systems, could offer 10-fold and even more performance improvement in terms of capacity, making 1Gbps wireless links a reality without additional transmit power or received SNR. No wonder their work incited tremendous scientific interest in this area: number of publications in MIMO area has been exhibiting rapid growth over the last decade (Fig. 2-2). Several special issues of IEEE journals were dedicated solely to MIMO communications ([1]-[4]). Some overview papers discussing the ever changing state of affairs in the area have been issued [5]-[8].

MIMO turns multipath propagation, traditionally a pitfall of wireless transmission, into its ally. This is a new paradigm in wireless communications, which requires new channel modeling, coding and signal processing techniques. The entire MIMO research area can thus be roughly divided into three smaller domains: channel modeling and capacity, space-time coding and receiver design. Below the thesis briefly outlines the recent advancements in the first two sub-areas and then dwells on MIMO receiver design as it constitutes its main topic.

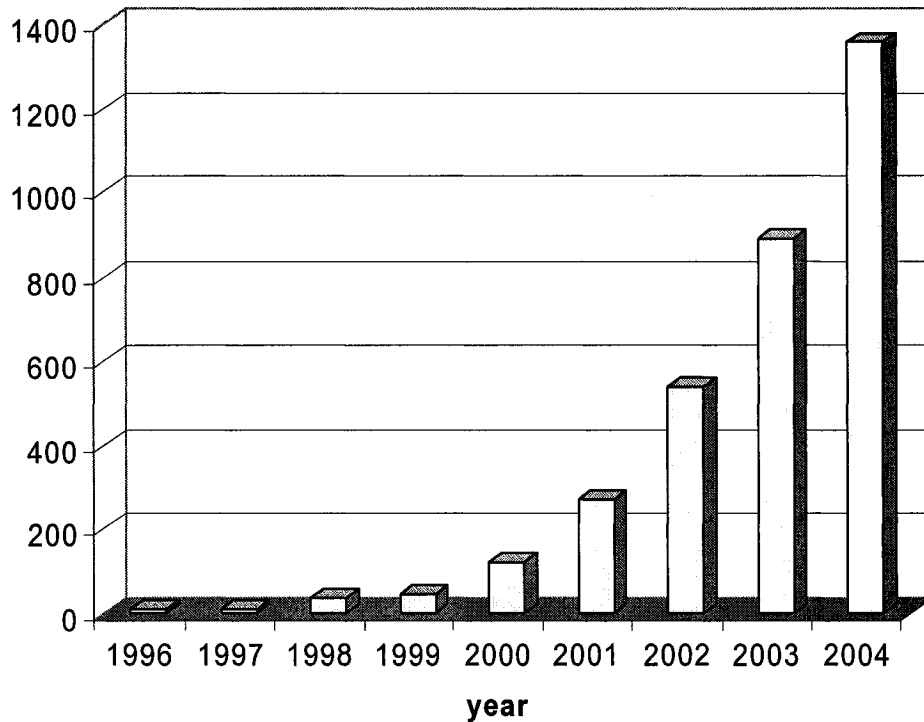


Fig. 2-2. Number of MIMO publications for the last decade¹

2.1. MIMO CHANNEL MODELING AND CAPACITY

Since profound understanding of MIMO channels is crucial in selecting proper signaling strategies in MIMO wireless networks, investigating the MIMO channel capacity in diverse environments and elaborating on proper channel models is one of the major trends in a broader MIMO research area. Pioneering studies [18][19] showed that in the presence of rich multipath leading to antenna decorrelation and full channel rank, MIMO links offer capacity gains that are proportional to the $\min(m, n)$, where m is the number of transmit antennas and n is the number of receive antennas. However, in real propagation environments, the fades are not independent due, for example, to insufficient spacing between antenna elements, and the channel capacity can be significantly smaller. [20] and [21] suggest simple MIMO channel models in the presence of spatial fading

¹ This data includes any published paper containing all of the keywords “MIMO”, “wireless”, “channel”, “space-time”, “communications” returned by the Google Scholar search engine.

correlation which allow to gain insight into the impact of propagation conditions on MIMO capacity. Chizhik et al. [22] go further and suggest a model which takes into account not only the spatial fading correlation but also the structure of scattering in the propagation environment. They point out the existence of pinhole channels that exhibit uncorrelated spatial fading between antennas but still have a poor rank property. H. Shin et al. [23] derive an analytical expression for the ergodic (average) capacity of such channels. However, the exact analytical expressions for the capacity of the MIMO system are mathematically intractable and hence are not very insightful. For that reason, many recent studies have been focused on deriving simple approximations and bounds for MIMO system capacity [24]-[26]. There have been many recent advances in this area, but many problems still remain open. An excellent tutorial and more detailed discussion on recent achievements in MIMO capacity evaluation can be found in [27].

2.2. SPACE-TIME CODING

The core idea in space-time coding (STC) is to complement time, a natural dimension of coding theory, with the spatial dimension arising from the use of multiple spatially separated antennas. The gain extracted from independence of multiple fading paths used by signal to travel from source to destination is called *diversity gain*. If the $m \cdot n$ links comprising the MIMO channel fade independently, the receiver can combine the arriving signals in such a way that the resultant signal exhibits considerably reduced amplitude variability in comparison to a SISO link and we get $m \cdot n$ -th order diversity. To extract total available spatial diversity in MIMO channel through appropriate construction of the transmitted space-time codewords is an objective of space-time diversity coding.

In the STC schemes, m code symbols are generated and transmitted simultaneously, one symbol per Tx antenna. The STC concept was originally revealed in

1998 in [28] in the form of trellis codes. Space-time trellis codes (STTC) provide the full diversity and coding gain, but require a multidimensional Viterbi decoder, the complexity of which grows exponentially with the number of antennas. In addressing the issue of decoding complexity of STTC, Alamouti proposed a simple space-time block coding (STBC) scheme for 2 Tx antennas [29]. STBC codes immediately gained a lot of attention because they can be decoded using simple linear processing, and yet they provide the full diversity gain. Alamouti scheme provides the maximum possible transmission rate allowed by the theory of orthogonal space-time block coding. The generalization of the Alamouti scheme for an arbitrary number of antennas [30] provides full spatial diversity but only half of the maximum possible rate. Despite the low complexity of the STBCs, they do not provide any coding gain, unlike the STTCs. Therefore, a few papers have appeared [31]-[33] in which the STBC is combined with an outer channel coding scheme to provide such coding gains. In most of these works, however, the conclusions are based on computer simulations, as performance analysis represents considerable difficulties. So far there have been some efforts to provide analytical tools which describe the performance of these space-time techniques [34]-[36], but still many open problems remain. This is not a surprise as with MIMO discovery an entire new dimension, a spatial one, was introduced to coding theory, opening new horizons for researchers.

2.3. SIGNAL PROCESSING AT THE MIMO RECEIVER: V-BLAST

As each Rx antenna in MIMO system sees a superposition of the Tx symbols (Fig. 2-1), the job of the MIMO receiver is to recover the original information from this mix in a reliable and computationally effective way. The Maximum Likelihood (ML) receiver yields the best performance, but its complexity is exponential in number of Tx antennas as exhaustive search over all possible transmitted vectors is required. Less complex

solution is to use a linear receiver interface, which uses complex combining weights to separate the transmitted data streams so that each stream can be decoded separately. But the error rate performance of such receivers is often unsatisfactory as linear combining enhances noise. Superior performance can be achieved by employing a nonlinear receiver interface, such as V-BLAST (Vertical Bell Laboratories Layered Space-Time), which was originally suggested by Foschini [37] in 1996. It is a comparatively simple algorithm and yet it achieves a significant portion of MIMO capacity. In [38], a laboratory result yielding 20 – 40 bit/s/Hz has been reported in indoor conditions with realistic SNR and error rates.

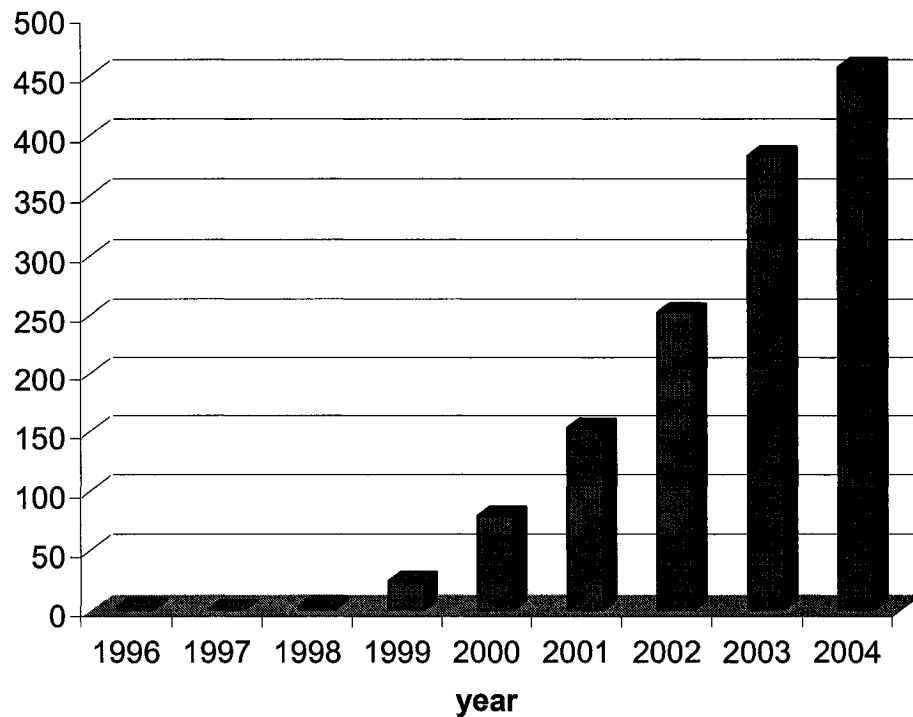


Fig. 2-3. Number of V-BLAST publications for the last decade²

² This data includes any published paper containing all of the keywords “BLAST”, “wireless”, “channel”, “space-time”, “communications” returned by the Google Scholar search engine.

The key idea behind V-BLAST is successive interference cancellation, namely, layer peeling where the individual data streams are decoded and stripped away layer-by-layer. The detection of a Tx symbol proceeds in steps and includes 3 major procedures at each step:

- (1) interference cancellation from already detected symbols,
- (2) interference nulling from yet-to-be-detected symbols,
- (3) optimal ordering (based on after-detection SNR).

A more detailed description of the algorithm can be found in Chapter 3.

V-BLAST has attracted significant attention in the recent years (Fig. 2-3) as it provides a good compromise between transmission rate, achievable diversity, and decoding complexity. However, the algorithm suffers from several drawbacks. Its computational complexity is still high for many applications, and, because of successive detection, its BER performance is degraded by the effect of error propagation. Thus, different modifications have been proposed to improve the algorithm in these directions [39]-[53].

Addressing the issue of the computational complexity of the original V-BLAST algorithm, Hassibi proposed a square root method for V-BLAST signal detection [39]. Original V-BLAST algorithm calculates pseudo-inverse of the channel matrix at each detection step. Square-root V-BLAST avoids direct computation of pseudo-inverse by using unitary transformations. Further improvement on the square-root algorithm was developed in [40], which speeds up the original square-root algorithm by 36% in terms of the number of multiplications and additions. Since it uses unitary transformations to avoid the computation of any matrix inversion or “squaring” operation, it maintains the advantages of the original square-root algorithm, such as robustness, hardware friendliness, and numerical stability. A recursive fast detection method, which avoids

inverting a matrix and finds the nulling weights via induction, was suggested in [43]. Compared to the improved square-root algorithm [40], it requires 13.6% less multiplications and 38.9% less additions. However, it is notable that in terms of numerical stability, the recursive algorithm yields to the improved square-root algorithm.

If the optimal ordering procedure is excluded from the algorithm, an efficient implementation based on QR decomposition is possible [41][42], which makes V-BLAST without optimal ordering an attractive low-complexity solution to space-time decoding.

Different research trend in the area is aimed at the reducing the BER, rather than complexity, of the original V-BLAST. Various modifications have been proposed in an effort to limit the error propagation effect. Among them, a joint ML and V-BLAST detection scheme [46], in which the ML detector is applied to the first (and hence most critical) subchannels to be decoded. In [47], low-diversity substreams are iteratively decoded by using decisions from high-diversity substreams, and in [48], all symbols are pre-estimated using the channel state information (CSI) and the most credible one is chosen to be detected first. Although these schemes do exhibit some performance improvement over the conventional V-BLAST, they often require a heavy feedback channel and also are more computationally intensive.

A popular approach to improve the error performance of the V-BLAST algorithm, which offers a reasonable complexity-performance tradeoff, is to decrease the error rates at lower steps by employing a non-uniform power allocation among the transmitters (Fig. 2-4).

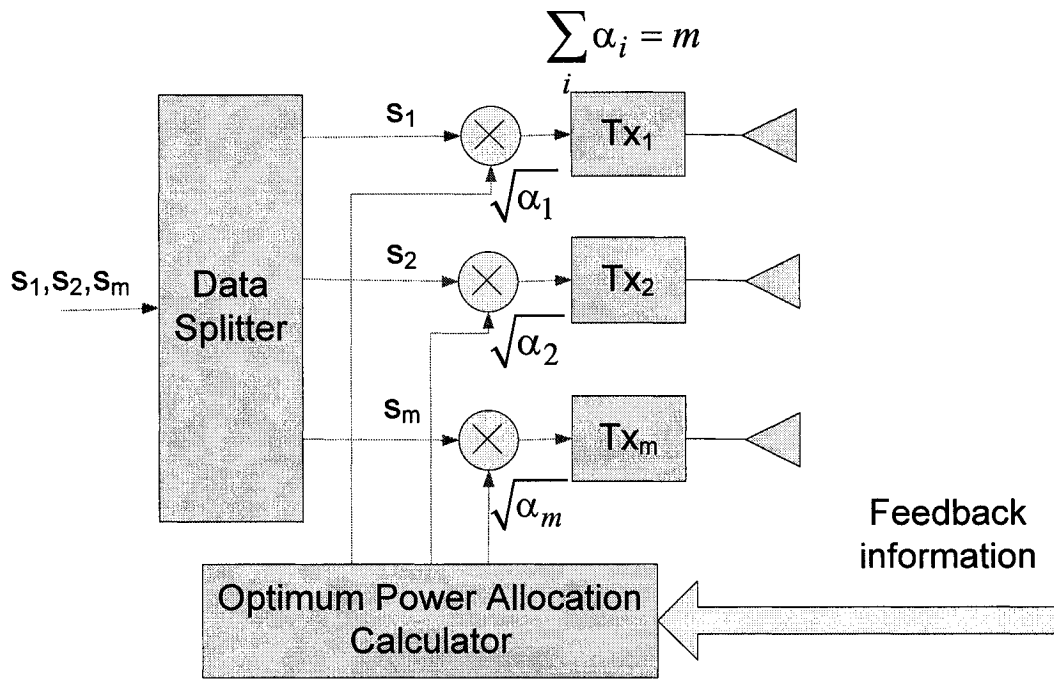


Fig. 2-4. V-BLAST with optimum power allocation

Several techniques have been reported that find the transmit (Tx) power allocation that minimizes the instantaneous (i.e. for given channel realization) total bit error rate (TBER) or block error rate (BLER) [49]-[50]. The TBER is defined as the error rate at the output stream to which all the individual sub-streams are merged after the detection [56]. Thus, it takes into account the actual number of errors at the transmitted symbol vector. The block error rate (BLER) is defined as the probability to have at least one error at the detected Tx symbol vector [56]. It does not take into account the *actual* number of errors, but just the fact of their presence, and is easier to analyze than the TBER.

In [49], an optimum transmit power allocation that minimizes instantaneous BLER for $2 \times n$ ordered V-BLAST is found numerically, and the SNR gain of 2 dB is demonstrated by simulation at the TBER of 10^{-3} .

In [50]-[52], the instantaneous TBER (rather than BLER) is considered as an optimization criterion. Because TBER includes explicitly the error propagation effect, its

exact analysis is very involved. Hence, various TBER approximations have been employed.

In [50][51], transmit power allocation that minimizes the instantaneous TBER when error propagation is neglected is found in closed form for $m \times n$ ZF V-BLAST with or without ordering. Error propagation analysis in [52] neglects the fact that there can be more than one error in decoded symbols. Authors claim that this assumption “may be justified at high SNR” but their simulation results show that their approximation of the TBER is not very accurate. However, it allows them to find a closed-form solution for $m \times n$ V-BLAST with either ZF or MMSE nulling. Detection ordering in a V-BLAST with this power allocation corresponds to the optimal ordering for uniform power allocation. Simulation results demonstrate that 4×4 V-BLAST with this power allocation provides 2.5-4.0 dB gain in SNR over the conventional V-BLAST at the TBER of 10^{-3} .

Although the instantaneous power allocation techniques proposed in [49]-[52] do demonstrate a few dB performance improvement over the original (unoptimized) V-BLAST, they also add considerably to the system complexity, since new feedback session and power reallocation are needed each time the channel matrix changes; the instantaneous per-stream (transmitter) SNRs also need to be sent to the Tx end.

A less complex approach is to use an average rather than instantaneous optimization, i.e. the optimum power allocation is found based on the error rate (BLER or TBER), averaged over all channel realizations. Since this ignores the small-scale fading, only occasional feedback sessions and power reallocations are required, when the average SNR changes, and only the average SNR needs to be fed back to the Tx end. This thesis adopts the latter approach but also studies some performance measures of the instantaneous optimization for comparison purposes. Similar approach has been taken up in [53][54]. The optimum power and rate allocation technique, based on minimizing the

average error rate for fixed total data rate, has been proposed in [53]. In [54], power allocation which minimizes the upper bound of the average BLER is suggested. However, only numerical techniques have been used in [53][54] to find the optimum power allocation, whereas this thesis develops an analytical approach to the average optimization of the V-BLAST power allocation, which provides more insight and also less demanding in terms of computational power. While the previous works [49]-[53] evaluated the performance of the optimized system through simulations only, by comparing optimized and non-optimized error rate curves, this thesis presents an analytical performance evaluation of both instantaneous and average optimization via a rigorous definition of the SNR gain of the optimization and via a measure of robustness.

2.4.SUMMARY

Discovery of MIMO, which is one of the most significant technological breakthroughs in modern communications, has inspired numerous research works in the areas of MIMO channel modeling, space-time coding and signal processing. Literature review outlining recent advances in these areas has been provided in this chapter. The main question that interests researchers and engineers is whether the enormous performance gains predicted by Foschini [37] and Telatar [18] can be reached in realistic operating scenarios. Several papers [49]-[54] have been published that propose employing non-uniform power allocation in the V-BLAST algorithm as a signal processing solution with reasonable complexity-performance tradeoff. However, these works lack analytical tools for analyzing the performance of the proposed system. This thesis addresses this issue by developing a unified analytical framework for optimization and analysis of the V-BLAST algorithm with non-uniform power allocation.

3. V-BLAST Algorithm and its Challenges

The following standard baseband discrete-time MIMO system model is employed in the thesis,

$$\mathbf{r} = \mathbf{H}\mathbf{s} + \boldsymbol{\xi} = \sum_{i=1}^m \mathbf{h}_i s_i + \boldsymbol{\xi}, \quad (3.1)$$

where $\mathbf{s} = [s_1, s_2, \dots, s_m]^T$ and $\mathbf{r} = [r_1, r_2, \dots, r_m]^T$ are the vectors representing the Tx and Rx symbols respectively, “T” denotes transposition, $\mathbf{H} = [\mathbf{h}_1, \mathbf{h}_2, \dots, \mathbf{h}_m]$ is the $n \times m$ matrix of the complex channel gains between each Tx and each Rx antenna, where \mathbf{h}_i denotes i -th column of \mathbf{H} , $n \geq m$, $\boldsymbol{\xi}$ is the vector of circularly-symmetric additive white Gaussian noise (AWGN), which is assumed to be $\mathcal{CN}(0, \sigma_0^2 \mathbf{I})$, i.e. independent and identically distributed (i.i.d.) in each receiver³. It is assumed that matrix \mathbf{H} is known at the receiver. In practice, channel knowledge at the receiver can be maintained via training, though not perfectly.

3.1. WHY V-BLAST? ALTERNATIVE RECEIVER ARCHITECTURES

The Maximum Likelihood (ML) detector bases its output on the following decision rule [5][8]:

$$\hat{\mathbf{s}} = \arg \min_{\mathbf{s}} |\mathbf{r} - \mathbf{H}\mathbf{s}|^2 \quad (3.2)$$

The ML receiver is optimal in terms of minimizing bit error rate. However, exhaustive search over all possible transmitted vectors (see (3.2)) renders a computing complexity of this receiver exponential in the number of Tx antennas. Hence, simpler receiver structures are needed that offer reasonable performance-complexity tradeoff.

³ the case of unequal noise power per Rx can also be considered within the present framework

The decoding complexity of the ML receiver can be significantly reduced by employing linear receiver front-ends to separate the transmitted data streams, and then independently decode each of the streams. The general form of a linear interface is given by

$$\mathbf{r}' = \mathbf{G}\mathbf{r}, \quad (3.3)$$

where $m \times n$ linear interface matrix \mathbf{C} is chosen so that the metric

$$|\mathbf{r}' - \mathbf{s}|^2 \quad (3.4)$$

can be used for decoding.

ZF (Zero-forcing) receiver: The ZF front-end minimizes (3.4) disregarding the presence of noise [8]:

$$\begin{aligned} \mathbf{G}_{ZF} &= \arg \min_{\mathbf{G}} |\mathbf{G}\mathbf{H}\mathbf{s} - \mathbf{s}|^2 \rightarrow \\ \mathbf{G}_{ZF} &= \mathbf{H}^{-1}, \end{aligned} \quad (3.5)$$

where $\mathbf{H}^{-1} = (\mathbf{H}^+ \mathbf{H})^{-1} \mathbf{H}^+$ denotes the Moore-Penrose pseudoinverse of the channel matrix \mathbf{H} , “+” denotes complex conjugate transposition. Obviously ZF receiver is not applicable for rank-deficient channel matrices as \mathbf{H}^{-1} does not exist in this case.

The output of the ZF receiver is obtained as

$$\mathbf{r}' = \mathbf{s} + \mathbf{H}^{-1}\boldsymbol{\xi} \quad (3.6)$$

Thus, the ZF front-end decouples the vector channel into m scalar channels with additive spatially-colored noise, completely removing inter-stream interference (that is why it is called zero-forcing). Each scalar channel is then decoded separately, and the processing complexity is significantly reduced. However, this receiver enhances noise, especially for ill-conditioned channel matrices, which results in considerable performance degradation compared to the ML decoder.

MMSE (Minimum mean-square error) receiver: The MMSE front-end is obtained from the condition of minimum mean-square error [8]:

$$\begin{aligned} \mathbf{G}_{MMSE} &= \arg \min_{\mathbf{G}} \langle \mathbf{G}(\mathbf{H}\mathbf{s} + \boldsymbol{\xi}) - \mathbf{s} \rangle_{\boldsymbol{\xi}}^2 \rightarrow \\ \mathbf{G}_{MMSE} &= (\mathbf{H}^{\dagger}\mathbf{H} + \sigma_0^2\mathbf{I}_m)^{-1}\mathbf{H}^{\dagger} \end{aligned} \quad (3.7)$$

\mathbf{I}_m is the $m \times m$ unity matrix, σ_0^2 is the noise power. MMSE receiver balances interference mitigation with noise enhancement, and yields better performance than ZF receiver. It is also more stable numerically as the inverse in (3.7) always exists⁴. However, its performance is still not satisfactory for most practical cases.

3.2. BASIC V-BLAST ALGORITHM

ML receiver is not feasible due to its complexity, whereas linear receiver interfaces are not feasible due to their unsatisfactory performance. V-BLAST is a suboptimum receiver interface that offers a good compromise between error rate and complexity.

The detection of a Tx symbol in the V-BLAST algorithm proceeds in steps and includes 3 major procedures at each step [37]:

(1) *The interference cancellation step:* when the signal from the i -th transmitter is detected, the interference from the $i-1$ already detected symbols is subtracted based on the knowledge of the channel matrix \mathbf{H}

$$\mathbf{r}'_i = \mathbf{r} - \sum_{j=1}^{i-1} \mathbf{h}_j \hat{s}_j \quad (3.8)$$

where \mathbf{h}_j is the j -th column of \mathbf{H} , and \hat{s}_j are the demodulated symbols.

(2) *The interference nulling step:* by applying a linear combining to received signals the amount of interference from yet-to-be-detected symbols is reduced (MMSE) or completely removed (ZF):

⁴ Note that $\mathbf{H}^{\dagger}\mathbf{H}$ is positive semidefinite and hence $\mathbf{H}^{\dagger}\mathbf{H} + \sigma_0^2\mathbf{I}_m$ is positive definite.

$$\hat{r}_i = \mathbf{w}_i^+ \mathbf{r}'_i = \mathbf{w}_i^+ \mathbf{h}_i s_i + \mathbf{w}_i^+ \sum_{j=1}^{i-1} \mathbf{h}_j e_j + \mathbf{w}_i^+ \xi, \quad (3.9)$$

where $e_j = \hat{s}_j - s_j$ is demodulation error at step j . (3.9) clearly shows that the errors from past decisions propagate to the current decision. The choice of the nulling vectors \mathbf{w}_i to satisfy either ZF or MMSE criteria categorizes the V-BLAST structure, giving rise to ZF-V-BLAST or MMSE-V-BLAST, respectively:

$$\mathbf{w}_i = \begin{cases} \text{1st column of } \mathbf{H}_{i-1} \left(\mathbf{H}_{i-1}^+ \mathbf{H}_{i-1} \right)^{-1}, & \text{ZF} \\ \text{1st column of } \mathbf{H}_{i-1} \left(\mathbf{H}_{i-1}^+ \mathbf{H}_{i-1} + \sigma_0^2 \mathbf{I}_{m-i+1} \right)^{-1}, & \text{MMSE} \end{cases}, \quad (3.10)$$

where $\mathbf{H}_i = [\mathbf{h}_{i+1}, \mathbf{h}_{i+2}, \dots, \mathbf{h}_m]$ is the matrix obtained from \mathbf{H} by removing its first i columns.

(3) *The optimal ordering procedure:* the strongest signal, among the remaining undecoded streams, is chosen to be detected next. The after-processing SNR at each step is given by

$$\gamma_i = \frac{|s_i|^2}{\sigma_0^2} \mathbf{w}_i^+ \mathbf{w}_i \quad (3.11)$$

The full optimal ordering detection algorithm can be summarized in Table 1 [37]:

If ZF nulling vectors are employed and the detection order is known beforehand, a series of calculation of the inverse can be replaced by applying the Gram-Schmitt Orthogonalization (GSO) process [41], leading to cost-efficient QR-implementation. Let us consider the QR decomposition of $\mathbf{H} = \mathbf{Q}\mathbf{R}$, where \mathbf{Q} is unitary and \mathbf{R} is lower-triangular. In a coordinate system associated with \mathbf{Q} , $\mathbf{Q}^+ \mathbf{r} = \mathbf{R}\mathbf{s} + \mathbf{Q}^+ \xi$, the channel matrix is lower-triangular, hence there is no interference from not yet detected symbols, and no need for the interference nulling step which involves calculation of the pseudo inverse; combining vectors are found as

$$[\mathbf{w}_1 \dots \mathbf{w}_m] = \mathbf{Q} \quad (3.12)$$

As was shown in [56][62], QR- and regular ZF-V-BLAST are equivalent in terms of basic algorithm steps, that is, regular V-BLAST in fact performs QR decomposition.

Table 1. V-BLAST algorithm with optimal ordering

Initialization:	$\mathbf{r}_0 = \mathbf{r}$ $\mathbf{H}_0 = \mathbf{H}$
Recursion:	$i \leftarrow 1 \dots m$ $\mathbf{G}_i = \begin{cases} \mathbf{H}_{i-1} (\mathbf{H}_{i-1}^+ \mathbf{H}_{i-1})^{-1}, & \text{ZF} \\ \mathbf{H}_{i-1} (\mathbf{H}_{i-1}^+ \mathbf{H}_{i-1} + \sigma_0^2 \mathbf{I}_{m-i+1})^{-1}, & \text{MMSE} \end{cases}$ $k_i = \arg \min_j \ (\mathbf{G}_i)_j\ $ - optimal ordering $\mathbf{w}_i = (\mathbf{G}_i)_{k_i}$ $\hat{r}_{k_i} = \mathbf{w}_i^+ \mathbf{r}$ - interference nulling $\hat{s}_{k_i} = D^{-1}(\hat{r}_{k_i})$ - quantization $\mathbf{r}_i = \mathbf{r}_{i-1} - \hat{s}_{k_i} \cdot \mathbf{h}_{k_i}$ - interference cancellation

3.3. COMPLEXITY-PERFORMANCE TRADEOFF IN DIFFERENT IMPLEMENTATIONS OF V-BLAST

Different variants of the V-BLAST algorithm generally exhibit different performance (Fig. 3-1). Optimally ordered MMSE-V-BLAST entails the most computational cost, but is capable of achieving excellent performance. Optimal ordering mitigates the effect of error propagation and allows to improve the error rate performance of the algorithm, yet it is a computationally intensive procedure. On the contrary, unordered ZF-V-BLAST ranks the worst in terms of performance. However, an efficient QR implementation makes it an attractive low-complexity solution to space-time

decoding [41]. Besides, orthogonality of ZF combining weights simplifies the error rate analysis of the algorithm, leading to analytical closed-form error rate expressions [54]-[56]. Hence optimization of the ZF-V-BLAST can be carried out analytically, leading to simpler and more insightful solutions. For these reasons, unordered ZF-V-BLAST is chosen as a baseline for optimization in the present thesis.

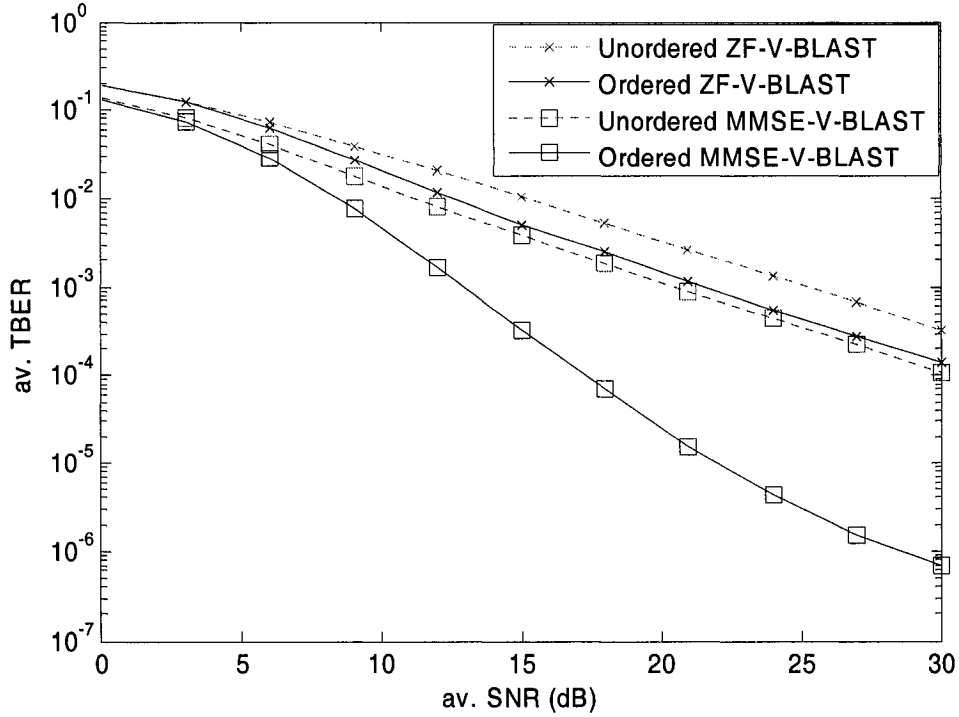


Fig. 3-1. TBER for ZF and MMSE V-BLAST, with and without optimal ordering, $n=m=3$, number of Monte Carlo simulations gradually increasing with SNR up to 10^8 , BPSK modulation, Rayleigh fading

3.4.ZF-V-BLAST WITH ORDERING AT 1ST STEP

The optimal ordering procedure has a significant computational complexity as it requires computation of $m-i+1$ SNRs at detection step i (or, equivalently, computation of the inverse of $(m-i+1) \times (m-i+1)$ matrix). Hence it is one of the major obstacles to cost-efficient implementation. On the contrary, when the detection order is known, only one QR decomposition is needed at the beginning of the algorithm.

Since the optimal detection order is not known beforehand, the suboptimal “ordering at 1st step” technique is suggested in the thesis⁵. According to this method, the columns of $\mathbf{H}(\mathbf{H}^+\mathbf{H})^{-1}$ are sorted in ascending order before successive nulling and cancellation, i.e. the optimal ordering procedure is performed at the first step only. QR implementation of ZF-V-BLAST with ordering at 1st step is compactly described as follows:

Table 2. ZF-V-BLAST algorithm with ordering at 1st step

Initialization:	$\mathbf{r}_0 = \mathbf{r}$ $\mathbf{G}_1 = \mathbf{H}(\mathbf{H}^+\mathbf{H})^{-1}$ - ZF $\{k_1 \dots k_m\} = \text{sort}_j \left\ (\mathbf{G}_1)_j \right\ $ - ascending order $\mathbf{G} = [(\mathbf{G}_1)_{k_1} \dots (\mathbf{G}_1)_{k_m}]$ $\mathbf{G} = \mathbf{QR}$ - \mathbf{Q} - unitary, \mathbf{R} - lower-triangular $[\mathbf{w}_1 \dots \mathbf{w}_m] = \mathbf{Q}$ - matrix of ZF weights
Recursion:	$i \leftarrow 1 \dots m$ $\hat{\mathbf{r}}_{k_i} = \mathbf{w}_i^+ \mathbf{r}_i$ $\hat{\mathbf{s}}_{k_i} = D^{-1}(\hat{\mathbf{r}}_{k_i})$ $\mathbf{r}_i = \mathbf{r}_{i-1} - \hat{\mathbf{s}}_{k_i} \cdot \mathbf{h}_{k_i}$

Since the strongest signal is decoded first, the credibility of the 1st step decision is increased. Because the overall performance is dominated by the first decoded stream [54][56], the proposed V-BLAST modification mitigates the error propagation effect. The simulation results demonstrate that V-BLAST with 1st step ordering performs nearly as well as the V-BLAST with optimal ordering (Fig. 3-2).

⁵ After this work was finished, we discovered that similar idea has already been proposed in [44], and its complexity has been analyzed in [45]

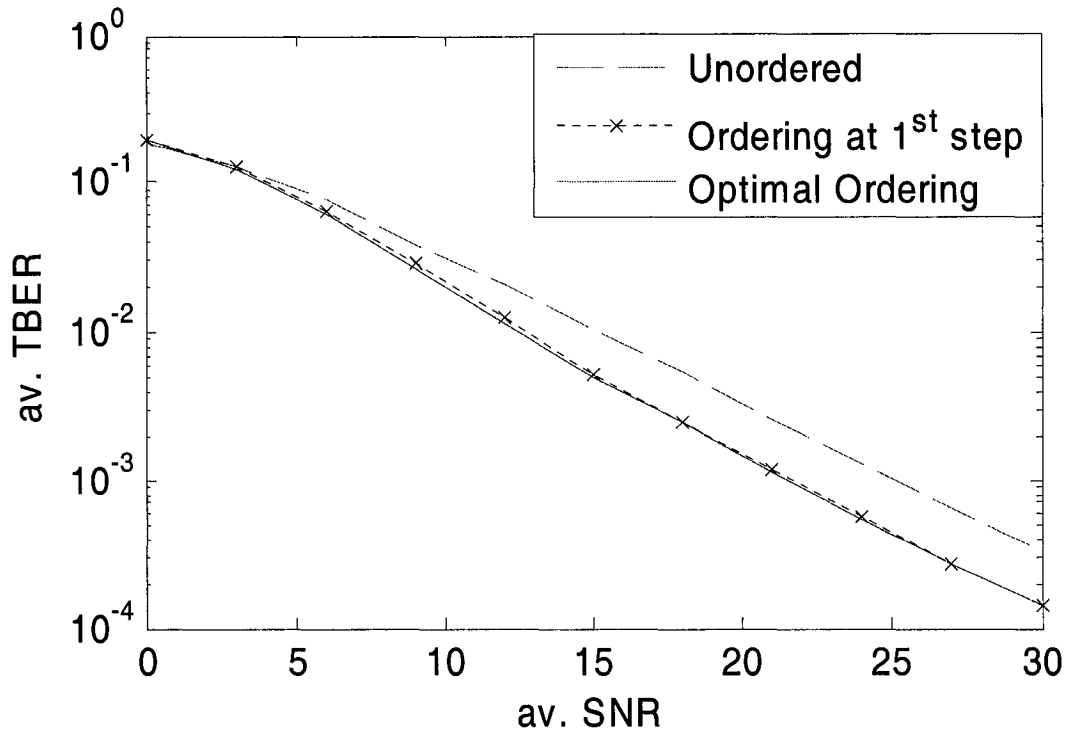


Fig. 3-2. TBER for ZF-V-BLAST with 1st step ordering and with optimal ordering, $n=m=3$, BPSK modulation, Rayleigh fading

Complexity analysis has been done in [45]. It demonstrates (see Table 3) significant complexity reduction the V-BLAST with 1st step ordering in comparison with the regular V-BLAST. The greater the total number of antennas, the greater the difference: thus, for 3×3 V-BLAST the total number of operations required the V-BLAST with 1st step ordering and for the optimally ordered V-BLAST equals 440 and 490, respectively, and the complexity reduction is 10%, whereas for 10×10 V-BLAST the corresponding numbers are 19123 and 45815, and the complexity reduction is 58%.

Table 3. Number of operations for the two variants of V-BLAST algorithm

V-BLAST with optimal ordering	V-BLAST with ordering at 1 st step
$4nm^3 + 6nm^2 + 2nm - \left(\frac{1}{3}m^3 + \frac{1}{2}m^2 + \frac{1}{6}m\right)$	$16nm^2 + \frac{13}{3}m^3 + \frac{14}{3}m + 3 - (4nm + 8m^2 + 6n)$

3.5. UNORDERED V-BLAST WITH OPTIMUM POWER ALLOCATION

Optimal ordering procedure attempts to decrease the error rate at lower steps by always detecting a symbol with the highest after-processing SNR first. Alternatively, the credibility of decisions at lower detection stages can be increased by employing a non-uniform power allocation among the transmitters (Fig. 2-4). It will be shown that the two approaches result in almost the same performance.

The standard MIMO system model (3.1) should be modified to account for a non-uniform power allocation,

$$\mathbf{r} = \mathbf{H}\mathbf{A}\mathbf{s} + \xi = \sum_{i=1}^m \mathbf{h}_i \sqrt{\alpha_i} s_i + \xi \quad (3.13)$$

where $\mathbf{A} = \text{diag}(\sqrt{\alpha_1}, \dots, \sqrt{\alpha_m})$, and α_i is the power allocated to the i -th transmitter. For the regular (unoptimized) V-BLAST, the total power is distributed uniformly among the transmitters, $\alpha_1 = \alpha_2 = \dots = \alpha_m = 1$. In the optimized system, α_i are chosen to minimize the TBER or the BLER, either average or instantaneous, leading to average and instantaneous optimization, accordingly. Instantaneous optimization is more demanding both in terms of the processing power and the feedback channel required as it needs new feedback session and computation of power allocation each time the channel matrix changes. The average optimization requires only occasional feedback when the average SNR is changed.

This thesis uses the unordered ZF-V-BLAST as a baseline for optimization for the following reasons:

- (i) Since the efficient QR implementation of ZF-V-BLAST can be applied when the order is known beforehand, the optimum power allocation is considered as a low complexity alternative to the optimal ordering. Yet it is capable of achieving almost the same error rate performance (see Chapter 5).

(ii) the optimal ordering presents serious difficulties for analytical performance evaluation, especially when no approximations are used [55][57]. For the case of ZF-V-BLAST without optimal ordering, the average TBER and the BLER were found in closed-form in uncorrelated Rayleigh fading in [54]-[56], which allows optimization to be carried out analytically and in closed-form.

The ZF-V-BLAST algorithm with optimum power allocation, assuming α_i are known, can be summarized as follows,

Table 4. ZF-V-BLAST algorithm with non-uniform power allocation

Initialization:	$\mathbf{r}_0 = \mathbf{r}$ $\mathbf{G} = \mathbf{H}(\mathbf{H}^+\mathbf{H})^{-1}$ - ZF $\mathbf{G} = \mathbf{QR}$ - \mathbf{Q} - unitary, \mathbf{R} - lower-triangular $[\mathbf{w}_1 \dots \mathbf{w}_m] = \mathbf{Q}$ - matrix of ZF weights
Recursion:	$i \leftarrow 1 \dots m$ $\hat{\mathbf{r}}_i = \mathbf{w}_i^+ \mathbf{r}_i$ $\hat{\mathbf{s}}_i = D^{-1}(\hat{\mathbf{r}}_i)$ $\mathbf{r}_i = \mathbf{r}_{i-1} - \sqrt{\alpha_i} \cdot \hat{\mathbf{s}}_i \cdot \mathbf{h}_{k_i}$

3.6. SUMMARY

Among different variants of the V-BLAST algorithm for space-time signal processing, unordered ZF-V-BLAST is an attractive choice due to its particular simplicity. Its performance however suffers from the error propagation effect. Introducing the optimal ordering procedure into the algorithm is one way to mitigate it. Unfortunately this solution is rather computationally intensive, which may be a limitation for some applications. As low-complexity alternatives to the optimal ordering, 1st step ordering and optimum power allocation techniques have been proposed. Both strategies yield almost the same performance as the V-BLAST with optimal ordering.

4. Error Rates

Analytical closed-form error performance evaluation of the un-ordered ZF-V-BLAST in uncorrelated Rayleigh fading channel has been reported in [54]-[56]. Below we outline the major results and extend them so that they can be used as a tool for the optimum power allocation. Following [56], BPSK modulation is assumed for simplicity, although the results below can also be generalized to other modulation formats (e.g M-QAM [54]), which results, however, in more cumbersome expressions.

Since this research relies on the V-BLAST error rate performance analysis in [54]-[56], it also adopts the same basic assumptions:

- (1) the channel is random, quasistatic (i.e. fixed for every frame of information bits but varying from frame to frame), frequency independent (i.e., negligible delay spread), Rayleigh fading;
- (2) the Tx signals, noise and channel gains are independent of each other;
- (3) perfect channel knowledge is available at the receiver;
- (4) there is no performance degradation due to synchronization and timing errors.

4.1. BLOCK ERROR RATE

The BLER is defined as a probability of having at least one error in the detected Tx symbol vector, which can be expressed as [54]-[56],

$$P_B = 1 - \prod_{k=1}^m (1 - P_{ei}) \quad (4.1)$$

where $P_{ei} = P_e(\gamma_i)$ is the instantaneous, i.e. for given channel realization, conditional (no errors at the previous steps) error rate at step i , γ_i is the after-processing instantaneous SNR at step i . The BLER is relatively easy to analyze as it does not require explicit error

propagation characterization. The average (over all channel realizations) BLER \bar{P}_B can be expressed in a similar way [54]-[56],

$$\bar{P}_B = 1 - \prod_{i=1}^m (1 - \bar{P}_{ei}) \quad (4.2)$$

where $\bar{P}_{ei} = \langle P_{ei} \rangle_{\mathbf{H}}$ is the average conditional error rate at step i , which is the same as the average error rate with $(n-m+i)$ -th order maximum ratio combining (MRC) $\bar{P}_{(n-m+i)}^{MRC}$, and is known in closed form for many modulation formats. Specifically, for BPSK modulation,

$$\bar{P}_{ei} = \bar{P}_{(n-m+i)}^{MRC}(\alpha_i \gamma_0) = \left[\frac{1 - \mu_i}{2} \right]^{n-m+i} \sum_{k=0}^{n-m+i-1} C_{n-m+i-1+k}^k \left[\frac{1 + \mu_i}{2} \right]^k, \quad (4.3)$$

$$\mu_i = \sqrt{\frac{\alpha_i \gamma_0}{1 + \alpha_i \gamma_0}}$$

where $C_{n-m+i-1+k}^k$ are the combinatorial coefficients, $\gamma_0 = 1/\sigma_0^2$ and $\alpha_i \gamma_0$ are the average per-Tx SNR for the unoptimized and optimized V-BLAST, respectively.

4.2. TOTAL BIT ERROR RATE

The TBER, i.e. the error rate in the output data stream to which all the individual Tx streams are merged, is given by

$$P_{et} = \frac{1}{m} \sum_{i=1}^m P_{ui}, \quad (4.4)$$

where $P_{ui} = P_{ui}(\gamma_1 \dots \gamma_i)$ is the unconditional error probability at step i , which includes the errors propagating from the preceding steps. To account for different combinations of errors in the first $i-1$ steps, the error vector is introduced: $\mathbf{E}_{i-1} = [e_1, e_2 \dots e_{i-1}]$, where $e_k = \hat{s}_k - s_k$ represents demodulation error at step k , $e_k \in \{0, \pm 2\}$, and \hat{s}_k denotes the symbol demodulated at step k . P_{ui} can then be expressed as:

$$P_{ui} = \sum_{\mathbf{E}_{i-1}} P_{ei|\mathbf{E}_{i-1}} P_{\mathbf{E}_{i-1}}, \quad (4.5)$$

where $P_{ei|\mathbf{E}_{i-1}} = P_{ei|\mathbf{E}_{i-1}}(\gamma_i)$ is the probability of error at i -th step conditioned on the error vector \mathbf{E}_{i-1} , and $P_{\mathbf{E}_{i-1}} = P_{\mathbf{E}_{i-1}}(\gamma_1 \dots \gamma_{i-1})$ is the probability that such error vector occurs, which can be expressed as:

$$P_{\mathbf{E}_{i-1}} = \prod_{k=1}^{i-1} \Pr\{e_k | \mathbf{E}_{k-1}\},$$

$$\Pr\{e_k | \mathbf{E}_{k-1}\} = \begin{cases} P_{ek|\mathbf{E}_{k-1}}, & e_k \neq 0 \\ 1 - P_{ek|\mathbf{E}_{k-1}}, & e_k = 0 \end{cases} \quad (4.6)$$

Rather than considering the TBER as a sum of unconditional BERs P_{ui} as in (4.4) [56], where each P_{ui} includes the errors propagating from steps 1 to $i-1$, the sum in (4.4) can be regrouped to emphasize the errors that occurred first at step i and then propagated further to steps $i+1, \dots, m$. Let us regroup the error vectors by the position of the first error, i.e. group i includes error vectors that can be written as $\tilde{\mathbf{E}}_{j-1} = [0, \dots, 0, \pm 2, e_{i+1} \dots e_{j-1}]$. The TBER can then be written as

$$P_{et} = \frac{1}{m} \sum_{i=1}^m a_i P_{ei} \prod_{k=1}^{i-1} (1 - P_{ek}),$$

$$a_i = 1 + P_{e_{i+1}|2} + \sum_{j=i+2}^m \sum_{[e_{i+1} \dots e_{j-1}]} P_{e_j|\tilde{\mathbf{E}}_{j-1}} \prod_{k=i+1}^{j-1} \Pr\{e_k | \tilde{\mathbf{E}}_{k-1}\}, \quad a_m = 1 \quad (4.7)$$

where a_i describes the after-effects of the error that first occurred at step i . If there were no error propagation, then all $a_i = 1$; the error propagation effect increases a_i , resulting in higher TBER. In many cases (i.e. intermediate to high SNR), (4.7) is easier to deal with than (4.4)-(4.6), since simple but accurate approximations are possible.

Note that (4.4)-(4.7) hold for both instantaneous and average error rates. In the latter case, similarly to [56], the average step BER conditioned on \mathbf{E}_{i-1} is:

$$\begin{aligned}\bar{P}_{ei|\mathbf{E}_{i-1}} &= \bar{P}_{(n-m+i)}^{MRC}(\gamma_i^{eff}), \\ \gamma_i^{eff} &= \frac{\alpha_i}{|\mathbf{E}_{i-1}\mathbf{A}_{i-1}|^2 + \sigma_0^2},\end{aligned}\quad (4.8)$$

where the unequal power distribution is taken into account by using $\mathbf{A}_{i-1} = \text{diag}(\sqrt{\alpha_1}, \dots, \sqrt{\alpha_{i-1}})$, and γ_i^{eff} is the ‘‘effective step SNR’’, which includes propagating errors from the past decisions as interference. The average TBER can be evaluated using (4.8) in (4.4)-(4.7). If there is no error in the earlier decisions, $\gamma_i^{eff} = \alpha_i/\sigma_0^2 = \alpha_i\gamma_0$. At intermediate to large SNR, earlier errors greatly reduce γ_i^{eff} since $|\mathbf{E}_{i-1}\mathbf{A}_{i-1}| \gg \sigma_0$.

To find the instantaneous TBER, we need to evaluate $P_{ei|\mathbf{E}_{i-1}}$. This can be accomplished by considering the decision variable at step i (after the interference cancellation and nulling – see (3.9)),

$$\hat{r}_i = \mathbf{w}_i^+ \mathbf{h}_i \sqrt{\alpha_i} s_i + \mathbf{w}_i^+ \sum_{j=1}^{i-1} \mathbf{h}_j \sqrt{\alpha_j} e_j + \mathbf{w}_i^+ \xi, \quad (4.9)$$

\mathbf{w}_i are ZF combining weights given by (3.10). \hat{r}_i is a Gaussian random variable for any given s_i , \mathbf{E}_{i-1} and \mathbf{H} ,

$$\hat{r}_i \square \mathcal{CN}\left(\mathbf{w}_i^+ \mathbf{h}_i \sqrt{\alpha_i} s_i + \mathbf{w}_i^+ \sum_{j=1}^{i-1} \mathbf{h}_j \sqrt{\alpha_j} e_j, \sigma_0^2\right), \quad (4.10)$$

and the binary decision rule applied to \hat{r}_i yields:

$$\begin{aligned}P_{ei|\mathbf{E}_{i-1}} &= \frac{1}{2}P(r_i'' > 0 | s_i = -1, \mathbf{E}_{i-1}) + \frac{1}{2}P(r_i'' < 0 | s_i = +1, \mathbf{E}_{i-1}) = \\ &= \frac{1}{2}Q\left(\text{Re}\left\{\mathbf{w}_i^+ \mathbf{h}_i \sqrt{\alpha_i} + \mathbf{w}_i^+ \sum_{j=1}^{i-1} \mathbf{h}_j \sqrt{\alpha_j} e_j\right\}\right) + \\ &+ \frac{1}{2}Q\left(\text{Re}\left\{\mathbf{w}_i^+ \mathbf{h}_i \sqrt{\alpha_i} - \mathbf{w}_i^+ \sum_{j=1}^{i-1} \mathbf{h}_j \sqrt{\alpha_j} e_j\right\}\right)\end{aligned}, \quad (4.11)$$

where $Q(x) = \sqrt{2\pi}^{-1} \int_x^\infty e^{-t^2/2} dt$ is the Q-function. The instantaneous TBER is obtained

by substituting (4.11) into (4.4)-(4.7).

Example. For $m = n = 2$, (4.11) reduces to,

$$\begin{aligned}
P_{e1} &= P_{e1|0} = Q\left(\text{Re}\left\{\mathbf{w}_1^+ \mathbf{h}_1 \sqrt{\alpha_1}\right\}\right) \\
P_{e2} &= P_{e2|0} = Q\left(\text{Re}\left\{\mathbf{w}_2^+ \mathbf{h}_2 \sqrt{\alpha_2}\right\}\right) \\
P_{e2|2} &= \frac{1}{2}Q\left(\text{Re}\left\{\mathbf{w}_2^+ \mathbf{h}_2 \sqrt{\alpha_2} + 2\mathbf{w}_2^+ \mathbf{h}_1 \sqrt{\alpha_1}\right\}\right) + \\
&+ \frac{1}{2}Q\left(\text{Re}\left\{\mathbf{w}_2^+ \mathbf{h}_2 \sqrt{\alpha_2} - 2\mathbf{w}_2^+ \mathbf{h}_1 \sqrt{\alpha_1}\right\}\right)
\end{aligned} \tag{4.12}$$

and the TBER is given by [56]:

$$P_{et} = \frac{1}{2} \left\{ \underbrace{P_{e1}}_{\substack{\text{1st step} \\ \text{BER}}} + \underbrace{P_{e2}(1-P_{e1})}_{\substack{\text{2nd step conditional} \\ \text{(on no error at 1st step) BER}}} + \underbrace{P_{e2|2}P_{e1}}_{\substack{\text{Error propagation} \\ \text{(from 1st to 2nd step)}}} \right\} \tag{4.13}$$

Due to the fast-decaying behavior of the Q-function, $P_{e1|E_{i-1}}$ is well approximated by

$$P_{e1|E_{i-1}} \approx Q(x_{\min})/2, \quad x_{\min} = \min \left[\text{Re} \left\{ \mathbf{w}_i^+ \mathbf{h}_i \sqrt{\alpha_i} \pm \mathbf{w}_i^+ \sum_{j=1}^{i-1} \mathbf{h}_j \sqrt{\alpha_j} e_j \right\} \right]. \tag{4.14}$$

Validity of analytical TBER expressions, instantaneous and average⁶, has been demonstrated through simulations. Fig. 4-1 compares analytical instantaneous TBER from (4.11), (4.4)-(4.7) averaged over all channel realizations, analytical average TBER from (4.4)-(4.8) and the TBER obtained by Monte-Carlo simulations. Both uniform and non-uniform power allocation are validated. As a non-uniform power allocation, the closed-form optimum power allocation $\boldsymbol{\alpha}^{opt}$ for optimization average optimization is used⁷. Fig. 4-2 plots exact and approximate instantaneous TBER given by (4.11),(4.14), (4.4)-(4.7) for two different channel realizations, versus γ_0 . Clearly both instantaneous and average TBER expressions are in agreement with TBER obtained by Monte Carlo simulations.

⁶ The average TBER expression was justified in [56] for uniform power allocation. This thesis extends this result for non-uniform power allocation.

⁷ See Chapter 5 for exact expression (eq. (5.7)), however, it is not the exact value of $\boldsymbol{\alpha}^{opt}$ that is important here, but the fact that the analytical TBER expressions hold for non-uniform power allocation as well.

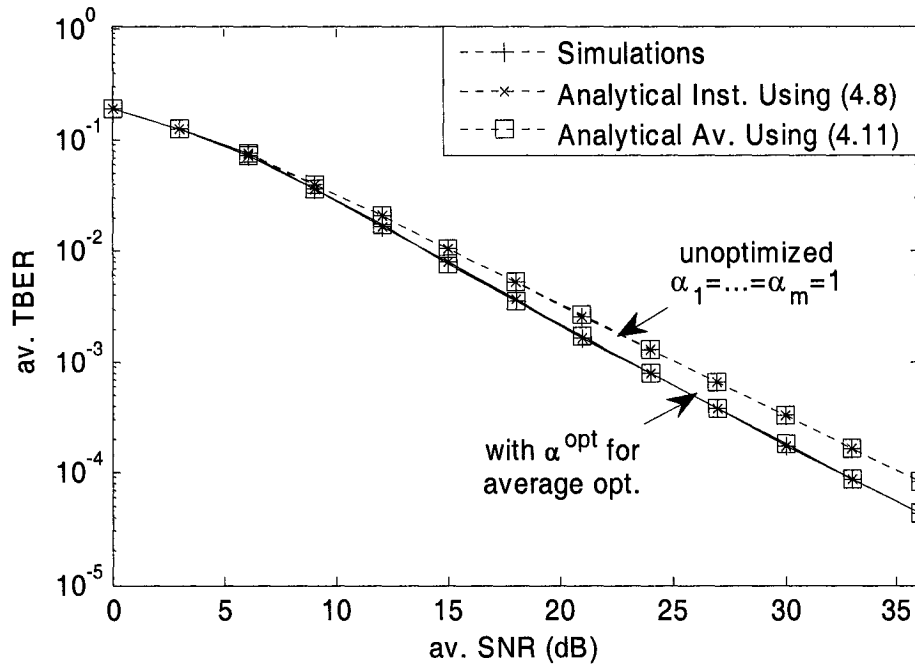


Fig. 4-1. TBER for 3×3 ZF-V-BLAST, analytical and simulated, number of Monte Carlo simulations gradually increasing with SNR up to $5 \cdot 10^6$, BPSK modulation, Rayleigh channel.

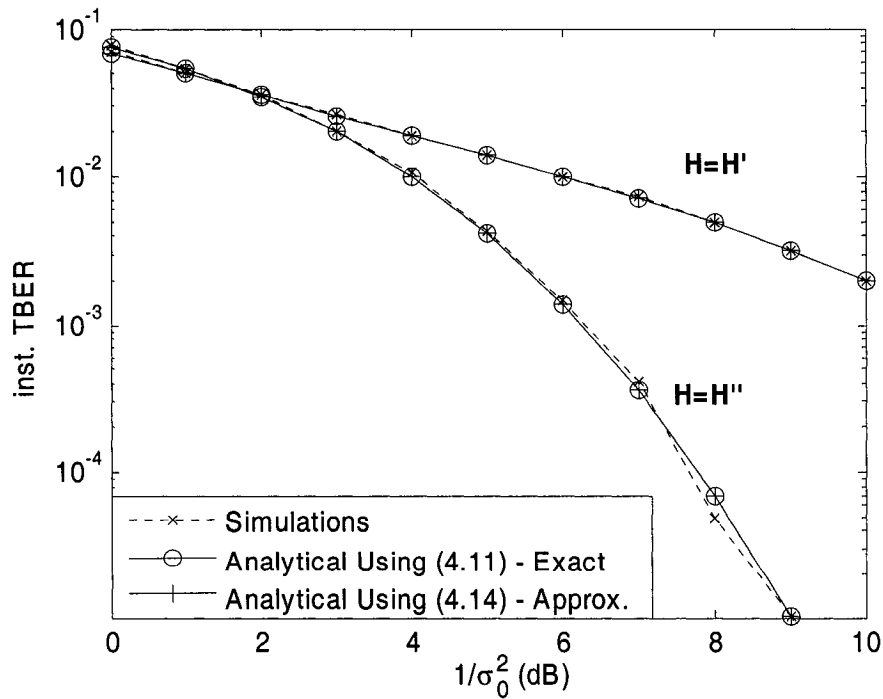


Fig. 4-2. Exact and approximate analytical instantaneous TBER compared to simulations, 3×3 ZF-V-BLAST with non-uniform power allocation given by (5.7), number of Monte-Carlo simulations 10^6 , BPSK modulation

4.3. AVERAGE ERROR RATES IN HIGH SNR REGION

An accurate high-SNR approximation of (4.2) for arbitrary fixed α can be obtained by approximating \bar{P}_{ei} and keeping only the leading term in each $\alpha_i\gamma_0$,

$$\begin{aligned}\bar{P}_B(\alpha) &\approx \sum_{i=1}^m \bar{P}_{ei} \approx \\ &\approx \sum_{i=1}^m \frac{C_{2i-1}^i}{(4\alpha_i\gamma_0)^{n-m+i}},\end{aligned}\quad (4.15)$$

Due to increasing diversity order with step number in unoptimized V-BLAST, $\alpha_1 = \alpha_2 = \dots = \alpha_m = 1$, the average BLER is well approximated by the first step BER [56],

$$\bar{P}_B \approx \bar{P}_{e1} \text{ for } \gamma_0 \gg 1, \quad (4.16)$$

As we demonstrate below, this approximation also holds for the optimized system (see Chapter 5).

Using (4.7), the high-SNR approximation of the average TBER for the unoptimized systems is as follows [56]:

$$\begin{aligned}\bar{P}_{ei} &\approx \frac{\bar{a}_1}{m} \bar{P}_{e1}, \\ \bar{a}_1 &= 1 + \bar{P}_{e2|2} + \sum_{i=3}^m \sum_{[e_2 \dots e_{i-1}]} \bar{P}_{ei|\tilde{\mathbf{E}}_{i-1}} \prod_{k=2}^{i-1} \Pr\{e_k | \tilde{\mathbf{E}}_{k-1}\}, \\ \bar{P}_{ei|\tilde{\mathbf{E}}_{i-1}} &\approx \bar{P}_{(n-m+i)}^{MRC} \left(|\tilde{\mathbf{E}}_{i-1}|^{-2} \right)\end{aligned}\quad (4.17)$$

where only the error patterns with an error at 1st step, $\tilde{\mathbf{E}}_{i-1} = [\pm 2, e_2 \dots e_{i-1}]$, are considered; \bar{a}_1 quantifies the contribution of the error propagation effect to the TBER and is independent of the average SNR. This expression will be instrumental in comparing the impacts of error propagation on the performance of the unoptimized and optimized systems. Since the 1st step BER has a dominant effect on the overall performance in the high SNR region, whether TBER or BLER is used as a performance criterion, it follows then that optimum power allocation algorithm should reduce the 1st step BER by

allocating most of the power to the 1st transmitter. As we demonstrate rigorously below, this is indeed the case.

For the optimized system at high SNR, the average TBER can be well approximated by using the high-SNR approximations of \bar{P}_{ei} (similarly to the average BLER approximation) and the approximated error propagation probability, $\bar{P}_{ei|\mathbf{E}_{i-1}} \approx 1/2$ if $|\mathbf{E}_{i-1}|^2 \neq 0$; see Chapter 5 for further details.

4.4.SUMMARY

The existent error rate expressions [54][56] of the unordered ZF-V-BLAST have been extended for the V-BLAST with non-uniform power allocation, so that they can be used as a tool for the power-optimization and the performance analysis of the optimized system. Exact instantaneous TBER has been derived in closed form. All novel error rate expressions have been validated through simulations.

5. Optimum Power Allocation

Under the total Tx power constraint, individual (per Tx or stream) powers can be optimally allocated in such a way as to minimize the TBER or the BLER, either instantaneous or average. While the instantaneous (i.e. for each channel realization) power allocation requires an instantaneous feedback in order to supply the Tx end with the optimum allocation for each channel realization, the average power allocation does not require instantaneous feedback (only the average⁸ SNR needs to be known at the Tx end) and hence does not incur significant penalty in complexity. A comparative analysis of the optimizations based on the BLER and the TBER, both instantaneous and average, is provided below.

The problem of optimum power allocation can be formulated as follows:

$$\text{minimize } P(\mathbf{\alpha}), \text{ subject to } \sum_{i=1}^m \alpha_i = m, \quad (5.1)$$

where P is the objective function equal to the BLER or the TBER, either instantaneous or average, whose argument is the power allocation coefficients $\mathbf{\alpha} = [\alpha_1, \alpha_2, \dots, \alpha_m]$ ⁹. For the unoptimized system (uniform power allocation), $\alpha_1 = \alpha_2 = \dots = \alpha_m = 1$.

5.1. UNIQUENESS OF THE SOLUTION

The optimization problem in (5.1) is a convex one and thus has a unique (global) solution when the BLER is used as the objective, $P(\mathbf{\alpha}) = P_B(\mathbf{\alpha})$ or $P(\mathbf{\alpha}) = \bar{P}_B(\mathbf{\alpha})$. This is the case not only for the BPSK but for a variety of modulation formats. For M-QAM, $M \geq 4$ modulation and $P(\mathbf{\alpha}) = \bar{P}_B(\mathbf{\alpha})$, the uniqueness of the solution has been demonstrated in

⁸ Over all channel realizations

⁹ It is also a function of γ_0 and, in the case of instantaneous optimization, of the instantaneous per-stream SNRs

[54]¹⁰ by noting that $\bar{P}_B(\boldsymbol{\alpha})$ is log-concave¹¹ as long as \bar{P}_{ei} is convex. In the case of the instantaneous BLER, $P(\boldsymbol{\alpha}) = P_B(\boldsymbol{\alpha})$, the uniqueness follows from the same argument. As demonstrated in [58], this result also extends, in a non-trivial way, to any 1-D or 2-D constellation, and also to some multi-dimensional constellations. The major results of [58] with application to the current problem are summarized below.

Theorem 5.1. P_{ei} is a convex function of the instantaneous SNR γ_i for any 1-D or 2-D constellation.

This covers such popular constellations as BPSK, BFSK, QPSK, QAM, M-PSK, OOK.

Theorem 5.2. For $N \geq 3$, where N is the constellation dimensionality, P_{ei} is convex in the large SNR mode,

$$\gamma_i \geq \frac{N + \sqrt{2N}}{d_{\min}^2} \quad (5.2)$$

where d_{\min} is the minimum distance to the boundary of the decision region among all constellation points (see Fig. 5-1).

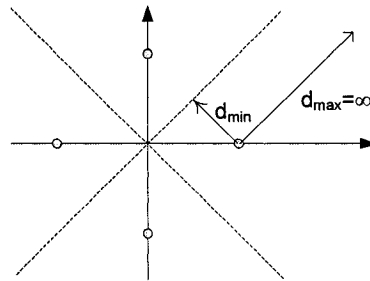


Fig. 5-1. Two-dimensional illustration of Theorem 2 geometry.

¹⁰ while QAM modulation has been considered in [54], the argument there holds true for BPSK modulation as well, by noting that $Q(\sqrt{\gamma})$ is a convex function. We note that this result also extends, in a non-trivial way, to any 1-D or 2-D constellation, and also to some multi-dimensional constellations [58][54].

¹¹ By definition, F is log-concave if $\log F$ is concave [13]

The idea behind the proof is as follows. The probability of correct decision is the integral of the probability density function (PDF) of the received signal over the correct decision region. Based on the fact that the decision regions of the minimum distance detector in AWGN channel are convex polyhedrons this integral can be bounded so that statements of theorems 1 and 2 follow. Detailed proofs are given in [58].

If (5.2) is not satisfied P_{ei} can have inflection points $P_{ei|Y_i}'' = 0$. One of the examples of non-convex P_{ei} is shown in Fig. 5-2.

Corollary. The optimization problem in (5.1) has a unique solution when instantaneous BLER is used as the objective, $P(\alpha) = P_B(\alpha)$ for any 1-D or 2-D constellation. It has a unique solution for any N-dimensional constellation, $N \geq 3$, if all instantaneous step SNRs satisfy (5.2).

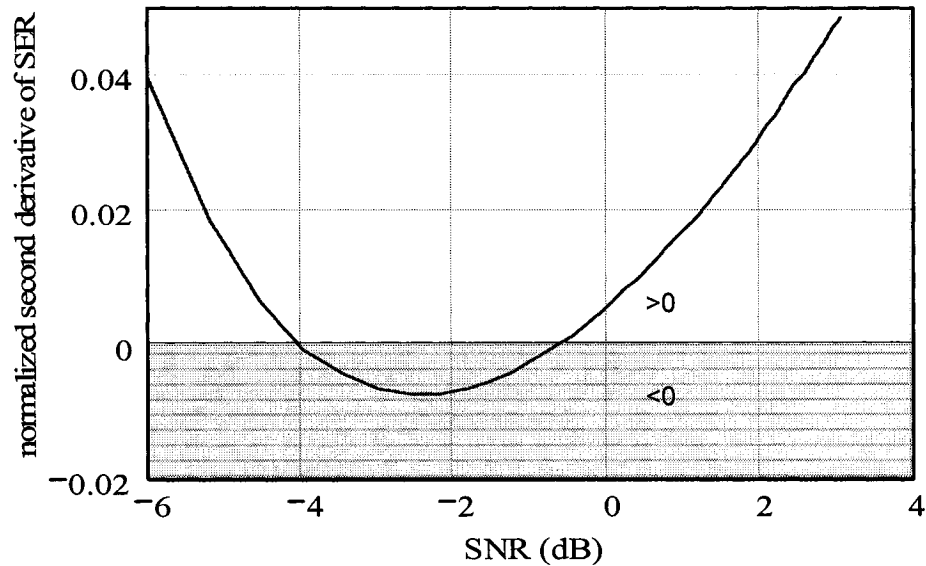


Fig. 5-2. Normalized closed-form second derivative (i.e. P_{ei}''/P_{ei}) of M-ary FSK SER in AWGN channel¹², M=50.

¹² Closed-form SER for M-ary FSK in AWGN channel can be found, for example, in [9]

Theorem 5.3. For any N-dimensional symmetric constellation (i.e. when the probability of error is the same for all constellation points), $1 - P_{ei}$ is log-concave in γ_i for any log-concave noise density (i.e. Gaussian, Laplacian, exponential, etc.).

The proof follows from the integration theorem for log-concave functions [13]

Corollary. The optimization problem in (5.1) has a unique solution when instantaneous BLER is used as the objective, $P(\mathbf{a}) = P_B(\mathbf{a})$, for any symmetric N-dimensional constellation.

This covers such popular modulation formats as N-ary orthogonal, biorthogonal and simplex signals.

Theorem 5.4. If the instantaneous BER P_{ei} is convex, the average BER \bar{P}_{ei} is convex for any fading (e.g. Rayleigh, Rice, Nakagami, log-normal, composite fading).

The proof follows from the convexity of the instantaneous BER and the observation that the fading PDF is nonnegative function.

Corollary. The optimization problem in (5.1) has a unique solution when average BLER is used as the objective, $F(\mathbf{a}) = \bar{P}_B(\mathbf{a})$, for any 1-D or 2-D constellation and any fading.

To sum up, the solution is unique in terms of average or instantaneous BLER for any 1-D or 2-D constellation. It is also unique in terms of instantaneous BLER for symmetric multi-dimensional constellations. This significantly simplifies the analysis since any found solution is automatically the global minimum.

If the instantaneous TBER is used as an objective, numerical results indicate that it can be non-convex, depending on a channel realization, i.e. some channel realizations produce convex $P(\mathbf{a}) = P_{et}(\mathbf{a})$, and some – non-convex one, so that the uniqueness of the

solution cannot be guaranteed. As an example, Fig. 5-3 shows the channel realization which produces the TBER with two minima, a local one and a global one.

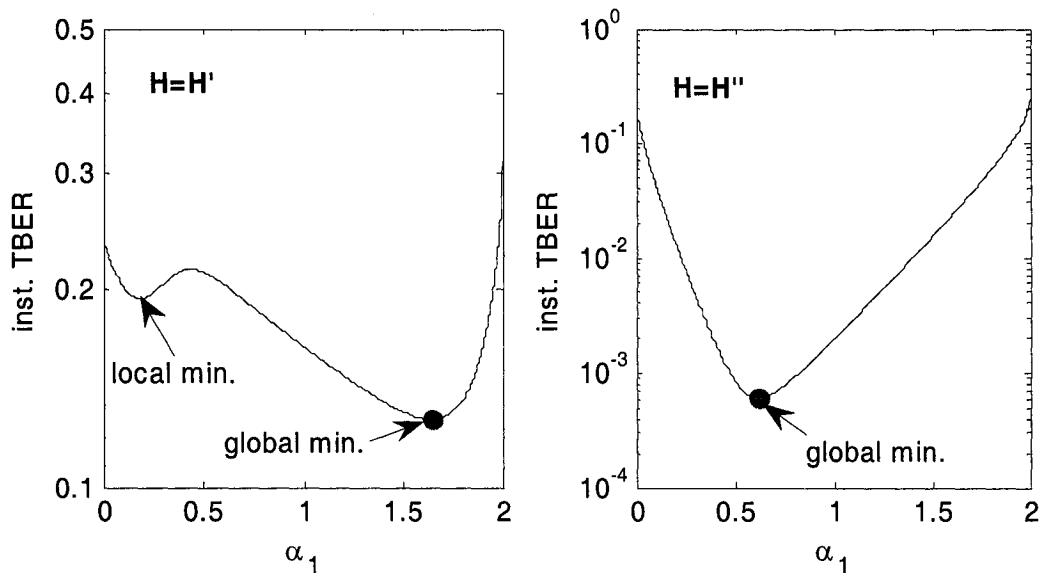


Fig. 5-3. Instantaneous TBER (for two different channel realizations) versus α_1 for 2×2 ZF-V-BLAST, BPSK modulation, SNR = 10 dB.

While the problem can be solved numerically, care should be taken when choosing a starting point in the numerical algorithm as it determines the particular local minimum that the algorithm will converge towards. It may also affect the convergence speed of the algorithm. In the case of average TBER, the uniqueness of the solution is an open problem. Extensive numerical evidence (see subsection) indicates that it is unique (i.e. only one global minimum). In the case of high average SNR, the uniqueness follows from the high-SNR approximation of the TBER which is convex (see subsection 5.4 for details).

5.2. INSTANTANEOUS POWER ALLOCATION

In this case, the best power allocation is found for each channel realization. Since an analytical solution is either not feasible or too complicated, with little insight available, a

numerical algorithm is used to minimize the instantaneous TBER (see (4.11), (4.6), (4.7)) or BLER (see (4.1)), subject to total power constraint, for every channel realization \mathbf{H} . Since instantaneous error rates expressions (4.1), (4.6), (4.7), (4.11) hold for both ZF and MMSE nulling vectors \mathbf{w}_i , both variants of V-BLAST can be optimized using this technique. Note that as P_{et} and P_{B} are functions of instantaneous per-channel SNRs, the instantaneous feedback of these SNRs is required. Fig. 5-4 plots the average TBER of optimized in this way MMSE-V-BLAST.

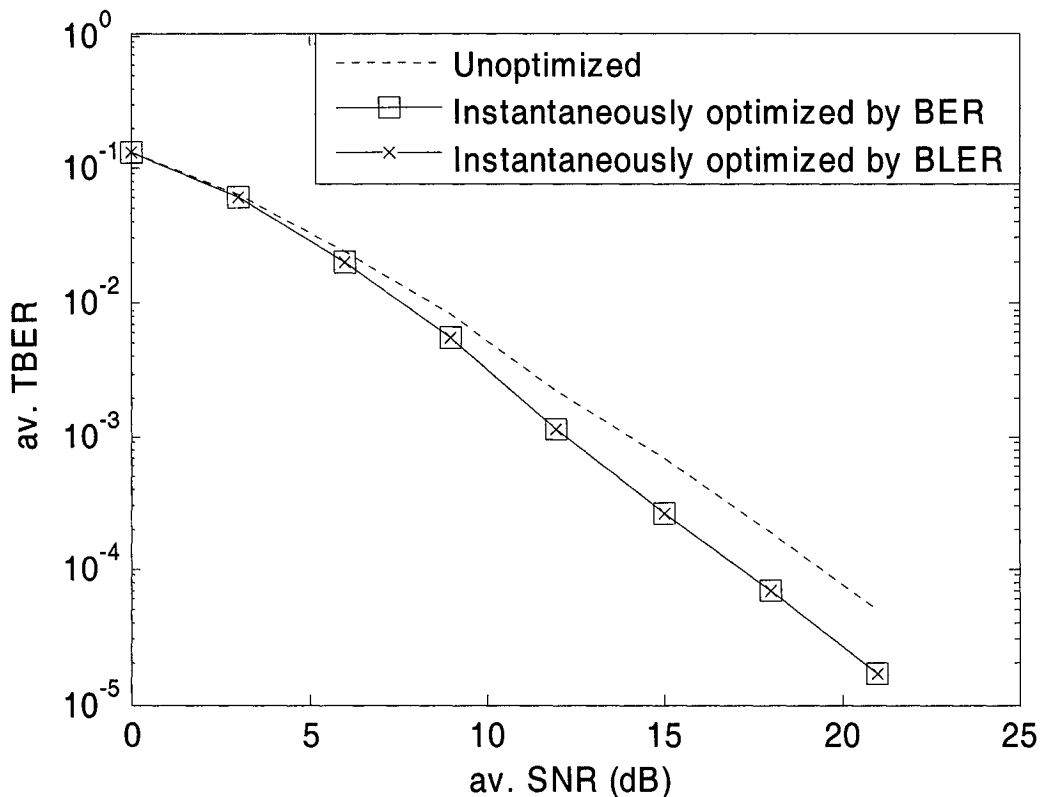


Fig. 5-4. TBER of 2x2 instantaneously optimized MMSE-V-BLAST with BPSK modulation.

As a numerical optimization algorithm, the MATLAB® implementation of Sequential Quadratic Programming (SQP) method (MATLAB function *fmincon* [15]) was used in this research. SQP closely mimics Newton's method for constrained optimization just as is done for unconstrained optimization. At each major iteration, the Hessian of the Lagrangian function is approximated using a quasi-Newton updating

method. This is then used to generate a subproblem whose solution is used to form a search direction for a line search procedure [15][16]. SQP methods represent the state of the art in nonlinear programming methods as they outperform other methods in terms of efficiency, accuracy, and percentage of successful solutions. In application to this research, termination tolerance values that are less than 10^{-8} have been experimentally shown to provide sufficient accuracy in finding the minimum of the instantaneous TBER/BLER (Fig. 5-3 – the dot at the curve indicates the solution found by the algorithm).

As indicated above, the optimum allocation in terms of the BLER is unique for a variety of modulation formats. This uniqueness facilitates numerical evaluation as there is only one global minimum and no local minima.

In the case of instantaneous TBER, the numerical algorithm converges to the local minimum which is the closest to the starting guess. The best strategy to insure that the global optimum is found for most of the channel realizations is to use several starting points which produce several local minima and choose the best one among them (curve labeled “min” in Fig. 5-5). Unfortunately this method has high computational complexity as it requires several runs of the numerical optimization algorithm for each channel realization. To save the processing power, it is desirable to stick to one starting point which finds the global optimum in most cases. According to Fig. 5-5, $\alpha_0 = [1,1]$ ranks the best among the starting points tested. For this reason, the uniform power allocation is used as a starting guess for numerical optimization throughout this work.

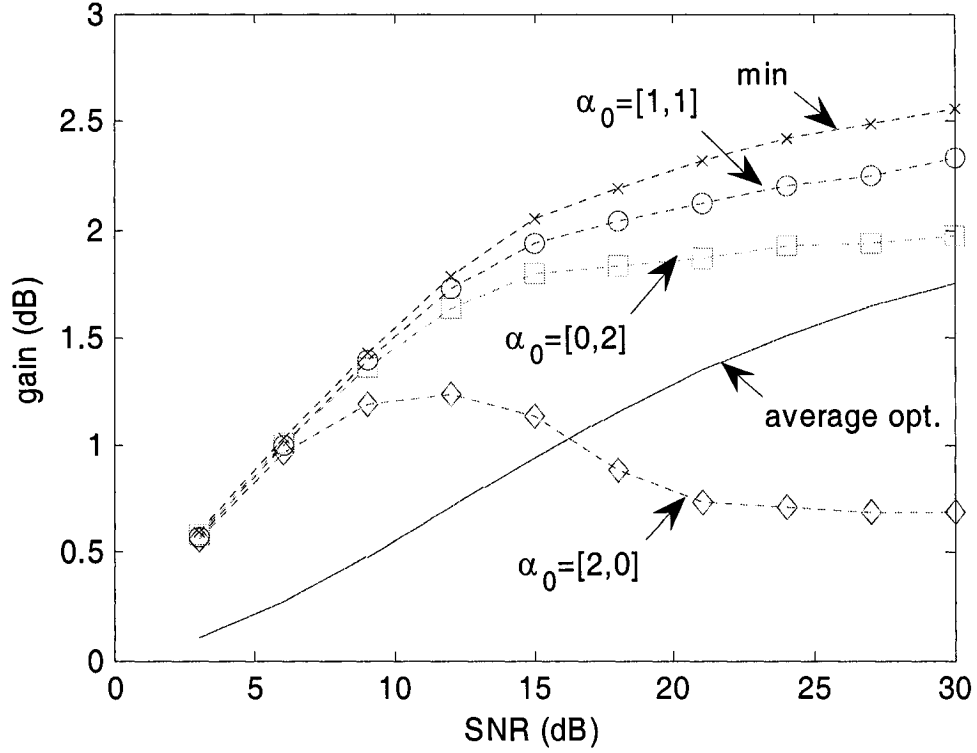


Fig. 5-5. SNR Gain for various starting points for numerical optimization, 2x2 ZF-V-BLAST, BPSK modulation.

5.3. OPTIMUM POWER ALLOCATION USING THE AVERAGE BLER

In this case, the average BLER is the objective function in (5.1), $P(\mathbf{a}) = \bar{P}_B(\mathbf{a})$.

Using the Lagrange multiplier technique for constrained optimization with the following Lagrangian,

$$L(\mathbf{a}) = \bar{P}_B(\mathbf{a}) + \lambda \left(\sum_{i=1}^m \alpha_i - m \right), \quad (5.3)$$

the optimum \mathbf{a} are found from

$$\partial L(\mathbf{a}) / \partial \alpha_i = \partial \bar{P}_B(\mathbf{a}) / \partial \alpha_i + \lambda = 0, \quad i = 1 \dots m \quad (5.4)$$

where $\lambda \geq 0$ is the Lagrange multiplier, which is found from the total power constraint,

$\sum_{i=1}^m \alpha_i(\lambda) = m$, i.e. (5.4) and the constraint are considered together as a system of

equations¹³. Since the objective is convex, the solution is the global minimum. Using (4.2) and after some manipulations, (5.4) reduces to,

$$\frac{\partial \ln(1 - \bar{P}_{ei})}{\partial \alpha_i} = -\frac{1}{1 - \bar{P}_{ei}} \frac{\partial \bar{P}_{ei}}{\partial \alpha_i} = \frac{\lambda}{1 - \bar{P}_B}, \quad i = 1 \dots m \quad (5.5)$$

Note that the optimality conditions (5.5) do not require all \bar{P}_{ei} be equal; rather, their normalized derivatives should be equal. Unfortunately, (5.5) together with the total power constraint is a system of nonlinear transcendental equations, which in general cannot be solved analytically in closed form. Thus, some approximations are required.

For high SNR, $\bar{P}_{ei}, \bar{P}_B \ll 1$, and (5.5) can be approximated as

$$\frac{\partial \ln(1 - \bar{P}_{ei})}{\partial \alpha_i} \approx -\frac{\partial \bar{P}_{ei}}{\partial \alpha_i} \approx \lambda, \quad i = 1 \dots m \quad (5.6)$$

so that the optimality requires all the derivatives $\partial \bar{P}_{ei} / \partial \alpha_i$ be equal, which is what one would intuitively expect based on the total power constraint.

A compact and accurate analytical solution of (5.6) can be obtained using the Newton-Raphson method and the approximation in (4.15) (see Appendix A.1 for details):

$$\alpha_i^{opt} \approx \frac{m \tilde{\alpha}_i}{\sum_{k=1}^m \tilde{\alpha}_k}, \quad (5.7)$$

$$\tilde{\alpha}_i \approx \frac{b_i}{(4\gamma_0)^{n-m+i+1}} \left(1 - \frac{b_2}{m c_1^{n-m+3} \sqrt[3]{4\gamma_0}} \right)^{c_i},$$

where the numerical coefficients b_i, c_i are given by

$$b_i = \frac{(n-m+i) m^{n-m+2} C_{2i-1}^i}{n-m+1}, \quad (5.8)$$

$$c_i = \frac{(n+1)!}{(n-m+1)!(n-m+i+1)}$$

¹³ strictly speaking, an additional constraint $\alpha_i \geq 0, i = 1 \dots m$, is required. However, since the solutions obtained always satisfy it, it is not included explicitly.

The first equality in (5.7) assures the total power constraint holds for the approximated allocation. Noting that $b_1 = m$, (5.7) can be further approximated as,

$$\begin{aligned}\alpha_1^{opt} &\approx m - \sum_{i=2}^m \alpha_i^{opt}, \\ \alpha_i^{opt} &\approx \frac{b_i}{(4\gamma_0)^{\frac{i-1}{n-m+i+1}}}, \quad i = 2, \dots, m,\end{aligned}\tag{5.9}$$

i.e. almost all the power goes to the 1st Tx as $\gamma_0 \rightarrow \infty$, and α_1^{opt} is quite close to m for finite but large γ_0 . Referring to (4.16), this is explained by the fact that 1st step has lowest diversity order ($n-m+1$) and hence its error rate dominates. The power allocation algorithm tries to reduce the BLER by allocating more power to the 1st stream and thus reducing the 1st step BER. Fig. 5-6 compares the approximate solutions above with the accurate numerical ones. It should be noted that while the approximation in (5.7) is more accurate, the approximation in (5.9) is simpler and more insightful. As Fig. 5-7 demonstrates, (5.7) yields the same gain¹⁴ as numerical optimization already for $\gamma_0 \geq 5dB$, and (5.9) approaches numerical optimization results at higher SNR. Hence (5.7) can be used instead of numerical optimization for the whole range of practical SNR, while (5.9) is instrumental in asymptotic analysis.

Example: the optimum power allocation for the 2×2 V-BLAST in terms of the average BLER,

$$\alpha_1^{opt} \approx 2 - \alpha_2^{opt}, \quad \alpha_2^{opt} \approx \sqrt[3]{6/\gamma_0},\tag{5.10}$$

As expected, optimization reduces the dominating 1st step BER,

$$\bar{P}_{el}^{opt} \approx 1/(8\gamma_0),\tag{5.11}$$

¹⁴ The *SNR gain of optimum power allocation* is defined as the difference in SNR required to achieve the same error rate in the optimized and unoptimized systems, see Chapter 7 for further details

if compared to the unoptimized one, $\bar{P}_{e1} = 1/(4\gamma_0)$ [56]. The low power allocated to the 2nd transmitter, α_2^{opt} , however, results in decreased diversity order at the 2nd step,

$$\bar{P}_{e2}^{opt} \approx \frac{3}{(4\alpha_2^{opt}\gamma_0)^2} \approx \frac{3}{16\sqrt[3]{36}\gamma_0^{4/3}}, \quad (5.12)$$

so that the optimized 2nd step BER is higher compared to that of the un-optimized system, $\bar{P}_{e2}^{opt} \gg \bar{P}_{e2} \approx 3/(4\gamma_0)^2$. The 1st step BER is therefore reduced at the price of increased 2nd step BER, but the dominant effect of 1st step BER is still preserved in the V-BLAST with optimum power allocation, since $\bar{P}_{e1}^{opt} \sim \bar{P}_{e2}^{opt}$ in high SNR region. However, this region is achieved at significantly higher SNR ($\sqrt[3]{\gamma_0} \gg 1$) compared to the un-optimized system ($\gamma_0 \gg 1$). Note also that \bar{P}_{e2}^{opt} exhibits a fractional diversity order.

In general, in the unoptimized V-BLAST step i exhibits $(n-m+i)$ -th order diversity, $\bar{P}_{ei} \sim (1/\gamma_0)^{n-m+i}$. In the optimized V-BLAST, step i has fractional diversity order,

$$\bar{P}_{ei}^{opt} \sim (1/\gamma_0)^{(n-m+2)\left(1-\frac{1}{n-m+i+1}\right)}, \quad (5.13)$$

but the diversity order still increases with the step number. Hence, high SNR approximations of the total BLER (4.15), (4.16) which were derived for a *fixed* power allocation, are applicable to the V-BLAST with *optimum* power allocation in which \mathbf{a} is a function of SNR. Using (5.9), (4.16), the average optimized BLER can be approximated as,

$$\bar{P}_B(\mathbf{a}^{opt}) \approx \frac{1}{(4m\gamma_0)^{n-m+1}} \quad (5.14)$$

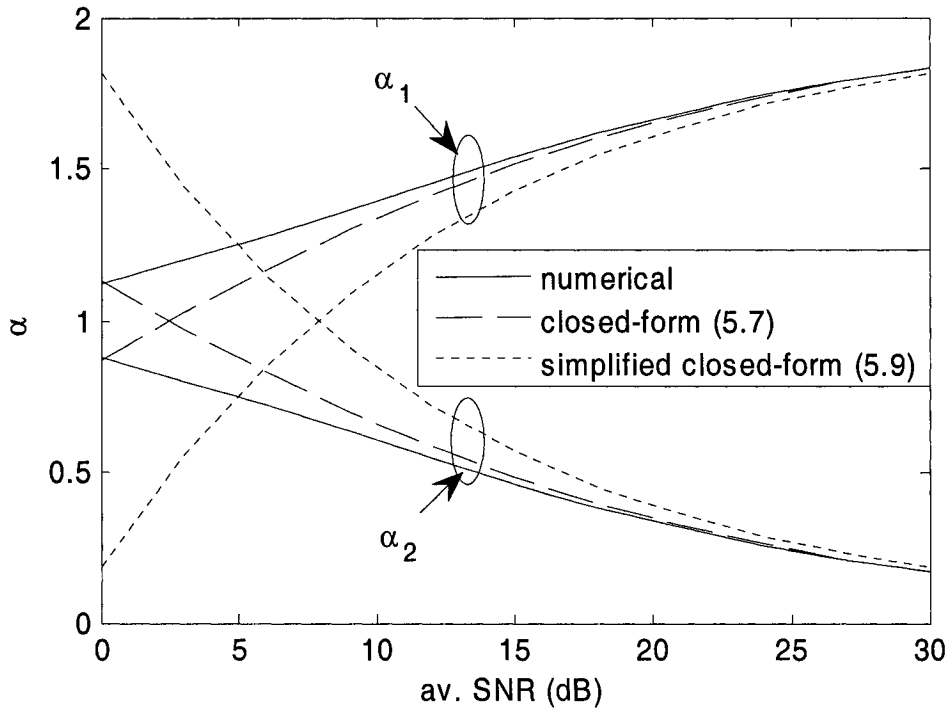


Fig. 5-6. Closed-form power allocation by (5.7) and (5.9) with b_i given by (5.8), 2x2 ZF-V-BLAST with BPSK modulation.

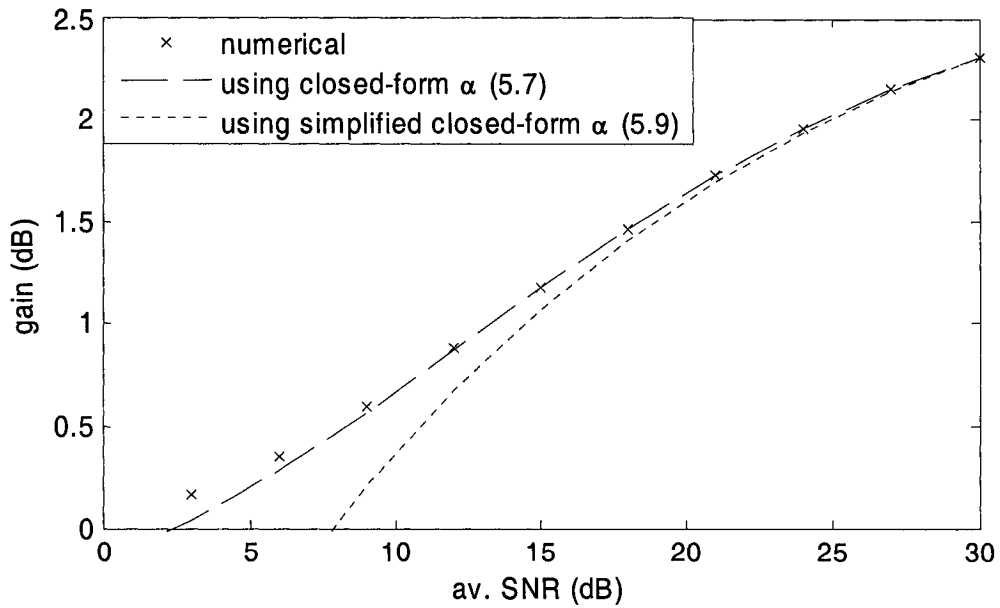


Fig. 5-7. SNR Gain of optimization by BLER using closed-form power allocation (5.8) and (5.9) with b_i given by (5.8), 2x2 ZF-V-BLAST, BPSK modulation.

5.4. OPTIMUM POWER ALLOCATION USING THE AVERAGE TBER

Similarly to the BLER-based optimization, the average TBER can be used in (5.3) as an objective function in the Lagrange multiplier technique to find the optimum power allocation. As it was indicated above, the average TBER is convex in α at high SNR; numerical evidence also suggests that it is convex at low to moderate SNR. Hence, the optimum power allocation is unique for arbitrary SNR. Closed-form analytical solution is not feasible due to the complexity of the problem¹⁵, but since the problem is convex, efficient numerical algorithms can be employed to solve it [13]. At high SNR mode, an accurate approximate closed-form solution can be obtained using the Newton-Raphson method. As in the case of BLER-based optimization, the 1st step BER has the dominant effect on the overall performance [56], and hence the optimization algorithm will have to reduce the 1st step BER by allocating most of the power to the first transmitter, i.e. $\alpha_1^{opt} \rightarrow m$, $\alpha_2^{opt}, \dots, \alpha_m^{opt} \rightarrow 0$ as $\gamma_0 \rightarrow \infty$. Therefore, for the V-BLAST with “close to optimum” power allocation at high SNR, γ_i^{eff} , $i = 2, \dots, m$, are small, and the probability of error propagation can be approximated as¹⁶

$$\bar{P}_{ei|\mathbf{E}_{i-1}} \approx \bar{P}_{(n-m+i)}^{MRC}(0) = 1/2 \text{ if } |\mathbf{E}_{i-1}|^2 \neq 0 \quad (5.15)$$

Using this, (4.7) can be approximated as

$$\begin{aligned} \bar{P}_{et}(\alpha) &\approx \frac{1}{2m} \sum_{i=1}^m (m-i+2) \bar{P}_{ei} \approx \\ &\approx \frac{1}{2m} \sum_{i=1}^m \frac{(m-i+2) C_{2i-1}^i}{(4\alpha_i \gamma_0)^{n-m+i}} \end{aligned} \quad (5.16)$$

The solution is similar to that for the BLER-based optimization, so that (5.7),(5.9) can be used with b_i given by (see Appendix A.1 for details):

¹⁵ As in the previous case, the Lagrange equations are the system of non-linear transcendental equations

¹⁶ For unoptimized system (5.15) is not applicable since in that case $\gamma_i^{eff} \approx 1/|\mathbf{E}_{i-1}|^2$ rather than 0 [56]

$$b_i = n-m+i+1 \sqrt{\frac{C_{2i-1}^i (n-m+i)(m-i+2)m^{n-m+2}}{(m+1)(n-m+1)}}, \quad (5.17)$$

but, as before, $b_1 = m$, which means that almost all the power goes to the 1st Tx at high SNR. The difference in the solution for the BLER and TBER-based optimizations is due to the fact that, in the latter case, the error propagation gives a contribution which does not appear in the former case. Since the probability of error propagation is small [56], this difference in the solutions is not large, as demonstrated below.

As before, the approximate solutions (5.7) are already accurate for intermediate to large SNR, $\gamma_0 \geq 5dB$ (see Fig. 5-8, Fig. 5-9). Moreover, as Fig. 5-10, Fig. 5-11 demonstrate, the BLER and TBER-based optimum power allocations are very close to each other and hence the choice of the optimization criteria does not affect significantly the final result. This is not a surprise as the 1st step error rate is dominant, due to the lowest diversity order, in terms of both the average BLER and TBER and hence most of the total power goes to the 1st transmitter, regardless of the criterion.

Similarly to the BLER-based optimization, fractional diversity order increasing with the step number is observed according to (5.13). Using (5.16) and (5.9), the average optimized TBER is,

$$\bar{P}_{et}(\mathbf{\alpha}^{opt}) \approx \frac{m+1}{2m} \frac{1}{(4m\gamma_0)^{n-m+1}} \quad (5.18)$$

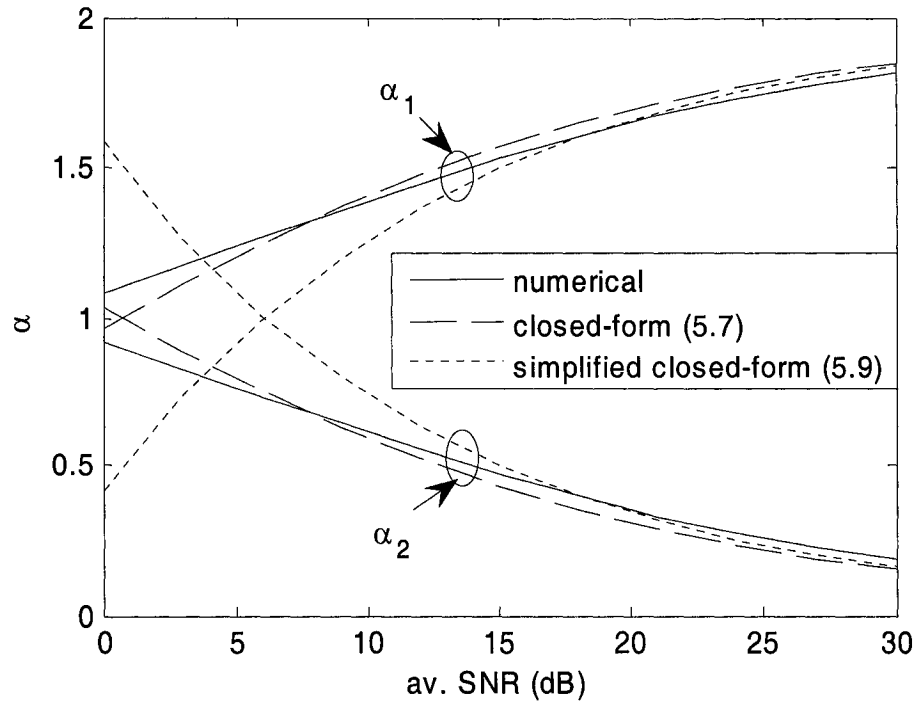


Fig. 5-8. Closed-form power allocation by (5.7) and (5.9) with b_i given by (5.17), 2x2 ZF-V-BLAST with BPSK modulation.

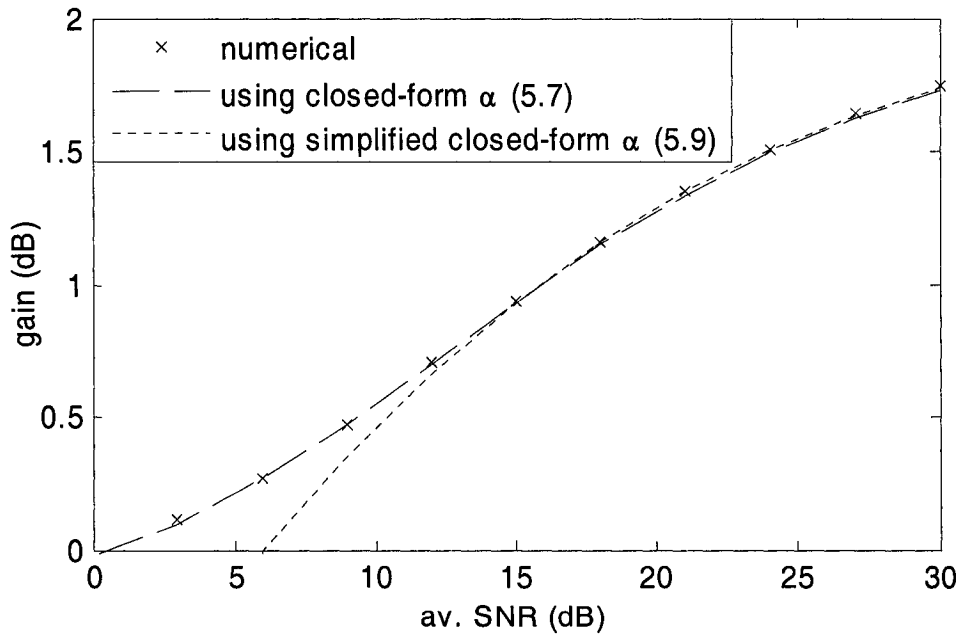


Fig. 5-9. SNR Gain of optimization by TBER using closed-form power allocation (5.8) and (5.9) with b_i given by (5.17), 2x2 ZF-V-BLAST, BPSK modulation.

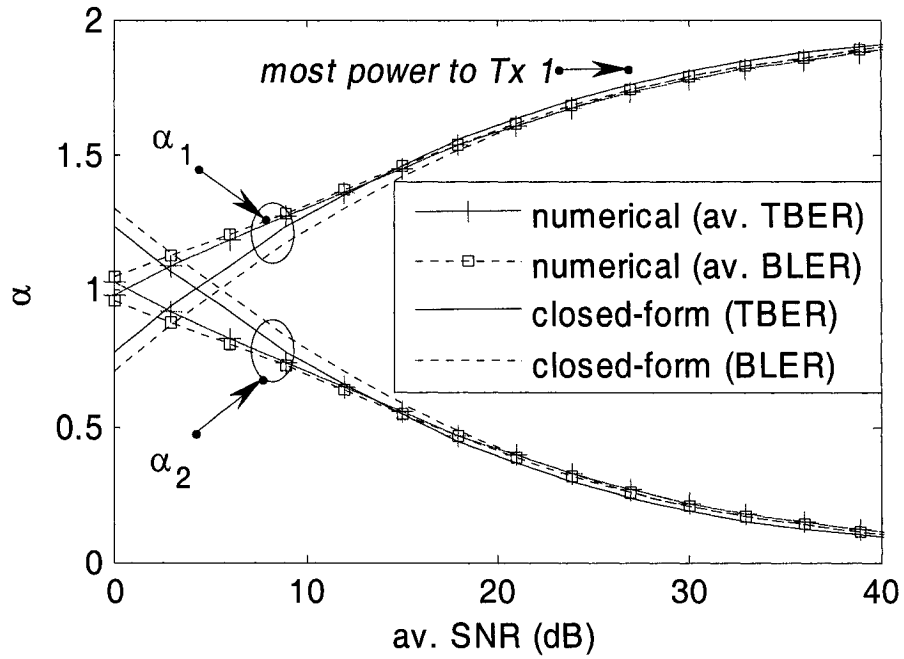


Fig. 5-10. Optimum power allocation for 2x2 ZF-V-BLAST with BPSK modulation for various optimization strategies.

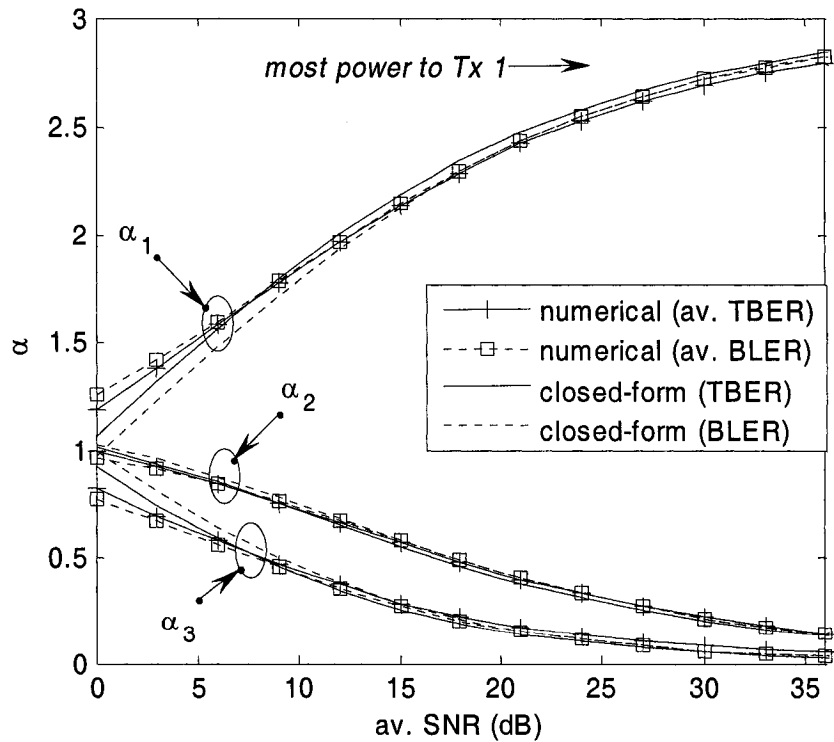


Fig. 5-11. Optimum power allocation for 3x3 ZF-V-BLAST with BPSK modulation for various optimization strategies.

5.5. INSTANTANEOUS VS. AVERAGE POWER ALLOCATION

The average TBER of instantaneous and average power optimizations is shown on Fig. 5-12, Fig. 5-13. Clearly, the results are quite close to each other, especially for $\gamma_0 \geq 20dB$. Essential difference between these two is that the instantaneous optimization performs better in terms of instantaneous TBER, especially for some channel realizations that do not favor the average power allocation. However, the cost of using the instantaneous optimization is higher as each channel instant requires its own optimization and feedback session. On the other hand, the average optimization requires only one computation of α^{opt} as long as the average SNR stays the same. Furthermore, no computationally-expensive numerical optimization is required as the approximate expressions above provide good accuracy, and only γ_0 needs to be fed back to the transmitter. The main conclusion here is that the average power optimization can be used instead of instantaneous one at high SNR without any visible penalty in the average error rate, but with much smaller complexity.

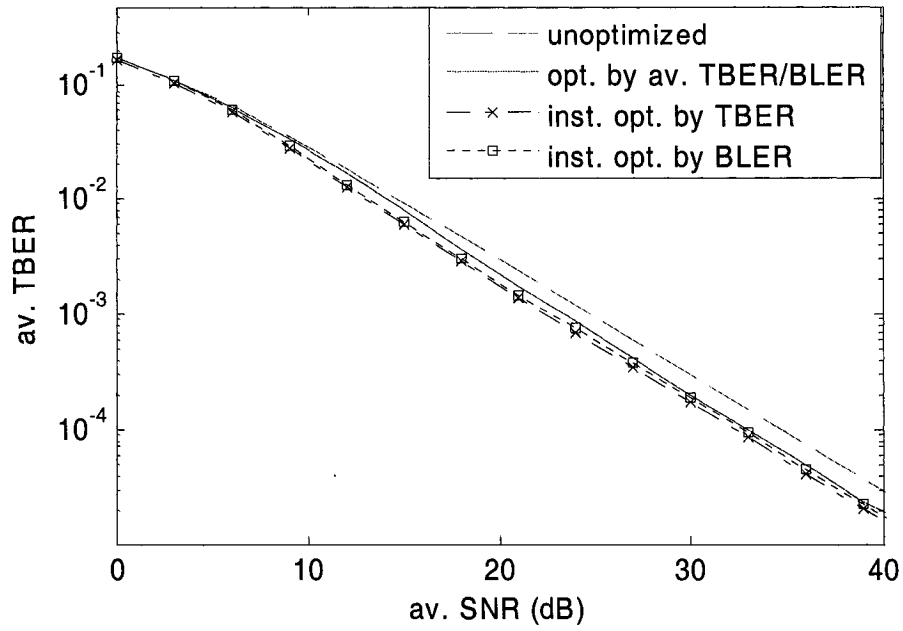


Fig. 5-12. TBER of 2x2 ZF-V-BLAST with BPSK modulation for various optimization strategies.

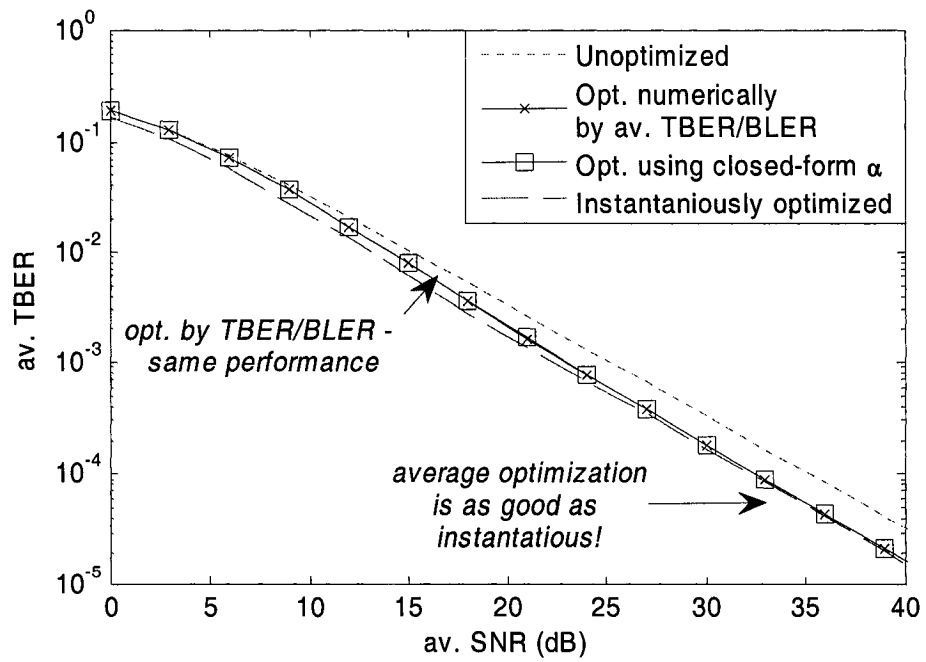


Fig. 5-13. TBER of 3x3 ZF-V-BLAST with BPSK modulation for various optimization strategies.

5.6.SUMMARY

Optimum power allocation techniques based on various criteria, i.e. average and instantaneous block and total error rates, have been studied. Compact closed form solutions have been derived for the optimum power allocation based on average BLER and TBER. Due to the dominant contribution of lower steps to the error rate, these steps get more power in the optimized system, with the 1st step getting most of it. The power allocation strategies based on the average BLER and TBER are almost the same, since in both cases 1st step is dominant in terms of the average error rate.

The error rate performance of the optimized system has been investigated; closed-form expressions for optimized error rates at high SNR have been obtained. Despite the non-uniform power allocation in the optimized system, 1st step still dominates in terms of the error rate. Conditional error rates of the higher steps exhibit fractional diversity order. While the instantaneous optimization requires instantaneous feedback and thus is more complex than the average one, which requires only the average SNR be fed back to the transmitter, its average error rate performance is only slightly better than that of the average optimization. At high SNR, both strategies exhibit the same average error rate.

BLER and TBER-based optimization strategies have been shown to result in the same performance improvement. BLER is a preferable choice of optimization criterion due to the especial simplicity of its analytical expressions, and also because the BLER-based optimization problem has been shown to have a unique solution for a variety of modulation formats in any fading channel, which facilitates numerical optimization.

6. Robustness of the Optimum Power Allocation

When the optimization algorithm is implemented in a practical system, there are various sources of inaccuracies and disturbances, which may affect its performance but which were ignored in the idealistic analysis of the previous chapter. These may include numerical inaccuracies of the optimization (due to, for example, using fixed point arithmetic devices, various approximations, etc.), inaccurate or outdated estimate of the average SNR etc., which result in inaccuracies in the optimum power allocation coefficients. A robust algorithm, which is insensitive to all of these factors, is desired from the practical perspective.

In order to estimate the impact of these factors on the system performance, let us introduce the measure of robustness δ (sensitivity) of the average optimized error rate (either BLER or TBER), $\bar{P} = \bar{P}(\mathbf{\alpha}^{opt})$, to the changes in some system parameter u ,

$$\delta = \left| \frac{\Delta \bar{P} / \bar{P}}{\Delta u / u} \right|. \quad (6.1)$$

where u may represent the total Tx power, $u = \sum_{i=1}^m \alpha_i$, or the power allocated to any of the transmitters, $u = \alpha_i$. The measure of robustness (6.1) is the ratio of the normalized variation in the performance $\Delta \bar{P} / \bar{P}$ to the normalized variation in the system parameter $\Delta u / u$, which causes this performance variation. Note that the use of normalized differences in the definition is essential as it makes the measure to be independent of the scale. The algorithm is robust to variations in the system parameter u if relatively small change in u leads to relatively small change in the error rate \bar{P} , i.e. when δ is small or moderate number.

6.1. LOCAL ROBUSTNESS

When both the perturbation in the system parameter Δu and in the system performance $\Delta \bar{P}$ are small enough, one can use the derivatives in (6.1) instead of the finite differences,

$$\delta \approx \delta' = \left| \frac{\partial \bar{P}}{\partial u} \frac{u}{\bar{P}} \right|, \quad (6.2)$$

so that $\partial \bar{P} / \partial u$ determines the algorithm robustness, and δ' serves as a measure of local robustness. If u is power allocated to any of the transmitters, $\partial \bar{P} / \partial u$ is found from (5.4)

as $\partial \bar{P} / \partial \alpha_i = -\lambda$. If u is the total Tx power,

$\partial \bar{P} / \partial u = \sum_{i=1}^m \partial \bar{P} / \partial \alpha_i \cdot \partial \alpha_i / \partial u = -\lambda \sum_{i=1}^m \partial \alpha_i / \partial u = -\lambda$, the last equality following from

differentiating the total power constraint, $\sum \partial \alpha_i / \partial u = 1$. Therefore, in both cases

$\partial \bar{P} / \partial \alpha_i = \partial \bar{P} / \partial u = -\lambda$, so that

$$\delta \approx \delta' = \frac{\lambda u}{\bar{P}} \quad (6.3)$$

Thus, the Lagrange multiplier λ , evaluated at the optimum point and appropriately normalized, is the measure of local sensitivity¹⁷ of the average error rate to variations in the total or individual Tx power. The normalized variation in the average error rate can be evaluated from the normalized variation in the system parameter using (6.3),

$$\frac{|\Delta \bar{P}|}{\bar{P}} = \delta \frac{|\Delta u|}{u} \approx \delta' \frac{|\Delta u|}{u}, \quad (6.4)$$

For the BLER-based optimization at high SNR, the Lagrange multiplier can be approximated as (see Appendix A.1),

$$\lambda \approx \frac{n-m+1}{m} \frac{1}{(4m\gamma_0)^{n-m+1}}, \quad (6.5)$$

¹⁷ an extended discussion of this issue in the general framework can be found in [13]

the average optimized BLER is given by (5.14). If the system parameter u is the total or the 1st transmitter power and its variations are small, substituting $u \approx \alpha_1 \approx m$, (5.14) and (6.5) into (6.3), one obtains the robustness measure with respect to the variations in the total or 1st transmitter power as

$$\delta_1' \approx n - m + 1, \quad (6.6)$$

i.e. equal to the diversity order of the system. The algorithm is locally robust as long as $(n - m)$ is not too large; $\delta_1' \approx 1$ and consequently $\Delta\bar{P}/\bar{P} \approx -\Delta u/u$ if $n = m$. This result is a consequence of the fact that the high-SNR average BLER is dominated by the 1st step BER (see (5.14)) so that its diversity order and hence the sensitivity to the Tx power is minimum when $n = m$; increasing $(n - m)$ results in increasing diversity order and hence in increasing sensitivity to the Tx power. Thus, the beneficial effect of higher diversity order with more Rx antennas is accompanied by the negative effect of higher sensitivity to variations in system parameters.

The robustness measure with respect to $\alpha_2 \dots \alpha_m$ is found by substituting (5.9), (5.14) and (6.5) into (6.3):

$$\delta_i' \approx \frac{n - m + 1}{m} \frac{b_i}{(4\gamma_0)^{\frac{i-1}{n-m+1+i}}} \square 1, \quad i = 2 \dots m, \quad (6.7)$$

where b_i is given by (5.8). Thus, the algorithm is also robust in terms of $\alpha_2, \dots, \alpha_m$ at high SNR. Furthermore, higher steps exhibit better robustness since, comparing (6.6) and (6.7), $\delta_1' > \delta_i'$, $i = 2 \dots m$. It should be noted that this robustness of the algorithm is a “free bonus”, which was not a goal of the original design.

For the TBER-based optimization, the Lagrange multiplier can be approximated at high SNR as (see Appendix A.1),

$$\lambda \approx \frac{(m+1)(n-m+1)}{2m^2} \frac{1}{(4m\gamma_0)^{n-m+1}}, \quad (6.8)$$

and, from (4.15), (4.16), (5.9), the average optimized TBER is,

$$\bar{P}_{et}(\mathbf{\alpha}^{opt}) \approx \frac{m+1}{2m} \frac{1}{(4m\gamma_0)^{n-m+1}} \quad (6.9)$$

As before, the robustness measure is given by (6.6) and (6.7), only b_i are now taken from (5.17). Hence the conclusions above hold true for TBER as well.

Fig. 6-1-Fig. 6-2 compare approximations (6.3), (6.6)-(6.7) with the exact robustness measures computed from (6.1), for BLER- and TBER-based optimization, accordingly. Clearly (6.6)-(6.7) give good estimate of δ' for $\gamma_0 \geq 10$ dB. For $\gamma_0 < 10$ dB they represent conservative estimates, the actual robustness being better than predicted by (6.6)-(6.7).

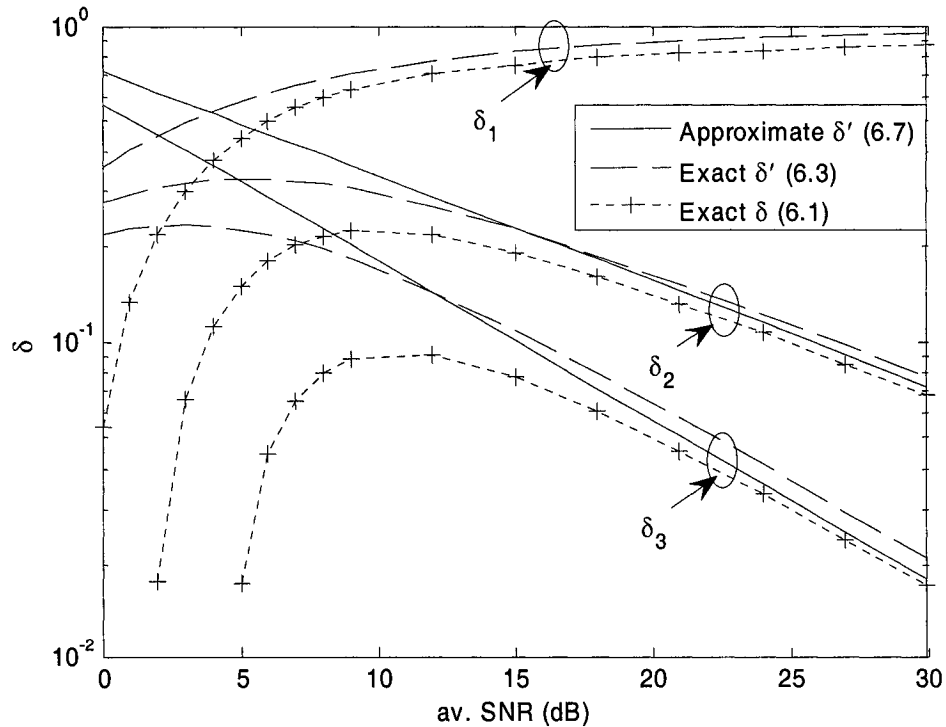


Fig. 6-1. The robustness measure of the BLER-based optimization with respect to the variations in $\alpha_1 \dots \alpha_m$, exact and approximate, versus SNR for 3×3 ZF-V-BLAST, BPSK modulation, $\Delta u/u = 10\%$.

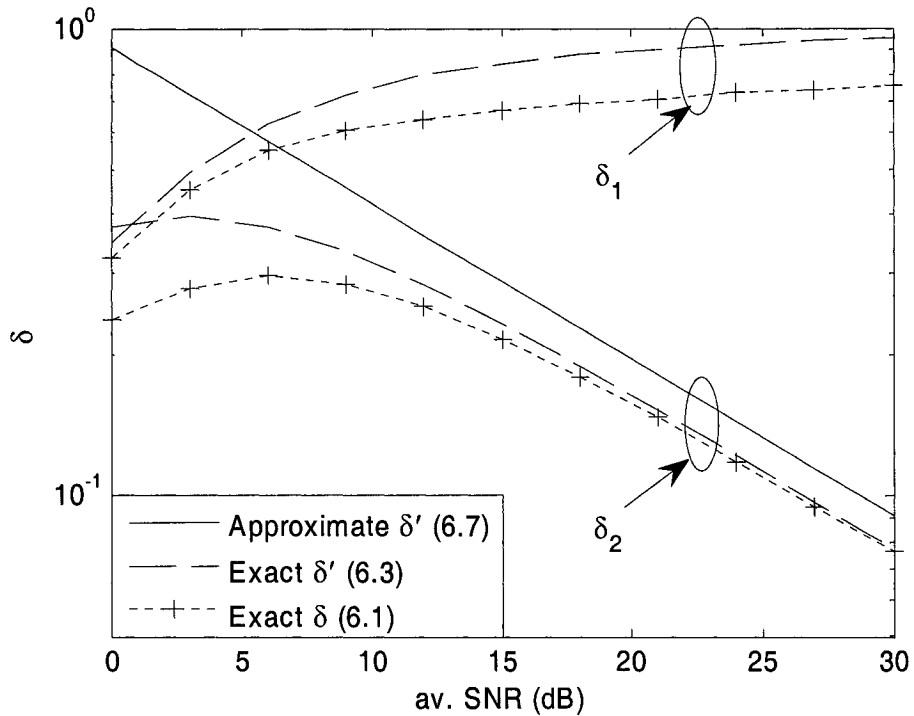


Fig. 6-2. The robustness measure of the TBER-based optimization with respect to the variations in $\alpha_1 \dots \alpha_m$, exact and approximate, versus SNR for 2×2 ZF-V-BLAST, BPSK modulation, $\Delta u/u = 20\%$

As an illustration of robustness of the TBER to small changes in α_1 , Fig. 6-3 shows the average TBER versus α_1 for 2×2 V-BLAST. When α_1 is far away from α_1^{opt} , the slope of the curves is quite steep and determined by the diversity order of the dominating step; thus, allocating too little power to the 1st Tx increases the 1st step BER, making it dominant, whereas giving too much power to the 1st Tx boosts the 2nd step BER. Note that the slope is steeper in the domain of the dominating 2nd step BER, apparently because of its greater diversity order. But as the power allocation algorithm attempts to balance these two extremes and approaches α_1^{opt} , the curves become very flat, confirming local (in the vicinity of α_1^{opt}) insensitivity of the TBER to variations in α_1 . The same conclusions hold for greater number of Tx antennas (Fig. 6-4) as well as BLER-based optimization (Fig. 6-5, Fig. 6-6).

Note that the instantaneous error rates are not robust to the changes in system parameters, at least for some channel realizations (see Fig. 5-3). This is because of the exponentially-decaying behavior of the Q-function, which makes the instantaneous TBER sensitive to changes in α .

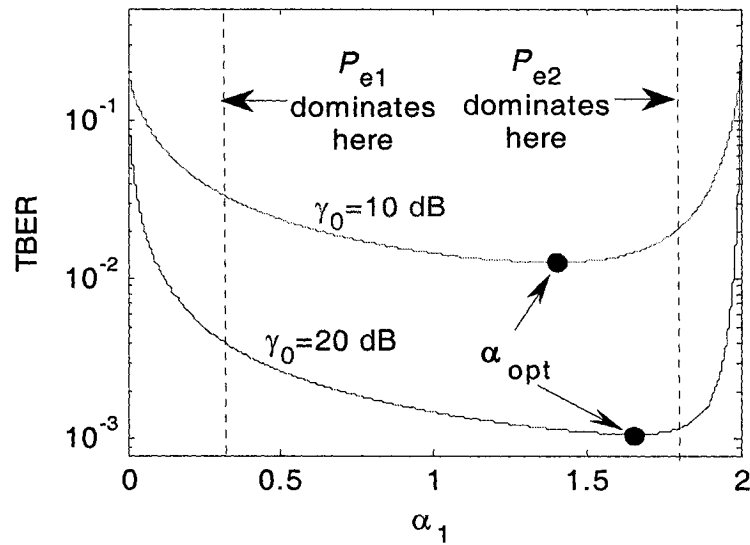


Fig. 6-3. Average TBER versus α_1 for 2x2 ZF-V-BLAST with BPSK modulation.

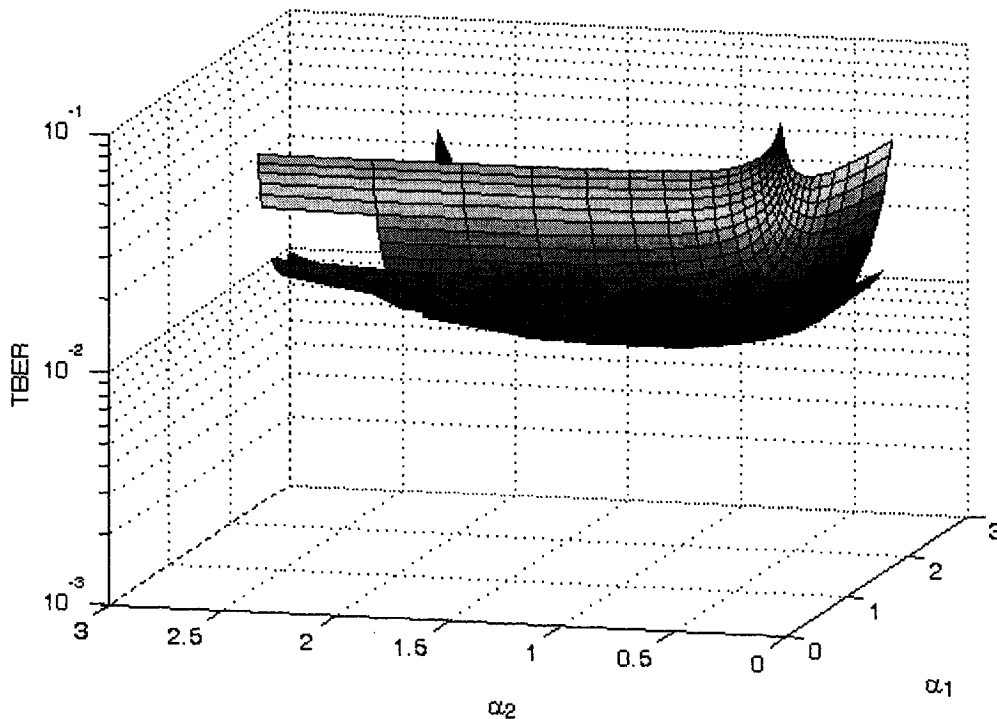


Fig. 6-4. Average TBER versus α_1, α_2 for 3x3 ZF-V-BLAST with BPSK modulation.

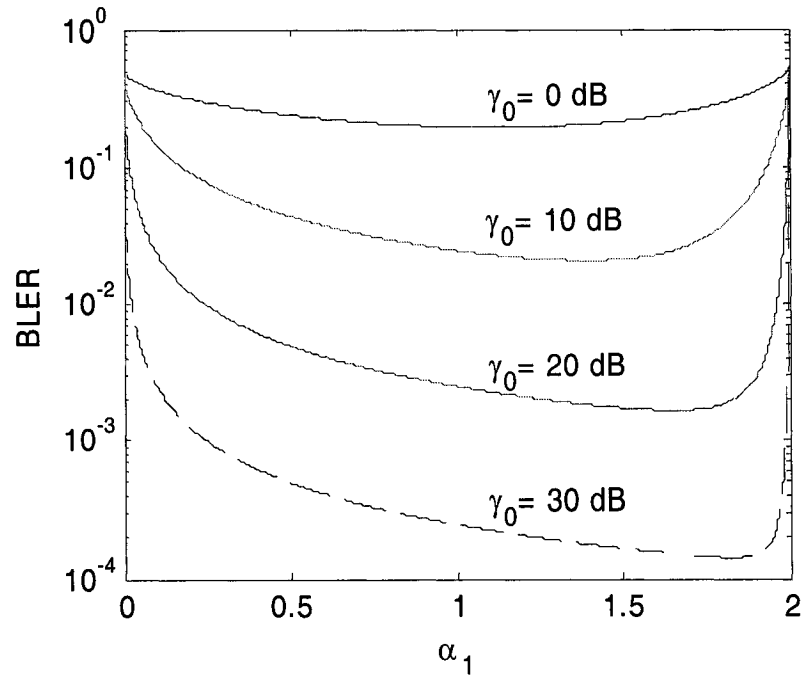


Fig. 6-5. Average BLER versus α_1 for 2x2 ZF-V-BLAST with BPSK modulation.

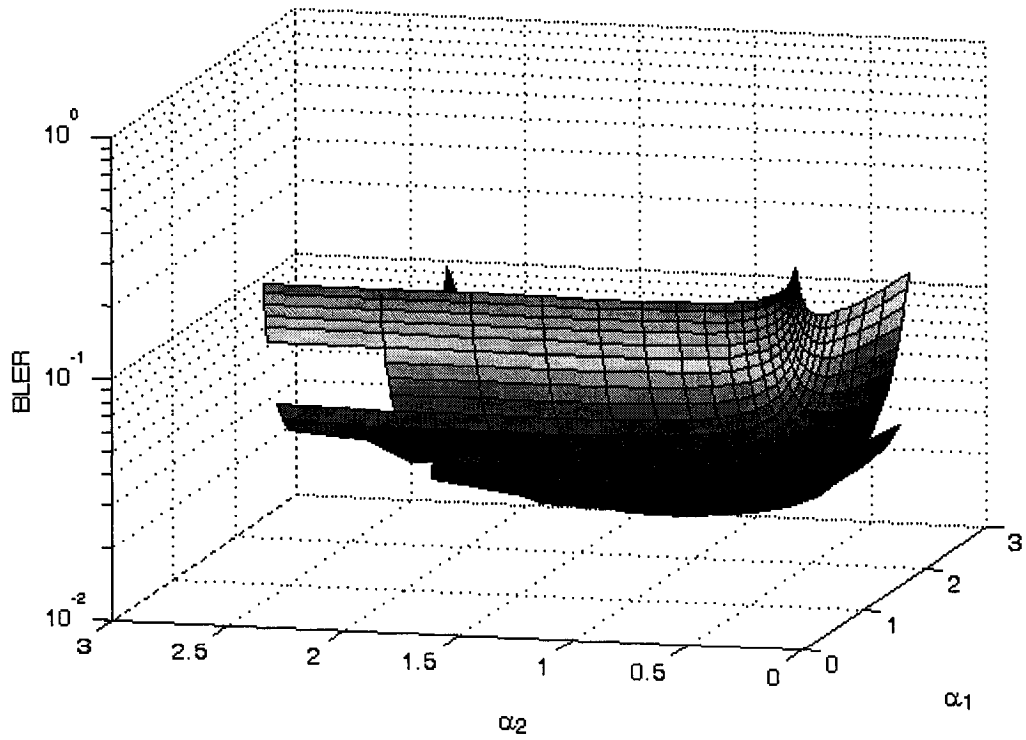


Fig. 6-6. Average BLER versus α_1, α_2 for 3x3 ZF-V-BLAST with BPSK modulation.

Local robustness of the solution means that small inaccuracies in α^{opt} do not affect the average error rate significantly. This explains why the approximate closed-form α^{opt} results in almost the same average error rate as the accurate numerical one. Fig. 5-7, Fig. 5-9, Fig. 5-13 show no performance gap between these two. Therefore, the closed-form approximate solution can be used instead of numerical optimization algorithm for the whole range of γ_0 , and not only for $\gamma_0 > 5\text{dB}$, where the closed-form solution is very accurate (see Fig. 5-10-Fig. 5-11). The choice of the optimization criteria (BLER or TBER) does not affect significantly the final result either (since they are indistinguishable on Fig. 5-12-Fig. 5-13, a single curve represents both). Thus, BLER or TBER can be used equally well as a performance criterion for optimization. From the analytical viewpoint, the BLER (either instantaneous or average) is preferable to use since it is convex and has a simple closed-form. It should also be remarked that the effect of the error propagation, which is what differentiates the TBER from the BLER, does not have any significant impact on the optimum power allocation, since both the TBER and BLER are dominated by the 1st step error rate [56]. Robustness of the algorithm also accounts for small difference between instantaneous and average optimization at high SNR.

6.2. V-BLAST WITH PRE-SET POWER ALLOCATION

Small sensitivity of the BLER/TBER to α suggests even further simplification in the optimization algorithm: since c changes slowly with the SNR (see Fig. 5-10-Fig. 5-11), we can pick up only one fixed value of α and still get performance improvement for a wide range of γ_0 . Such simplified algorithm does not require any feedback at all, and yet, as Fig. 6-7 demonstrates, it attains almost the same performance as the dynamically optimized system. In this example, the 3x3 V-BLAST with $\alpha = [2 \ 0.6 \ 0.4]$ (this power allocation is optimum for $\gamma_0 = 15\text{ dB}$, see Fig. 5-11) is

considered, and its performance is very close to the optimized V-BLAST in the range of $\gamma_0 = 15 \pm 10$ dB.

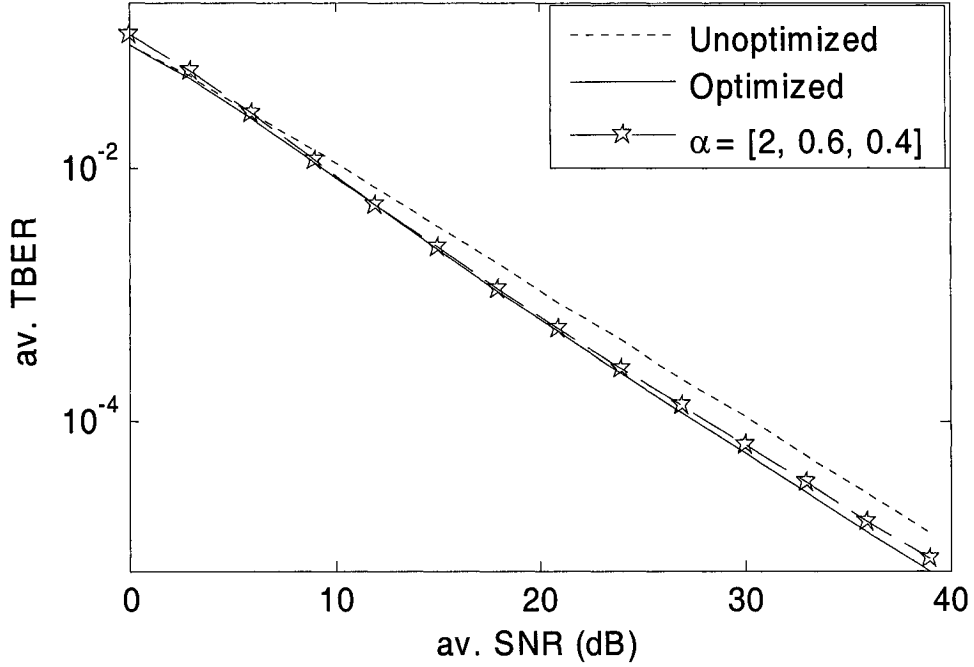


Fig. 6-7. TBER of 3x3 ZF-V-BLAST with BPSK modulation for fixed power allocation.

6.3. GLOBAL ROBUSTNESS

The robustness considered above is *local* robustness, i.e. for small variations in the vicinity of the unperturbed values of the system parameter. When variations are not small, the finite differences in (6.1) cannot be accurately approximated by the derivatives and the approximations in (6.2), (6.3), (6.6), (6.7) may not be accurate. In such a case, one has to consider a measure of *global* robustness. To this end, let us consider the average error rate of the perturbed system $\bar{P}(\mathbf{a}; u + \Delta u)$, where Δu is not necessarily small and u is the total Tx power. Let $\mathbf{a}_{\Delta u}^{opt}$ denote the optimum power allocation of the perturbed system, so that the optimum allocation for the unperturbed system is $\mathbf{a}_0^{opt} = \mathbf{a}_{\Delta u=0}^{opt}$, the optimized average error rate of the unperturbed system is $\bar{P}(\mathbf{a}_0^{opt}; u)$,

and the optimized average error rate of the perturbed system is $\bar{P}(\mathbf{\alpha}_{\Delta u}^{opt}; u + \Delta u)$. From the general theory of convex optimization [13], the last two quantities are related by the following global inequality,

$$\Delta P = \bar{P}(\mathbf{\alpha}_{\Delta u}^{opt}; u + \Delta u) - \bar{P}(\mathbf{\alpha}_0^{opt}; u) \geq -\lambda \Delta u, \quad (6.10)$$

where λ is evaluated at $\Delta u = 0$, and the equality is achieved for $\Delta u = 0$. It follows immediately that:

- if Δu is positive, i.e. the total Tx power is increased, the optimal value of \bar{P} decreases by *no more* than $\lambda \Delta u$;
- if Δu is negative, i.e. the total Tx power is decreased, the optimal value of \bar{P} is guaranteed to increase by *at least* $\lambda |\Delta u|$.

Dividing (6.10) by \bar{P} , one obtains

$$\frac{\Delta \bar{P}}{\bar{P}} \geq -\delta' \frac{\Delta u}{u}, \quad (6.11)$$

where δ' is given by (6.3). Therefore, δ' , which was introduced as a measure of *local* robustness in (6.3), also serves as a measure of *global* robustness in (6.11). It gives the lower bound on the normalized variation in the error rate due to any (not necessarily small) variation Δu in the total Tx power. The inequality in (6.11) transforms into the approximate equality for small perturbations (see (6.4)). Thus, the Lagrange multiplier λ plays a key role not only in the local but also in the global robustness.

Note that the Lagrange multiplier λ at $\Delta u = 0$ is required in (6.10), (6.11). Since it is not known in closed-form for arbitrary SNR, the high-SNR approximation in (6.5) can be used with reasonable accuracy for $\gamma_0 > 0$ dB, as Fig. 6-8 demonstrates.

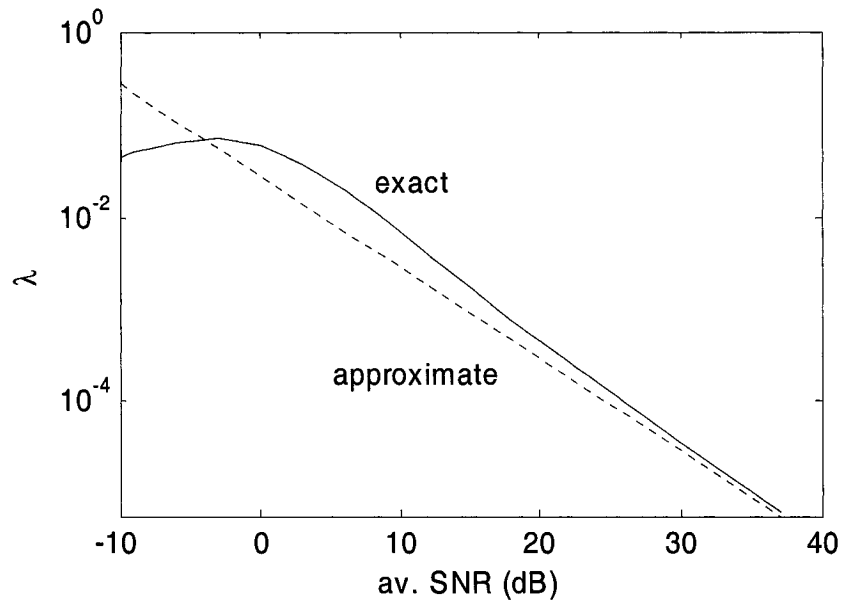


Fig. 6-8. The Lagrange multiplier for the BLER-based optimization versus SNR for 3x3 ZF-V-BLAST.

6.4.SUMMARY

Robustness of the optimized algorithm in terms of variations in system parameters have been studied. It is demonstrated that robustness, local and global, is quantified by the value of the Lagrange multiplier of the power-optimization problem. Using the measure of robustness introduced, it has been demonstrated that the optimized algorithm is not sensitive to small variations in total and individual Tx powers. This suggests a simplified power allocation strategy, which does not require any feedback at all but relies on pre-set values of transmit powers. It has been demonstrated that the pre-set power allocation can provide almost the same performance improvement in the wide range of SNR as the adaptive power allocation strategy.

7. SNR Gain of Optimum Power Allocation

This chapter explores some properties of the SNR gain of optimization using mostly analytical techniques, and uses numerical results only as the last resort. The analysis and conclusions below are valid for any modulation format, unless otherwise stated.

The *SNR gain of optimum power allocation* is defined as the difference in SNR required to achieve the same error rate in the optimized and unoptimized systems, i.e.

$$P(\alpha_1^{opt}, \dots, \alpha_m^{opt}) = P(\alpha, \dots, \alpha), \quad (7.1)$$

where P is the performance criterion, i.e. the BLER or the TBER, either instantaneous or average, the left-hand side represents the optimized error rate under the total power constraint $\sum_{i=1}^m \alpha_i^{opt} = m$, the right-hand side represents the error rate for the uniform power allocation, $\alpha_i = \alpha$, and the SNR gain is $G = \alpha$.

For the average optimization, the average error rate is used in (7.1). For the instantaneous optimization, one may use both instantaneous and average error rate in (7.1). In the former case, one obtains the instantaneous gain of the instantaneous optimization, and in the latter case, one obtains the average gain (i.e. in terms of the average error rate) of the instantaneous optimization. To be able to compare the instantaneous and average optimizations below, the average gain of the instantaneous optimization G_{inst} is used. It compares to the gain of the average optimization G_{av} as follows

$$G_{inst} \geq G_{av} \quad (7.2)$$

i.e. the instantaneous optimization is at least as good as the average one. This follows from the inequality $\overline{\min_x \{f(x, y)\}} \leq \min_x \{\overline{f(x, y)}\}$, where the expectation is over y . If the instantaneous gain of instantaneous optimization is averaged over \mathbf{H} , it is also greater that

the gain of the average optimization G_{av} , since instantaneous optimization outperforms average one for each channel realization. Averaged over \mathbf{H} gain of instantaneous optimization should not be confused with G_{inst} , which is defined in terms of average, rather than instantaneous, error rate.

According to the definition (7.1), the properties of the SNR gain are determined by the criterion chosen to measure performance and hence might be different depending on whether TBER or BLER is used in (7.1). To avoid confusion, this chapter will consider separately the SNR gain defined by the BLER and TBER and later demonstrate that they share many similarities. Note that G can be considered to be a function of the targeted error rate or the SNR at which this error rate is attained. In this analysis, G is considered to be a function of γ_0 , where γ_0 is the average SNR at which the *optimized* system attains the targeted error rate, see Fig. 7-1.

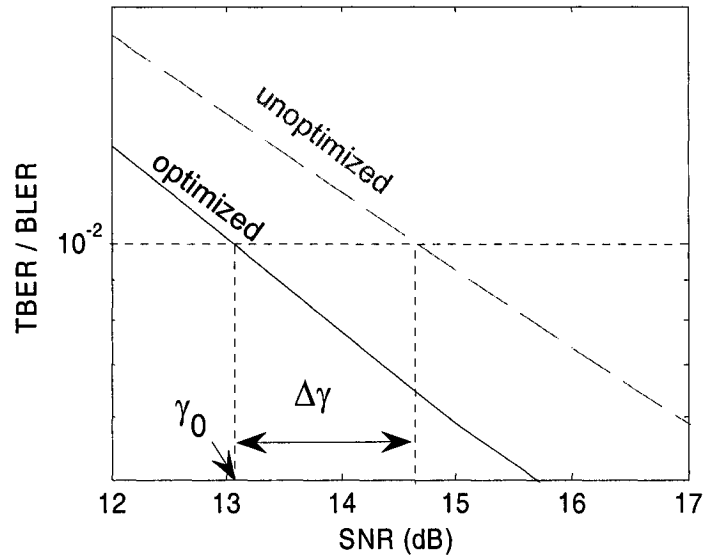


Fig. 7-1. Definition of the SNR gain.

7.1. BLER SNR GAIN OF THE OPTIMUM POWER ALLOCATION

Presented below are the universal bounds on the BLER SNR gain, either instantaneous or average, which hold for arbitrary modulation, arbitrarily-fading channel and an optimization strategy which is based on reducing the BLER

Theorem 7.1. The BLER SNR gain of optimum power allocation, either instantaneous or average, is bounded as follows

$$1 \leq G \leq m \quad (7.3)$$

Proof. The key to the proof is the fact that the BLER, either instantaneous or average, is a monotonically decreasing function in each argument $\alpha_1, \dots, \alpha_m$, which follows from (4.1), (4.2), and the fact that P_{ei} is monotonically decreasing function of the SNR.

Based on this fact and also on the inequality $P_B(\alpha_1^{opt}, \dots, \alpha_m^{opt}) \leq P_B(1, \dots, 1)$, which simply states that the optimized system is at least as good as the unoptimized one, the lower bound in (7.3) follows.

For the upper bound, using the monotonic-decreasing property of the BLER and the fact that $\alpha_i \leq m$, which follows from the total power constraint, one concludes that $P_B(\alpha_1^{opt}, \dots, \alpha_m^{opt}) \geq P_B(m, \dots, m)$. Comparing this inequality with the definition of the gain in (7.1) in view of the monotonic-decreasing property of the BLER, the upper bound follows. *Q.E.D.*

The small-SNR behavior of the SNR gain in terms of the average BLER, which is related to the lower bound in Theorem 7.1, for the BLER-based optimization and for a variety of modulation formats, is described by

Theorem 7.2. Small-SNR behavior of the BLER SNR gain for the average BLER-based optimization is as follows:

$$G_{av} \rightarrow G_0 \geq 1 \text{ as } \gamma_0 \rightarrow 0, \quad (7.4)$$

where

$$G_0 = \begin{cases} \frac{m \sum_i a_i^2}{\left(\sum_i a_i\right)^2}, a_i = \frac{\partial \bar{P}_{ei}}{\partial \sqrt{\alpha_i \gamma_0}} \Big|_{\alpha_i \gamma_0 = 0}, & \text{coherent detection} \\ \frac{\max_i |b_i|}{m \sum_i |b_i|}, b_i = \frac{\partial \bar{P}_{ei}}{\partial (\alpha_i \gamma_0)} \Big|_{\alpha_i \gamma_0 = 0}, & \text{noncoherent detection} \end{cases} \quad (7.5)$$

and a_i, b_i are the coefficients at the 1st term of the Taylor series expansion of \bar{P}_{ei} at $\alpha_i \gamma_0 = 0$. The equality in (7.4) is achieved, i.e. $G_0 = 1$, if and only if all a_i or all b_i are equal, for coherent and non-coherent detection respectively.

Proof. See Appendix A.2.

This result is valid for a variety of modulation formats for which the error rate admits MacLaurin's series expansion in SNR or $\sqrt{\text{SNR}}$ about SNR=0. In most cases, the strict inequality in (7.4) holds, i.e. there is an SNR gain of optimization even at very low SNR, since different \bar{P}_{ei} exhibit different behavior so that the expansion coefficients are also different. For coherent BPSK and non-coherent BFSK,

$$\begin{aligned} a_i^{BPSK} &= \frac{n-m+i}{2} - \frac{1}{2^{n-m+i}} \sum_{k=0}^{n-m+i-1} C_{n-m+i+k-1}^k \frac{k}{2^k}, \\ b_i^{BFSK} &= a_i^{BPSK} / 2, \end{aligned} \quad (7.6)$$

and for 2×2 V-BLAST, $G_0 = 0.17$ dB and 0.79 dB respectively.

Theorem 7.2 also applies to the instantaneous gain of the instantaneous optimization, in which case P_{ei} should be used in (7.5) instead of \bar{P}_{ei} , and the coefficients a_i, b_i and hence the gain depend on the channel realization, as long as the derivatives in (7.5) exist and are not all equal to zero simultaneously.

The average SNR gain of instantaneous optimization is also lower bounded by G_0 in (7.5), $G_{inst} \geq G_0 \geq 1$, because of (7.2). Thus, we conclude that (7.4) holds for a variety of scenarios for BLER-based optimization.

The following theorem states that the upper bound in (7.3) is achieved at high SNR:

Theorem 7.3. High-SNR behavior of the average BLER SNR gain for the BLER-based optimization, both instantaneous and average, with BPSK modulation in Rayleigh fading channel, is as follows:

$$G \rightarrow m \text{ as } \gamma_0 \rightarrow \infty \quad (7.7)$$

Proof. From the high SNR approximation of the average BLER (4.15) with α^{opt} given by (5.9), one concludes that

$$\bar{P}_B \rightarrow \bar{P}_{el} = \begin{cases} \bar{P}_{n-m+1}^{MRC}(\gamma_0), \text{ unoptimized} \\ \bar{P}_{n-m+1}^{MRC}(m\gamma_0), \text{ optimized} \end{cases} \text{ as } \gamma_0 \rightarrow \infty \quad (7.8)$$

i.e. the first step dominates for both unoptimized and optimized systems. Using this in the gain definition in (7.1), one concludes that for the average optimization, $G_{av} \rightarrow m$ as $\gamma_0 \rightarrow \infty$. Using (7.3) and (7.2), this also holds for the average gain of the instantaneous optimization, $G_{inst} \rightarrow m$ as $\gamma_0 \rightarrow \infty$. *Q.E.D.*

It should be noted that this result also extends to any modulation/fading for which (7.8) holds, i.e. for which the first step error rate dominates the BLER. Based on the diversity order argument, this condition should hold for most modulation formats in Rayleigh-fading channel.

For the average-BLER based optimization with BPSK modulation, a high-SNR approximation of the average BLER gain is given by (see Appendix A.3 for derivation)

$$G_{av} \approx \frac{m}{n-m+1 \sqrt{1 + \frac{c_{m,n}}{n-m+3 \sqrt{4\gamma_0}}}}, \quad (7.9)$$

$$c_{m,n} = \frac{(n-m+1)b_2^{n-m+3} + 3m^{n-m+2}}{mb_2^{n-m+2}},$$

and b_2 is given by (5.8). Note that (7.9) reduces to (7.7) for $\gamma_0 \rightarrow \infty$, as it should be. The convergence rate to the upper bound in (7.7) is however small, since the convergence condition is $n-m+3\sqrt{\gamma_0} \gg 1$.

It follows from (7.9) that the average BLER gain of the average BLER-base optimization with BPSK modulation is an increasing function of the average SNR in the high-SNR range. Numerical evidence indicates that this also holds for low to intermediate SNR, see Fig. 6.

Theorem 7.4. Under the total power constraint $\sum_{i=1}^m \alpha_i = u$, where u is the total Tx power, the BLER SNR gain of BLER-based optimization in (7.1), either instantaneous or average, is a monotonically increasing function of u :

$$\frac{\partial G}{\partial u} = -\frac{\lambda}{\partial P_B(\alpha \dots \alpha) / \partial \alpha} \geq 0 \quad (7.10)$$

Proof. see Appendix A.4.

7.2. TBER SNR GAIN OF THE OPTIMUM POWER ALLOCATION

To extend the results of the previous section to the SNR gain defined in terms of the average TBER, we will need the following generic properties of the average TBER, which serve as a substitution to the monotonically decreasing property of the BLER¹⁸.

¹⁸ Unfortunately, the TBER is not necessarily monotonically decreasing in $\alpha_1 \dots \alpha_m$ since increasing power of the lower step transmitters increases inter-stream interference to the higher step transmitters due to the effect of error propagation. Hence, the TBER may potentially increase if the error propagation effect is strong enough.

Property 1. For regular (unoptimized) V-BLAST, the average TBER decreases with SNR or total Tx power,

$$\partial \bar{P}_{et}(\alpha, \dots, \alpha) / \partial \alpha < 0 \quad (7.11)$$

This property is supported by the results in [12], [56], and also by research on the error rate performance of diversity systems with co-channel interference [59]-[62]¹⁹, since the error propagation in V-BLAST effectively “creates” co-channel interference and thus it is similar to diversity combining with interference. Note that since all the Tx powers are increased in (7.11) simultaneously, the effective signal-to-interference ratio for propagating errors stays the same or even decreases due to decrease in the probability of error propagation [56].

Property 2. For a partially-optimized V-BLAST, in which α_i^{opt} are used up to the stream $k < m$, the TBER decreases when the SNR at the unoptimized streams increases:

$$\partial \bar{P}_{et}(\alpha_1^{opt}, \dots, \alpha_k^{opt}, \alpha, \dots, \alpha) / \partial \alpha < 0 \quad (7.12)$$

This property follows from Property 1 and (4.4), since first k errors rates P_{u1}, \dots, P_{uk} are fixed and the others are those of the unoptimized system and behave according to Property 1, i.e. decrease with the SNR. The same reasoning also holds for instantaneous TBER.

Property 3. For the average TBER-based optimization, the following inequality holds,

$$\alpha_{k-1}^{opt} \geq \alpha_k^{opt}, \quad k = 2 \dots m \quad (7.13)$$

The rationale behind this property is the fact that according to the optimum power allocation strategy, more power is granted to the more significant source of error. Since

¹⁹ to the best of our knowledge, it has never been observed in the literature that error rate may increase with SNR, even when co-channel interference is present. This strongly supports Property 1.

lower steps generate on average more errors due to lower average after-processing SNR²⁰ and the effect of error propagation, they are allocated more power. This property is also supported by numerical evidence. This, however, does not necessarily hold for the instantaneous TBER-based optimization since some channel realization may “favor” lower steps, which may thus have higher SNR and fewer errors than higher steps, so that they will get less Tx power. This is demonstrated in Fig. 7-2 where the distribution of α_1^{opt} for instantaneous optimization (α_1^{opt} is a random variable since \mathbf{H} is random) for 2×2 V-BLAST is shown. Clearly with non-negligible probability $\alpha_1^{opt} \leq 1$, and hence $\alpha_1^{opt} \leq \alpha_2^{opt}$.

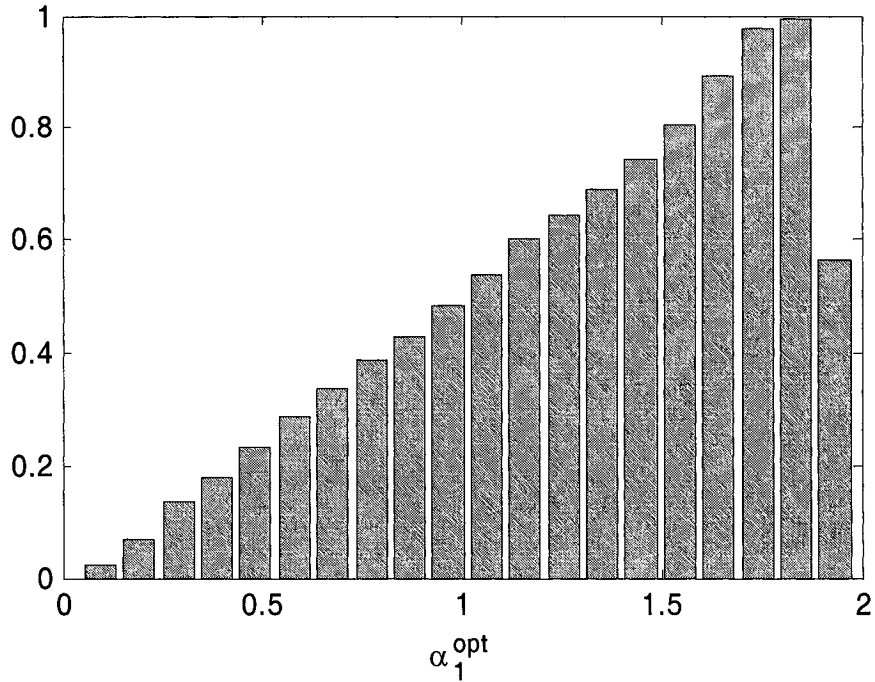


Fig. 7-2. Empirical PDF of instantaneous α_1^{opt} for 2×2 ZF V-BLAST, BPSK modulation, Rayleigh channel, SNR = 20dB, number of trials 10^4

²⁰ projecting out interference from yet-to-be-detected higher-step symbols results in SNR loss. Since the dimensionality of the projected out space decreases for higher steps, the SNR loss decreases as well.

It can be now shown that Theorem 7.1 also holds for the average TBER SNR gain. The lower bound in (7.3) follows from the fact that optimization can not increase the TBER, so that $\bar{P}_{et}(\boldsymbol{\alpha}^{opt}) \geq \bar{P}_{et}(1, \dots, 1)$; using Property 1 gives the lower bound.

To prove the upper bound in (7.3), note that by Property 2 for $k = m - 1$, $\bar{P}_{et}(\alpha_1^{opt}, \dots, \alpha_{m-1}^{opt}, \alpha)$ is a decreasing function of α , and by Property 3, $\alpha_{m-1}^{opt} \geq \alpha_m^{opt}$; therefore, $\bar{P}_{et}(\alpha_1^{opt}, \dots, \alpha_{m-1}^{opt}, \alpha_m^{opt}) \geq \bar{P}_{et}(\alpha_1^{opt}, \dots, \alpha_{m-1}^{opt}, \alpha_{m-1}^{opt})$. Repeating this for $k = m - 2, \dots, 1$, one obtains

$$\bar{P}_{et}(\boldsymbol{\alpha}^{opt}) \geq \dots \geq \bar{P}_{et}(\alpha_1^{opt}, \dots, \alpha_1^{opt}) \geq \bar{P}_{et}(m, \dots, m) \quad (7.14)$$

The last inequality here is due to Property 1 and $\alpha_i \leq m$, which follows from the total power constraint. Using (7.14) in the gain definition in (7.1) and relying on Property 1, the upper bound follows.

For the SNR gain defined in terms of instantaneous TBER for instantaneous optimization, analytical proof of the upper-bound in (7.3) presents serious difficulties, but numerical evidence suggests that it is still valid.

Theorem 7.2 still holds for the average TBER SNR gain, with the substitution of $\bar{P}_{ei} \rightarrow \bar{P}_{et}$ in (7.5).

Theorem 7.3 is no longer valid, i.e. the upper bound m is never attained if the gain is defined in terms of the TBER. Instead, the following holds.

Theorem 7.5. High SNR behavior of the average TBER SNR gain for the average optimization is as follows:

$$G_{av} \rightarrow G_{\infty} < m \text{ as } \gamma_0 \rightarrow \infty, \quad G_{\infty} = m \left(\frac{2\tilde{a}_1}{m+1} \right)^{\frac{1}{n-m+1}} < m, \quad (7.15)$$

where \tilde{a}_1 is given by (4.17).

Proof. From the high SNR approximations of the average TBER for optimized and unoptimized systems in (4.17) and (5.16), one concludes that

$$\bar{P}_{el} \approx \begin{cases} \frac{\tilde{a}_1}{m} \frac{1}{(4\gamma_0)^{n-m+1}}, & \text{unoptimized} \\ \frac{m+1}{2m} \frac{1}{(4m\gamma_0)^{n-m+1}}, & \text{optimized} \end{cases}, \quad (7.16)$$

Using (7.16) in (7.1), it follows that $G_{av} \rightarrow G_\infty$ as $\gamma_0 \rightarrow \infty$.

Thus, the improvement in average TBER is less than the upper-bound in (7.3). The reason for this is the increased power of propagating errors for the optimized system (due to greater power going to lower steps) compared to the unoptimized one. For example, the optimum power allocation algorithm gives most of the power to the 1st Tx trying to avoid the errors at the 1st step. But if the error *does* occur at the 1st step, its amplitude is higher than for the unoptimized system, which makes the error propagation effect more severe.

The high-SNR approximation of the TBER SNR gain is similar to that in (7.9):

$$G_{av} \approx \frac{G_\infty}{\sqrt[n-m+1]{1 + \frac{c_{m,n}}{n-m+3} \sqrt[n-m+3]{4\gamma_0}}}, \quad \text{where} \quad (7.17)$$

$$c_{m,n} = \frac{(m+1)(n-m+1)b_2^{n-m+3} + 3m^{n-m+3}}{m(m+1)b_2^{n-m+2}},$$

with G_∞ given by (7.15) and b_2 is given by (5.17).

7.3. EXAMPLES AND COMPARISONS

Let us consider the 2×2 V-BLAST. The average BLER in this case is,

$$\bar{P}_B \approx \begin{cases} \bar{P}_{el}(\gamma_0) \approx 1/(4\gamma_0), & \text{unoptimized} \\ \bar{P}_{el}(2\gamma_0) \approx 1/(8\gamma_0), & \text{optimized} \end{cases} \quad (7.18)$$

so that $G_{av} = 2$ (3 dB) at high SNR, which is the same as upper-bound in (7.3). This is not the case for the average TBER SNR. At high SNR, the probability of error propagation for the unoptimized V-BLAST is $\bar{P}_{e2|2} \approx 1/5$ [56] (4.17), and $\bar{P}_{e2|2} \approx 1/2$ (5.15) for the optimized V-BLAST. The average TBER is,

$$\bar{P}_{et} \approx \frac{1}{2} \bar{P}_{e1} (1 + \bar{P}_{e2|2}) \approx \begin{cases} \frac{3}{5} \bar{P}_{e1}(\gamma_0) \approx \frac{3}{20\gamma_0}, & \text{unoptimized} \\ \frac{3}{4} \bar{P}_{e1}(2\gamma_0) \approx \frac{3}{32\gamma_0}, & \text{optimized} \end{cases} \quad (7.19)$$

In this case, $G_{av} = 8/5$ (2 dB) at high SNR, which is less than the 3 dB upper-bound in (7.3). The high-SNR behavior of the average BLER and TBER gains is as follows,

$$G_{av,BLER} \approx 2 \left[1 + \frac{9}{2\sqrt[3]{36\gamma_0}} \right]^{-1}, \quad (7.20)$$

$$G_{av,TBER} \approx \frac{8}{5} \left[1 + \frac{3}{2\sqrt[3]{2\gamma_0}} \right]^{-1}$$

The simulation results validate these conclusions. Fig. 7-3 demonstrates that the average BLER gain of the optimized 2×2 V-BLAST monotonically increases with SNR and tends to 3 dB, which is the upper bound. The average BLER gain of the instantaneous optimization also tends to 3 dB and attains this bound, but much faster than that of the average optimization. The average TBER SNR gain of the same system tends to 2 dB, monotonically and slowly increasing (see Fig. 7-4). For the instantaneous optimization, the gain is higher but still does not exceed the 3 dB upper bound. Note that the averaged over \mathbf{H} gain of instantaneous optimization reaches the upper bound fastest. This is explained by the fact that it is defined in terms of instantaneous error rate, which decreases exponentially with SNR, resulting in steeper slope of this gain in comparison with the gain defined in terms of the average error rate.

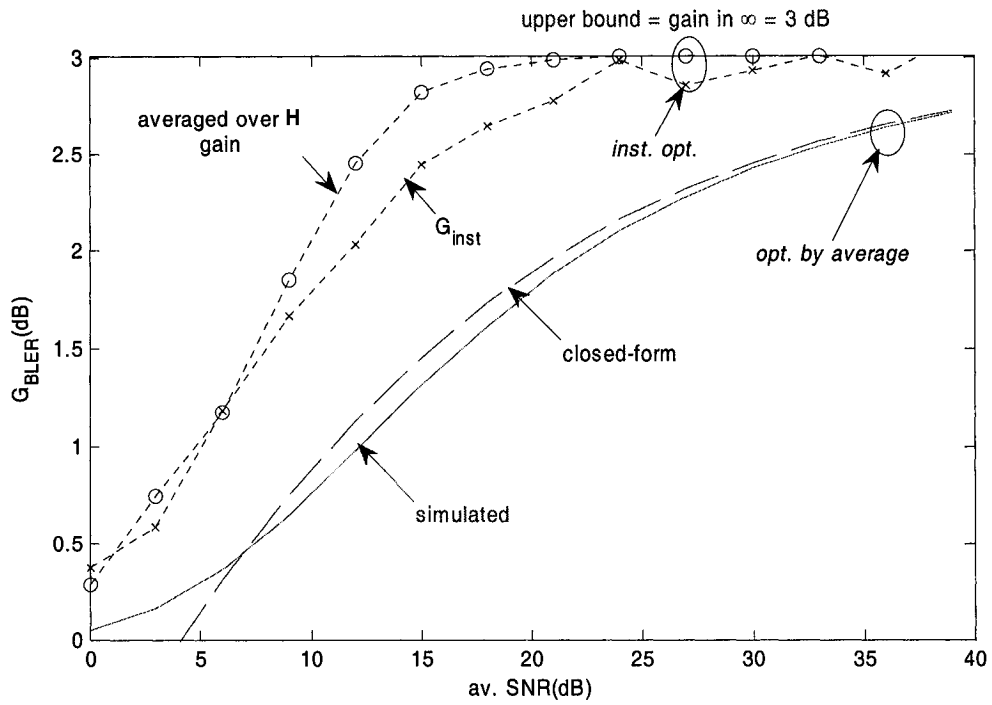


Fig. 7-3. Average BLER SNR gain vs. SNR for 2x2 ZF-V-BLAST with BPSK modulation.

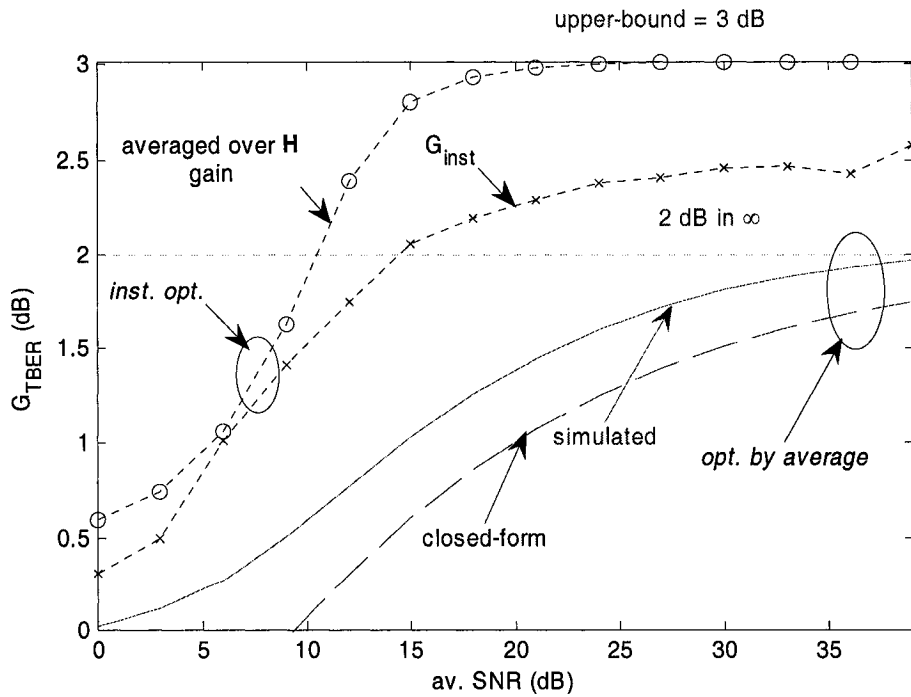


Fig. 7-4. Average TBER SNR gain vs. SNR for 2x2 ZF-V-BLAST with BPSK modulation.

The SNR gain of the optimum power allocation is almost the same, at high SNR, as that of the optimal ordering procedure (see [55] for details). The computational complexity, however, of the former is much less than that of the latter. Hence, the average power optimization can be used instead of the optimal ordering with roughly the same performance.

Let us now turn our attention to the small SNR behavior of the optimized 2×2 V-BLAST. According to (7.6), the first coefficients in the Taylor series of \bar{P}_{e1} and \bar{P}_{e2} are given by $a_1^{BPSK} = 1/2$ and $a_1^{BPSK} = 3/4$ accordingly, and the low SNR approximation of the BLER is given by (see Appendix A.2)

$$\bar{P}_B(\boldsymbol{\alpha}) \approx \frac{3}{4} - \frac{1}{2}\sqrt{\alpha_1\gamma_0} - \frac{3}{4}\sqrt{\alpha_2\gamma_0}, \quad (7.21)$$

which means that the higher steps have more impact on the overall performance. This is exactly opposite to the behavior of the system in high SNR mode. Approximation (7.21) is verified in Fig. 7-6, and the asymptotic low SNR gain is found from (7.5) as $G_0 = 1.04$ (0.17 dB). Fig. 7-7 corroborates this low SNR limit. Note that the average BLER SNR gain is a decreasing function of SNR in small SNR region, reaches 0 dB at about $\gamma_0 \approx -5$ dB and monotonically increases for $\gamma_0 \geq -5$ dB. The average TBER SNR gain exhibits similar behavior, as Fig. 7-8 demonstrates. This can be justified as follows. As the contribution of the lower steps into the total error rate is smaller in low SNR region, less power is allocated to them. But as the SNR increases, lower steps begin to have more impact on the overall performance and hence receive more and more power (see Fig. 7-5). At the transition region, when the contributions of all step BERs into the total error rate are roughly the same, little can be done with the optimum power allocation. Optimum power allocation in this case is very close to the uniform power allocation and hence the least gain is observed.

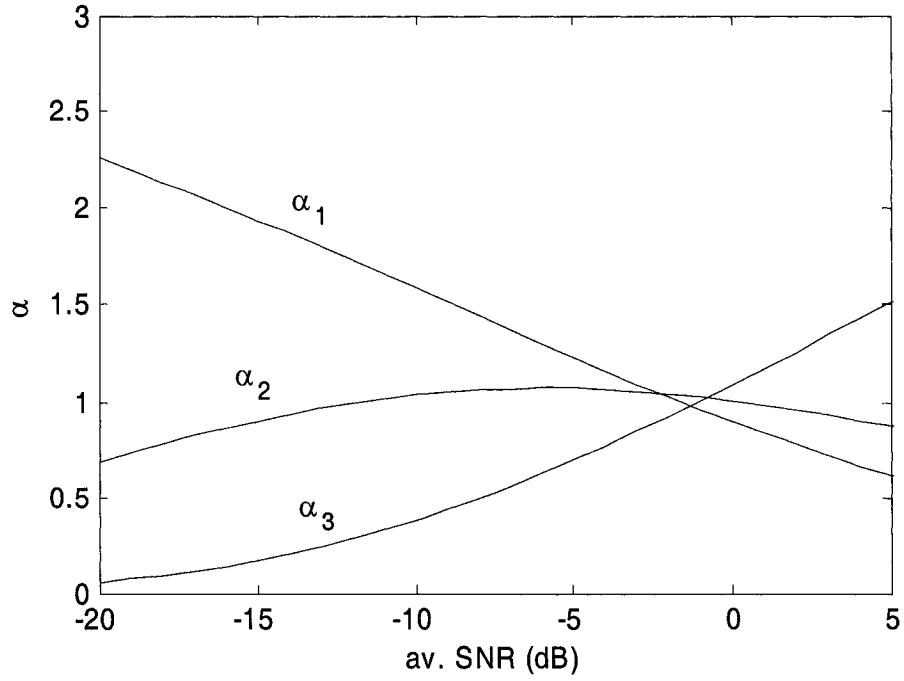


Fig. 7-5. Optimum power allocation at low SNR for average BLER-based optimization, 3x3 ZF-V-BLAST with BPSK modulation.

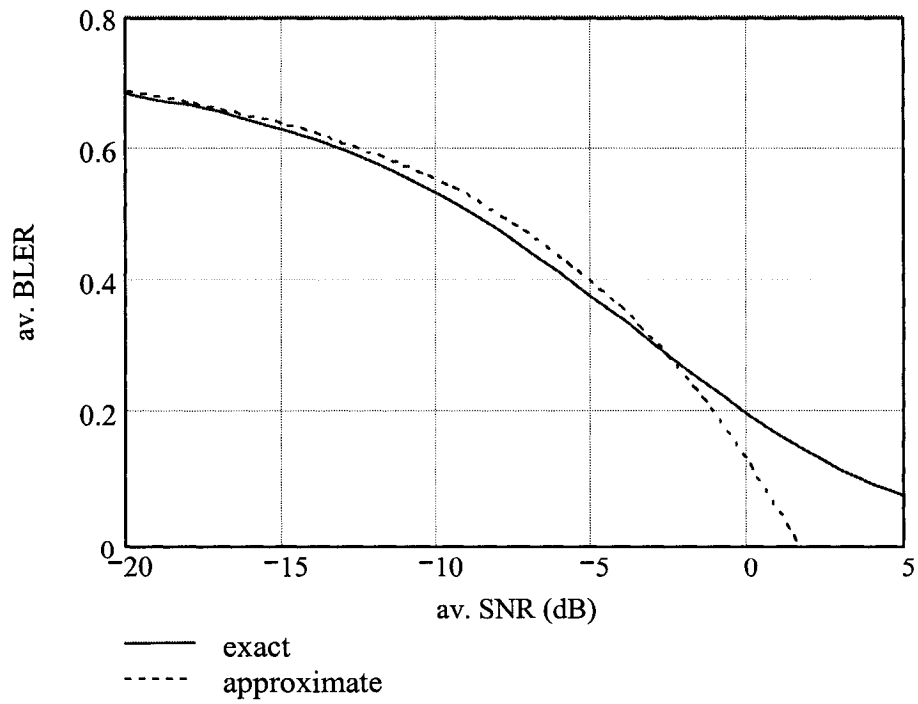


Fig. 7-6. Average BLER at low SNR for unoptimized 2x2 ZF-V-BLAST with BPSK modulation, exact and approximate by (7.21)

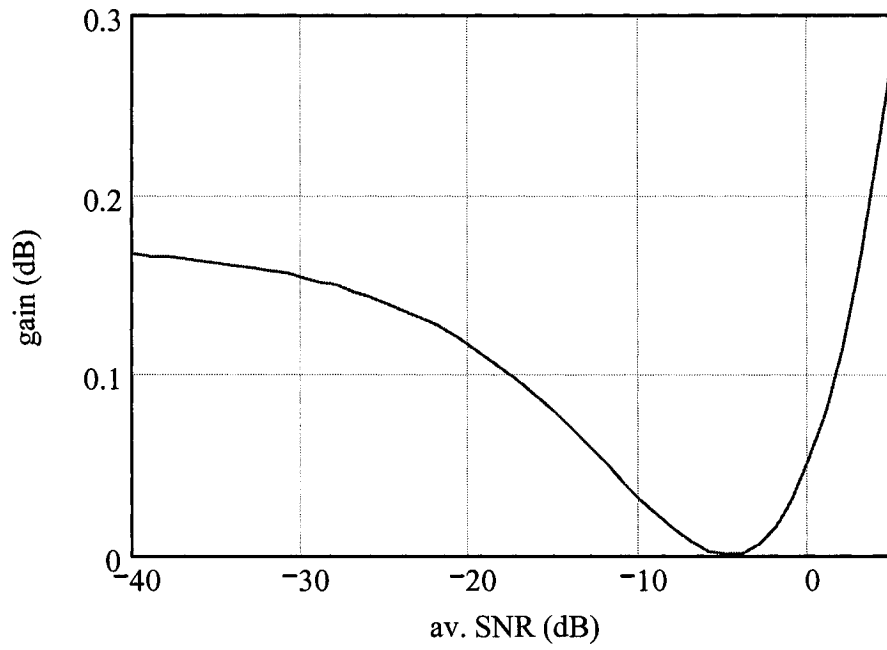


Fig. 7-7. Average BLER SNR gain at low SNR for 2x2 ZF-V-BLAST with BPSK modulation.

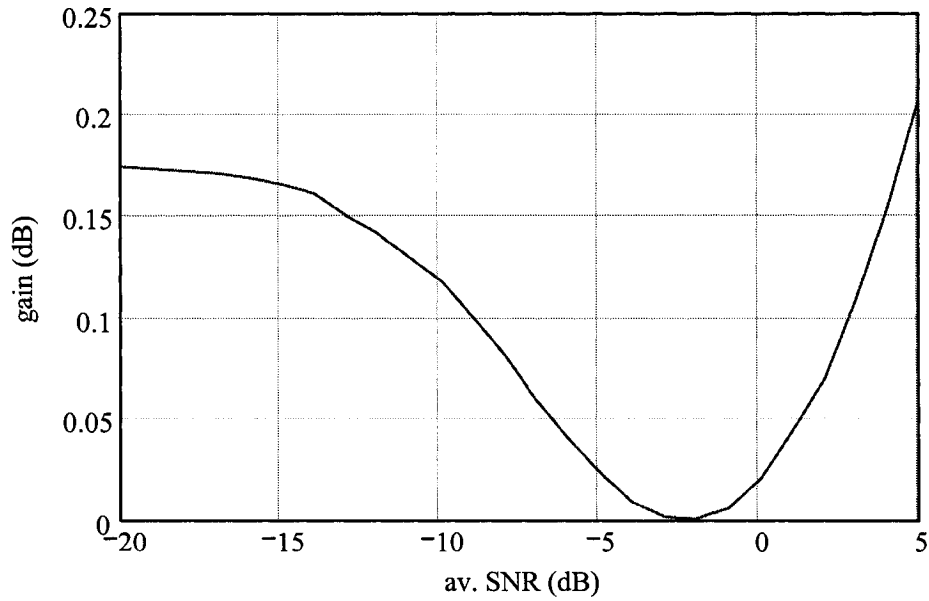


Fig. 7-8. Average TBER SNR gain at low SNR for 2x2 ZF-V-BLAST with BPSK modulation.

Whether the gain is defined using the TBER or the BLER, it exhibits roughly the same behavior: it is bounded as in (7.3), it approaches the lower bound at low SNR, and it increases monotonically with the SNR. In both cases, the instantaneous optimization attains the upper-bound at $\gamma_0 \approx 20...25$ dB. In both cases, the gain of average optimization increases with the SNR much slower than that of the instantaneous one. The only significant difference is that the BLER gain of average optimization attains the upper bound = m , and the TBER gain does not. However, since the upper bound is achieved by the BLER gain at rather high SNR, this difference seems to be less important from practical perspective. As indicated by Fig. 7-3 and Fig. 7-4, both gains are close to each other at practical SNR range.

7.4.SUMMARY

The SNR gain of the optimization has been rigorously defined for various criteria (average and instantaneous BLER and TBER) and investigated. Universal bounds have been derived, which hold true for any optimization strategy, modulation format and channel fading type. Specifically, the gain is upper bounded by the number of transmit antennas. The upper bound is achieved at high SNR for the average BLER-defined gain, but is not for the TBER-defined gain, which we attribute to increased power of the error propagation in the optimized system. Closed-form high SNR approximations of the gain have been obtained. Low SNR behavior of the SNR gain has also been studied. There is a nonzero gain at very low SNR, and the gain is a decreasing function of SNR in low SNR region.

8. Conclusion

8.1. SUMMARY OF THE THESIS

Among different variants of the V-BLAST algorithm for space-time signal processing, unordered ZF-V-BLAST is an attractive choice due to its simplicity. Its performance however suffers from the error propagation effect. Introducing the optimal ordering procedure into the algorithm is one way to mitigate it. Unfortunately this solution is rather computationally intensive, which may be a limitation for some applications. As low-complexity alternatives to the optimal ordering, 1st step ordering and optimum power allocation techniques have been proposed (Chapter 3). Both have been shown to provide almost the same performance improvement as optimal ordering.

Optimum power allocation techniques based on various criteria, i.e. average and instantaneous block and total error rates, have been systematically studied and compared to each other. Accurate high-SNR approximations in a compact closed form have been derived for the optimum power allocation based on average BLER and TBER (Chapter 5). Due to the dominant contribution of lower steps to the error rate, these steps get more power in the optimized system, with the 1st step getting most of it. The power allocation strategies based on the average BLER and TBER are almost the same, since in both cases the 1st step is dominant in terms of the average error rate.

The error rate performance of the optimized system has been investigated (Chapter 5); closed-form expressions for optimized error rates at high SNR have been obtained. Despite the non-uniform power allocation in the optimized system, 1st step still dominates in terms of the error rate. Conditional error rates of the higher steps exhibit fractional diversity order. To the best of our knowledge, this is the first time when fractional diversity order is observed in a practical system in a Rayleigh fading channel.

BLER and TBER-based optimization strategies have been shown to result in the same performance improvement. BLER is a preferable choice of optimization criterion due to the especial simplicity of its analytical expressions. Besides, BLER-based optimization problem has been shown to have a unique solution for a variety of modulation formats in any fading channel, which facilitates numerical optimization.

While the instantaneous optimization requires instantaneous feedback and thus is more complex than the average one, which requires only the average SNR be fed back to the transmitter, its average error rate performance is only slightly better than that of the average optimization. At high SNR, both strategies exhibit the same average error rate.

The SNR gain of the optimization has been rigorously defined for various criteria (average and instantaneous BLER and TBER) and investigated (Chapter 7). Universal bounds have been derived, which hold true for any optimization strategy, modulation format and channel fading type. Specifically, the gain is upper bounded by the number of transmit antennas. The upper bound is achieved at high SNR for the average BLER-defined gain, but is not for the TBER-defined gain, which we attribute to increased power of the error propagation in the optimized system. Closed-form high SNR approximations of the gain have been obtained.

Robustness of the optimized algorithm in terms of variations in total and individual Tx powers have been studied (Chapter 6). Using the measure of robustness introduced, it has been demonstrated that the optimized algorithm is not sensitive to small variations in the above-mentioned parameters. This suggests a simplified power allocation strategy, which does not require any feedback at all but rather relies on pre-set values of transmit powers.

The analytical results and approximations above have been validated through simulations.

8.2. FUTURE RESEARCH

A unified analytical approach for the optimization and analysis of the V-BLAST, which has been developed in the thesis, can be adopted to power-optimize the V-BLAST in various operating scenarios. For example, the BPSK modulation has been assumed for simplicity in this research. An obvious extension would be to generalize the analysis for other modulation formats. Except for more cumbersome expressions, this generalization is quite straightforward within the framework developed.

Another limitation of the analytical analysis of the current research is that it assumed the unordered ZF-V-BLAST as a baseline for power-optimization. A desirable extension would be to generalize the results of the thesis for the V-BLAST with MMSE nulling and the V-BLAST with optimal ordering. The major difficulty here is that the optimal ordering procedure, as well as the MMSE nulling, complicates considerably the analytical performance evaluation of the algorithm.

The approaches used in the thesis to evaluate the performance of the optimized system can be applied to study different power-optimization strategies as long as the performance criterion is known in closed form. In particular, the measure of robustness and the definition of the SNR gain introduced can be directly applied to analyze the behavior of the optimized system once the function quantifying its performance is defined.

This thesis has touched some issues that obviously need further research. For example, the convexity of the average TBER has been observed numerically but not proven analytically; the small SNR behavior of the V-BLAST requires better understanding; implications of two different ways to define the SNR gain of instantaneous optimization should be elaborated further, etc. So, this work is only a beginning towards full understanding of the power-optimized V-BLAST.

9. References

9.1. OVERVIEWS AND HANDBOOKS

- [1] Special Issue on MIMO Systems, IEEE Transactions on Signal Processing, v. 50, N. 10, Oct. 2002
- [2] Special Issue on MIMO Systems, IEEE Journal Selected Areas Comm., v. 21, N. 3 and 5, April and June 2003
- [3] Special Issue on Space-Time Transmission, Reception, Coding and Signal Processing, IEEE Trans. Information Theory, v. 49, N. 10, Oct. 2003
- [4] Special Issue on Gigabit Wireless, Proceedings of the IEEE, v. 92, N.2, Feb. 2004
- [5] I. Berenguer, X. Wang, Coding and Signal Processing for MIMO Communications - A Primer, Journal of Computer Science and Technology, v. 18, No. 6, pp. 689-702, Nov. 2003
- [6] D. Gesbert, M. Shafi, D. Shiu, P. J. Smith, A. Naguib, From theory to practice: An overview of MIMO space-time coded wireless systems, IEEE Journal Selected Areas Comm., v. 21, No. 3, 2003
- [7] G. J. Foschini, D. Chizhik, MJ Gans, C. Papadias, R. A. Valenzuela, Analysis and Performance of Some Basic Space-Time Architectures, IEEE Journal Selected Areas Comm., v. 21, N. 3, pp. 281-320, April 2003.
- [8] A. J. Paulraj, D. Gore, R. U. Nabar, H. Bolcskei, An Overview of MIMO Communications—A Key to Gigabit Wireless, Proceedings of the IEEE, v. 92, No. 2, 2004
- [9] J. G. Proakis, Digital Communications, McGraw Hill, Boston, 2001
- [10] H. L. Van Trees, Optimum Array Processing, Wiley, New York, 2002

- [11] S. Verdu, *Multiuser Detection*, Cambridge University Press, Cambridge, UK, 1998
- [12] M. K. Simon, M.-S. Alouini, *Digital Communication over Fading Channels*, 2nd ed., Wiley, New York, 2005
- [13] S. Boyd, L. Vandenberghe, *Convex Optimization*, Cambridge University Press, Cambridge, UK, 2004
- [14] F. Zhang, *Matrix theory*, Springer, New York, 1999
- [15] MATLAB® Help, 1994-2005, The MathWorks, Inc.
- [16] R. Fletcher, *Practical Methods of Optimization*, Wiley, New York, 1987
- [17] G. A. Korn, T. M. Korn, *Mathematical Handbook for Scientists and Engineers*, Dover, New York, 2000

9.2.MIMO CHANNELS/CAPACITY

- [18] I. E. Telatar, *Capacity of Multi-Antenna Gaussian Channels*, AT&T Bell Lab. Internal Tech. Memo., Jun. 1995 (European Trans. Telecom., v.10, N.6, Dec.1999)
- [19] G. J. Foschini and M. J. Gans, *On limits of wireless communications in a fading environment when using multiple antennas*, *Wireless Personal Comm.*, v. 6, N.3, pp. 311–335, 1998
- [20] D. Shiu, G. J. Foschini, M. J. Gans, and J. M. Kahn, *Fading correlation and its effect on the capacity of multi-element antenna systems*, *IEEE Trans. Commun.*, v. 48, N.3, pp. 502–513, Mar. 2000
- [21] H. Bölcskei, D. Gesbert, and A. J. Paulraj, *On the capacity of OFDM based spatial multiplexing systems*, *IEEE Trans. Comm.*, v. 50, N.2, pp. 225–234, Feb. 2002
- [22] D. Chizhik, G. J. Foschini, M. J. Gans, and R. A. Valenzuela, *“Keyholes, correlations, and capacities of multielement transmit and receive antennas,”* *IEEE Trans. Wireless Comm.*, v. 1, N. 2, pp. 361–368, Apr. 2002

- [23] H. Shin and J. H. Lee, Capacity of Multiple-Antenna Fading Channels: Spatial Fading Correlation, Double Scattering, and Keyhole, *IEEE Transactions on Information Theory*, v. 49, N. 10, Oct. 2003
- [24] Q. T. Zhang, X. W. Cui, X. M. Li, Very tight capacity bounds for MIMO-correlated Rayleigh-fading channels, *IEEE Trans. Wireless Comm.*, v. 4, N. 2, pp. 681 – 688, Mar. 2005
- [25] M. R. McKay, I. B. Collings, General Capacity Bounds for Spatially Correlated Rician MIMO Channels, *IEEE Trans. Information Theory*, v. 51, N. 9, pp. 3121 – 3145, Sep. 2005
- [26] M. Webb, M. Beach, A. Nix, Matrix structure and capacity bounds of MIMO channels in interference, *IEE Proceedings Comm.*, v. 153, N. 4, pp. 476 – 481, Aug. 2006
- [27] A. Goldsmith, S. A. Jafar, N. Jindal, S. Vishwanath, Capacity limits of MIMO channels, *IEEE Journal Selected Areas Comm.*, v. 21, N. 5, pp. 684 – 702, Jun. 2003

9.3. SPACE-TIME CODES

- [28] V. Tarokh, N. Seshadri, A. R. Calderbank, Space-Time Codes for High Data Rate Wireless Communication: Performance Criterion and Code Construction, *IEEE Trans. Information Theory*, v. 44, N. 2, pp. 744-765, Mar. 1998.
- [29] S.M. Alamouti, A simple transmit diversity technique for wireless communications, *IEEE Journal Selected Areas Comm.*, v. 16, No. 8, pp. 1451 – 1458, Oct. 1998
- [30] V. Tarokh, H. Jafarkhani, A. R. Calderbank, Space-time block codes from orthogonal designs, *IEEE Trans. Information Theory*, v. 45, N. 5, pp. 1456 – 1467, Jul. 1999
- [31] S. Baro, G. Bauch, A. Hansmann, Improved codes for space-time trellis-coded modulation, *IEEE Comm. Letters*, v. 4, N. 1, pp. 20–22, Jan. 2000

- [32] Y. Liu, M. P. Fitz, O. Y. Takeshita, Full rate space–time turbo codes, *IEEE Journal Selected Areas Comm.*, v. 19, N. 5, pp. 969–980, May 2001
- [33] Y. Gong, K. B. Letaief, Concatenated space–time block coding with trellis coded modulation in fading channels, *IEEE Trans. Wireless Comm.*, v. 1, N. 4, pp. 580–590, Oct. 2002
- [34] H. Bouzekri, S. L. Miller, An upper bound on turbo codes performance over quasi-static fading channels, *IEEE Comm. Letters*, v. 7, N. 7, pp. 302-304, Jul. 2003
- [35] K. Wu, B. Bai, and L. Ping, Performance analysis of cascade trellis block space-time codes, *IEEE Trans. Comm.*, v. 52, N. 3, pp. 355-358, Mar. 2004
- [36] H. Jingyu, S. L. Miller, Performance analysis of convolutionally coded systems over quasi-static fading channels, *IEEE Trans. Wireless Comm.*, v. 5, N. 4, pp. 789 – 795, Apr. 2006

9.4.V-BLAST

- [37] G. J. Foschini, Layered space-time architecture for wireless communication in a fading environment when using multiple antennas, *Bell Lab. Tech. J.*, v. 1, N. 2, pp. 41-59, 1996
- [38] P. W. Wolniansky, G. J. Foschini, G. D. Golden, R. A. Valenzuela, V-BLAST: An architecture for realizing very high data rates over the rich scattering wireless channel, *In Proc. Int. Symposium on Advanced Radio Technologies*, Boulder, CO, Sep. 1998
- [39] B. Hassibi, A fast square-root implementation for BLAST, *Signals, Conf. Record of the 34-th Asilomar Conf. Signals Systems and Computers*, Pacific Grove, CA, USA, v. 2, pp. 1255–1259, 2000
- [40] H. Zhu, Z. Lei, F. P. S. Chin, An Improved Square-Root Algorithm for BLAST, *IEEE Sig. Proc. Letters*, v. 11, N. 9, pp. 772-775, Sep. 2004

- [41] D. Wubben, R. Bohnke, J. Rinas, V. Kuhn, K. D. Kammeyer, Efficient algorithm for decoding layered space-time codes, *Electronics Letters*, v. 37, N. 22, pp. 1348 – 1350, Oct. 2001
- [42] D. Wubben, R. Bohnke, V. Kuhn, K. D. Kammeyer, MMSE extension of V-BLAST based on sorted QR decomposition, *Vehicular Technology Conference 2003*, v. 1, pp. 508- 512, Oct. 2003
- [43] J. Benesty, Y. Huang, J. Chen, A fast recursive algorithm for optimum sequential signal detection in a BLAST system, *IEEE Trans. Signal Processing*, v. 51, N. 7, pp. 1722 – 1730, Jul. 2003
- [44] W. K. Wai, C.-Y. Tsui, R. S. Cheng, A low complexity architecture of the V-BLAST system, *IEEE Wireless Communications and Networking Conference, Chicago, IL, USA*, v.1, pp. 310 - 3141, Sep. 2000
- [45] N. Boubaker, K. B. Letaief, R. D. Murch, A low complexity multicarrier BLAST architecture for realizing high data rates over dispersive fading channels, *Vehicular Technology Conference, Rhodes, Greece*, v. 2, pp. 800-804, 2001
- [46] W.-J. Choi, R. Negi, J. M. Cioffi, Combined ML and DFE decoding for the V-BLAST system, *IEEE International Conference Comm., New Orleans, LA, USA*, v. 3, pp. 1243 - 1248, Jun. 2000
- [47] C. Shen, H. Zhuang, L. Dai, S. Zhou, Detection algorithm improving V-BLAST performance over error propagation, *Electronics Letters*, v. 39, N. 13, pp. 1007–1008, Jun. 2003
- [48] X Jing, H Wang, C Ming, S. Cheng, A novel BLAST detection algorithm based instantaneous error ordering, *IEEE Int. Conf. Comm.*, v. 5, pp. 3056-3060, Mar. 2003

- [49] R. Kalbasi, D. D. Falconer, A. H. Banihashemi, Optimum power allocation for a V-BLAST system with two antennas at the transmitter, *IEEE Communications Letters*, v. 9, No. 9, pp. 826 – 828, Sep. 2005
- [50] N. Wang, S. D. Blostein, Minimum BER Transmit Power Allocation for MIMO Spatial Multiplexing Systems, 2005 IEEE International Conference on Communications, San Diego, California, USA, May 2005
- [51] N. Wang, S.D. Blostein, Minimum BER Transmit Power Allocation and Beamforming for Two-Input Multiple-Output Spatial Multiplexing Systems, 2005 Canadian Workshop on Information Theory, Montreal, Canada, Jun. 2005
- [52] S. H. Nam, O. S. Shin, K. B Lee, Transmit Power Allocation for a Modified V-BLAST System, *IEEE Trans. Comm.*, v. 52, N. 7, pp.1074-1079, Jul. 2004
- [53] Z. Yan, K. M. Wong, Z. Q. Luo, Optimal diagonal precoder for multiantenna communication systems, *IEEE Trans. Signal Processing*, v. 53, N. 6, pp. 2089 – 2100, Jun. 2005
- [54] N. Prasad, M. K. Varanasi, Analysis of decision feedback detection for MIMO Rayleigh-fading channels and the optimization of power and rate allocations, *IEEE Trans. Inform. Theory*, v. 50, No. 6, Jun. 2004
- [55] S. Loyka, F. Gagnon, Performance Analysis of the V-BLAST Algorithm: an Analytical Approach, *IEEE Trans. Wireless Comm.*, v. 3, No. 4, pp. 1326-1337, Jul. 2004
- [56] S. Loyka, F. Gagnon, V-BLAST without Optimal Ordering: Analytical Performance Evaluation for Rayleigh Fading Channels, *IEEE Transactions on Communications*, v. 54, N. 6, pp. 1109-1120, Jun. 2006
- [57] S. Loyka, F. Gagnon, Analytical Framework for Outage and BER Analysis of the V-BLAST Algorithm, 2004 IEEE International Zurich Seminar on Communications, ETH Zurich, Switzerland, pp. 120-123, Feb. 2004

- [58] S. Loyka, V. Kostina, F. Gagnon, On Convexity/Concavity Properties of Error Rates of the ML Detector and Their Applications, *IEEE Trans. Information Theory*, submitted, 2006
- [59] A. Shah, A.M. Haimovich, Performance analysis of maximal ratio combining and comparison with optimum combining for mobile radio communications with cochannel interference, *IEEE Trans. Vehicular Technology*, v. 49, N. 4, pp.1454 – 1463, Jul. 2000
- [60] J.S. Kwak, J. H. Lee, Closed-form expressions of approximate error rates for optimum combining with multiple interferers in a Rayleigh fading channel, *IEEE Trans. Vehicular Technology*, v. 55, N. 1, pp. 158 – 166, Jan. 2006
- [61] M. Chiani, M. Z. Win, A. Zanella, Error probability for optimum combining of M-ary PSK signals in the presence of interference and noise, *IEEE Trans. Comm.*, v. 51, N. 11, pp. 1949 – 1957, Nov. 2003
- [62] G. Ginis, J.M. Cioffi, On the Relation Between V-BLAST and the GDFE, *IEEE Communications Letters*, v. 5, N. 9, pp. 364-366, Sep. 2001

Appendix A. Mathematical Derivations

A.1. CLOSED-FORM EXPRESSIONS FOR OPTIMUM POWER ALLOCATION

In the high SNR range, \bar{P}_b is approximated by (4.15), and (5.4) is transformed into

$$\frac{\partial L(\boldsymbol{\alpha})}{\partial \alpha_i} = -\frac{(n-m+i)C_{2i-1}^i}{(4\gamma_0)^{n-m+i}\alpha_i^{n-m+i+1}} + \lambda = 0, \quad i=1 \dots m \quad (\text{A.1})$$

It follows that each α_i can be expressed via the single parameter λ :

$$\alpha_i = \frac{a_i}{n-m+i+1 \sqrt{(4\gamma_0)^{n-m+i} \lambda}}, \quad (\text{A.2})$$

$$a_i = n-m+i+1 \sqrt{(n-m+i) C_{2i-1}^i}$$

Substituting (A.2) into the total power constraint $\sum_{i=1}^m \alpha_i = m$ and introducing a new variable $x = \lambda^{-(n+1)!/(n-m+1)!}$, we obtain the following equation for x :

$$\sum_{i=1}^m (4\gamma_0)^{-\frac{n-m+i}{n-m+i+1}} a_i x^{c_i} = m, \quad (\text{A.3})$$

$$c_i = \frac{(n+1)!}{(n-m+1)!(n-m+i+1)}$$

Following the Newton-Raphson method [17], the zero-order approximate solution to (A.3) is found when only the leading term ($i=1$) is kept in (A.3),

$$x_0 = \sqrt[n-m+1]{m(4\gamma_0)^{\frac{n-m+1}{n-m+2}} / a_1} \quad (\text{A.4})$$

First-order approximate solution can be written as $x = x_0(1+\delta)$, where δ is a small increment. By substituting x into the left-hand side of (A.3), one obtains

$$\sum_{i=1}^m a_i x_0^{c_i} (1+\delta)^{c_i} = \sum_{i=1}^m b_i (1+\delta)^{c_i} (4\gamma_0)^{\frac{1-i}{n-m+i+1}} = m, \quad (\text{A.5})$$

$$b_i = a_i a_1^{-\frac{n-m-2}{n-m+i+1}} m^{\frac{c_i}{n-m+i+1}} = n-m+i+1 \sqrt{\frac{(n-m+i) m^{n-m+2} C_{2i-1}^i}{n-m+1}}$$

Keeping only the first two leading terms in (A.5), $i = 1, 2$, one obtains:

$$m(1 + c_1\delta) + b_2(4\gamma_0)^{-1/(n-m+3)} = m, \quad (\text{A.6})$$

from which it follows that

$$\delta = -b_2(mc_1)^{-1}(4\gamma_0)^{-1/(n-m+3)} \quad (\text{A.7})$$

and

$$\begin{aligned} x &= x_0(1 + \delta) = \sqrt[n-m+2]{a_1^{-1}m(4\gamma_0)^{n-m+2}} \left[1 - \frac{b_2}{mc_1^{n-m+3}\sqrt[n-m+2]{4\gamma_0}} \right], \\ \lambda &= x^{-(n-m+2)c_1} = \frac{1}{(4\gamma_0)^{n-m+1}} \left(\frac{a_1}{m} \right)^{n-m+2} \left[1 - \frac{b_2}{mc_1^{n-m+3}\sqrt[n-m+2]{4\gamma_0}} \right]^{-(n-m+2)c_1} \end{aligned} \quad (\text{A.8})$$

Finally, the optimum power allocation α^{opt} is found by substituting λ from (A.8) into (A.2):

$$\tilde{\alpha}_i = b_i(4\gamma_0)^{\frac{1-i}{n-m+i+1}} \left(1 - \frac{b_2}{mc_1^{n-m+3}\sqrt[n-m+2]{4\gamma_0}} \right)^{c_i}, \quad \alpha_i^{\text{opt}} = m\tilde{\alpha}_i / \sum_{k=1}^m \tilde{\alpha}_k \quad (\text{A.9})$$

The last equality here is to assure the total power constraint for the approximate solution.

When \bar{P}_{et} is used as objective, due to similarity of high SNR approximations (4.15)

and (5.16), the above argument can be applied directly with substitution

$$a_i = \sqrt[n-m+i+1]{\frac{(m-i+2)(n-m+i)C_{2i-1}^i}{2m}} \quad (\text{A.10})$$

in (A.2) and

$$b_i = a_i a_1^{-\frac{n-m-2}{n-m+i+1}} m^{c_i} = \sqrt[n-m+i+1]{\frac{C_{2i-1}^i (n-m+i)(m-i+2)m^{n-m+2}}{(m+1)(n-m+1)}} \quad (\text{A.11})$$

in (A.5).

A.2. THE GAIN OF OPTIMIZATION FOR SMALL SNR

The main idea of the proof of Theorem 2 is to use the small SNR approximations of \bar{P}_B to find α^{opt} . The gain is then found in closed form using the definition (7.1). The

small SNR approximation of \bar{P}_{ei} is found via the MacLaurin's series expansion. For coherent modulation formats (e.g. M-ary PSK, coherent binary FSK), the error rate is a function of $\sqrt{\text{SNR}}$ [9] so that the expansion in $\sqrt{\alpha_i \gamma_0}$ about zero is used²¹ as a low-SNR approximation,

$$\begin{aligned} \bar{P}_{ei} &\approx \frac{1}{2} + a_i \sqrt{\gamma_0}, \\ a_i &= \left. \frac{\partial \bar{P}_{ei}}{\partial \sqrt{\alpha_i \gamma_0}} \right|_{\alpha_i \gamma_0 = 0}. \end{aligned} \quad (\text{A.12})$$

where we keep only the two leading terms. For the BPSK modulation, a_i^{BPSK} are given by (7.6). The small SNR approximation of the BLER is obtained by using (A.12) in (4.2) and keeping only first-order terms in $\sqrt{\alpha_i \gamma_0}$,

$$\bar{P}_B(\boldsymbol{\alpha}) \approx 1 - \frac{1}{2^m} + \frac{\sqrt{\gamma_0}}{2^{m-1}} \sum_{i=1}^m a_i \sqrt{\alpha_i}. \quad (\text{A.13})$$

Using (A.13) as the objective function in (5.4), one finds $\boldsymbol{\alpha}^{opt}$:

$$\left. \begin{aligned} \frac{\partial L(\boldsymbol{\alpha})}{\partial \alpha_i} \Big|_{\boldsymbol{\alpha} = \boldsymbol{\alpha}^{opt}} &= -\frac{a_i \sqrt{\gamma_0}}{2^m \sqrt{\alpha_i^{opt}}} + \lambda = 0 \\ \sum_{i=1}^m \alpha_i^{opt} &= m \end{aligned} \right\} \rightarrow \alpha_i^{opt} = \frac{m a_i^2}{\sum a_i^2}. \quad (\text{A.14})$$

The optimized BLER can now be expressed as $\bar{P}_B(\boldsymbol{\alpha}^{opt}) = 1 - 2^{-m} + 2^{-m+1} \sqrt{m \gamma_0} \sqrt{\sum_i a_i^2}$.

Comparing it to the non-optimized one in the gain definition in (7.1),

$\bar{P}_B(\alpha, \alpha, \dots, \alpha) = 1 - 2^{-m} + 2^{-m+1} \sqrt{\alpha \gamma_0} \sum_i a_i$, one finds the gain $G_0 = \alpha$,

$$G_0 = \frac{m \sum_i a_i^2}{\left(\sum_i a_i \right)^2} \geq 1 \quad (\text{A.15})$$

²¹ recall that \sqrt{x} cannot be expanded in MacLaurin's series.

By the Cauchy-Schwartz inequality, the equality holds if all a_i are equal.

For the instantaneous BLER the approximation in (A.12) applies for BPSK as well as for some other modulation formats [9] hence (A.15) also holds.

For non-coherent modulation formats (e.g. DPSK, FSK), the MacLaurin's series expansion in terms of SNR can be used as a low-SNR approximation of the error rate,

$$\bar{P}_{ei} \approx \frac{1}{2} + b_i \gamma_0, \quad b_i = \left. \frac{\partial \bar{P}_{ei}}{\partial (\alpha_i \gamma_0)} \right|_{\alpha_i \gamma_0 = 0}, \quad (\text{A.16})$$

For the BFSK detected non-coherently, b_i^{BFSK} are given by (7.6). Similarly to the coherent case, the small SNR approximation of the BLER is,

$$\bar{P}_B(\boldsymbol{\alpha}) \approx 1 - \frac{1}{2^m} + \frac{\gamma_0}{2^{m-1}} \sum_{i=1}^m b_i \alpha_i. \quad (\text{A.17})$$

The derivatives $\partial L(\boldsymbol{\alpha}) / \partial \alpha_i = -b_i 2^{m-1} \gamma_0 + \lambda$ cannot be now all equal to zero simultaneously unless all b_i are the same, which means that there exists no stationary point inside of the feasible region and the solution is located on the region boundary. It follows from (A.17) that the BLER is minimized when all the power is allocated to the stream for which $|b_i|$ is maximum²²,

$$\alpha_{i_{\max}}^{opt} = m, \quad \alpha_i^{opt} = 0, \quad i \neq i_{\max}, \quad \text{where } i_{\max} = \arg \max_i |b_i| \quad (\text{A.18})$$

When all b_i are equal, any power allocation gives the same BLER, so that (A.18) can also be used. Finally, using the optimum allocation in the definition of the SNR gain, one obtains:

$$G_0 = m \frac{\max_i |b_i|}{\sum_i |b_i|} \geq 1. \quad (\text{A.19})$$

²² the magnitude is required since all b_i are non-positive

The equality holds if all b_i are equal, in which case, as expected, there is no gain due to the optimization. It should be pointed out that the argument above holds for the instantaneous BLER as long as the approximation in (A.16) holds, which is the case for many non-coherent modulation formats [9]. Thus, (A.19) also applies to the instantaneous gain of the instantaneous optimization, in which case b_i and hence the gain depend on channel realization.

For the instantaneous BLER-based optimization, the averaged over \mathbf{H} gain cannot be worse than that of the average optimization, see (7.2), hence the former is also subject to the inequalities in (A.19) and (A.15).

A.3. THE GAIN OF OPTIMIZATION FOR HIGH SNR

This approximation follows along the lines of the proof of Theorem 7.3: high SNR approximations of the average BLER of the optimized and unoptimized systems are used in the gain definition in (7.1) to obtain (7.9).

The high SNR approximation of the optimized BLER (4.16) is improved by keeping the first two terms (rather than one) of the Taylor series expansion of the exact BLER expression at $1/\gamma_0 = 0$ (see (4.15), (5.9),(5.8)):

$$\begin{aligned}
\bar{P}_B(\boldsymbol{\alpha}^{opt}) &\approx \sum_{i=1}^m \frac{C_{2i-1}^i}{[4\alpha_i^{opt}\gamma_0]^{n-m+i}} \approx \\
&\approx \frac{1}{\left[4\left(m-b_2(4\gamma_0)^{-\frac{1}{n-m+3}}\right)\gamma_0\right]^{n-m+1}} + \sum_{i=2}^m \frac{C_{2i-1}^i}{\left(4\left(b_i(4\gamma_0)^{-\frac{i-1}{n-m+i+1}}\right)\gamma_0\right)^{n-m+i}} \approx \\
&\approx \frac{1}{(4m\gamma_0)^{n-m+1}} \left(m + \frac{(n-m+1)}{m} b_2(4\gamma_0)^{-\frac{1}{n-m+3}}\right) + \frac{3}{(4\gamma_0)^{n-m+1}} \frac{(4\gamma_0)^{-\frac{1}{n-m+3}}}{b_2^{n-m+2}},
\end{aligned}$$

which can be compactly written as

$$\begin{aligned}\bar{P}_B(\mathbf{a}^{opt}) &\approx \frac{1}{(4m\gamma_0)^{n-m+1}} \left[1 + \frac{c_{m,n}}{n-m+3\sqrt[3]{4\gamma_0}} \right], \\ c_{m,n} &= \frac{(n-m+1)b_2^{n-m+3} + 3m^{n-m+2}}{mb_2^{n-m+2}},\end{aligned}\tag{A.20}$$

where b_2 is given by (5.8). From (4.16), the unoptimized BLER is approximates as $\bar{P}_B(\alpha, \alpha, \dots, \alpha) \approx 1/(4\alpha\gamma_0)^{n-m+1}$, and comparing it to the optimized one from (A.20) in the gain definition in (7.1), one finds the gain $G_0 = \alpha$ as:

$$G_{av} \approx \frac{m}{n-m+1\sqrt[3]{1 + \frac{c_{m,n}}{n-m+3\sqrt[3]{4\gamma_0}}}}\tag{A.21}$$

When \bar{P}_{et} is used to define the SNR gain, the argument above applies with minor changes (see (5.16),(5.9),(5.17)),

$$\begin{aligned}\bar{P}_B(\mathbf{a}^{opt}) &\approx \frac{1}{2m} \sum_{i=1}^m \frac{(m-i+2)C_{2i-1}^i}{[4\alpha_i^{opt}\gamma_0]^{n-m+i}} \approx \\ &\approx \frac{1}{2m} \left\{ \frac{m+1}{(4m\gamma_0)^{n-m+1}} \left(m + \frac{(n-m+1)}{m} b_2 (4\gamma_0)^{-\frac{1}{n-m+3}} \right) + \frac{3m}{(4\gamma_0)^{n-m+1}} \frac{(4\gamma_0)^{-\frac{1}{n-m+3}}}{b_2^{n-m+2}} \right\} \\ &= \frac{m+1}{2m} \frac{1}{(4m\gamma_0)^{n-m+1}} \left[1 + \frac{c_{m,n}}{n-m+3\sqrt[3]{4\gamma_0}} \right], \text{ where } c_{m,n} = \frac{(m+1)(n-m+1)b_2^{n-m+3} + 3m^{n-m+3}}{m(m+1)b_2^{n-m+2}}\end{aligned}$$

where b_2 is given by (5.17). Using the high SNR approximation of the unoptimized TBER (4.17), one finds the gain by definition in (7.1) from

$$\left\{ \begin{aligned}\bar{P}_B(\mathbf{a}^{opt}) &\approx \frac{m+1}{2m} \frac{1}{(4m\gamma_0)^{n-m+1}} \left[1 + \frac{c_{m,n}}{n-m+3\sqrt[3]{4\gamma_0}} \right] \\ \square \\ \bar{P}_B(\alpha, \dots, \alpha) &\approx \frac{1}{m} \frac{1}{(4\alpha\gamma_0)^{n-m+1}}\end{aligned}\right.\tag{A.22}$$

as

$$G_{av} = \alpha \approx \frac{m \cdot n - m + 1 \sqrt{2\tilde{\alpha}_1 / (m+1)}}{n - m + 1 \sqrt{1 + \frac{c_{m,n}}{n - m + 3} \sqrt{4\gamma_0}}} \quad (\text{A.23})$$

A.4. PROOF OF THEOREM 7.4

From the total power constraint,

$$\sum_{i=1}^m \frac{\partial \alpha_i^{opt}}{\partial u} = 1, \quad (\text{A.24})$$

and from the optimality condition (5.3)

$$\frac{\partial \bar{P}_B(\mathbf{\alpha}^{opt})}{\partial \alpha_i^{opt}} = -\lambda \leq 0 \quad (\text{A.25})$$

Taking the derivative of (7.1) with respect to α_i^{opt} ,

$$\begin{aligned} \frac{\partial \bar{P}_B(\mathbf{\alpha}^{opt})}{\partial \alpha_i^{opt}} &= \frac{\partial \bar{P}_B(\alpha \dots \alpha)}{\partial \alpha} \frac{\partial \alpha}{\partial \alpha_i^{opt}}, \\ \rightarrow \frac{\partial \alpha}{\partial \alpha_i^{opt}} &= \frac{\partial \bar{P}_B(\mathbf{\alpha}^{opt})}{\partial \alpha_i^{opt}} \bigg/ \frac{\partial \bar{P}_B(\alpha \dots \alpha)}{\partial \alpha}, \end{aligned} \quad (\text{A.26})$$

Using (A.24)-(A.26), one obtains:

$$\frac{\partial \alpha}{\partial u} = \sum_{i=1}^m \frac{\partial \alpha}{\partial \alpha_i^{opt}} \frac{\partial \alpha_i^{opt}}{\partial u} = -\frac{\lambda}{\partial \bar{P}_B(\alpha \dots \alpha) / \partial \alpha} \geq 0 \quad (\text{A.27})$$

The same reasoning holds true if the instantaneous BLER is used to define the SNR gain.

Appendix B. Matlab Code

B.1. AUXILIARY FUNCTIONS

Q-function

```
function Q = Q(gamma) %Q-function
    Q = 1/2*erfc(gamma/sqrt(2));
end
```

Adaptive Change of Number of Monte-Carlo Simulations

```
function out = numberOfTrials(SNR)
%Changes adaptively the number of Monte-Carlo trials based on the SNR to
optimize the calculation time
%The higher the SNR, the smaller is the error rate, hence more
simulations
%are required for reliable results
%
%SNR (dB) - scalar integer from 0 to 40

persistent N

if isempty(N)
    N= 10^3
end

switch SNR
    case 9
        N = N*10
    case 12
        N = N*10
    case 21
        N = N*10
    case 33
        N = N*10
    case 36
        N = N*2
end
out = N;
end
```

Difference in SNR Between two BER(SNR) Curves

```
function out = gain(BERe, BERd,SNRe)
%returns gain in SNR versus SNR: given BERe at SNRe for unoptimized
system,
%SNR required to reach the same BER is found for optimized system.
%Difference among the two is returned

%BERe - etalon BER: vector of BERs for unoptimized system
%BERd - data: vector of BERs for optimized system
%SNRe - etalon SNR: vector of SNRs

BERe = -log(BERe);
BERd = -log(BERd);
SNRd = interp1(BERd,SNRe,BERe);
out = SNRe - SNRd;
end
```

MMSE-BLAST Weights

```
function out = wMMSE(H, gamma)
%Returns complete matrix of MMSE weights
%
%H - channel matrix
%gamma - scalar SNR (W)

    m = size(H,1);
    G = H; %Allocate
matrix from which we'll be successively deleting columns
    for i=1:m
        P = inv(G'*G + gamma*eye(m-i+1));
        tmp = G*P;
        w(:,i) = tmp(:,i); %MMSE-BLAST
weights
        w(:,i) = w(:,i)/norm(w(:,i)); %normalize
weights
        G(:,i)=0; %null next
column
    end
    out = w;
end
```

ZF-BLAST Weights

```
function out = wZF(H, gamma)
%Returns complete matrix of ZF weights
%
%H - channel matrix
%gamma - scalar SNR (W) (not needed, only added for consistency to use
with function handles)

    m = size(H,1);
    G = H; %Allocate
matrix from which we'll be successively deleting columns
    for i=1:m
        G(:,i)=[]; %Delete
next column
        Gq = null(G'); % null
space basis
        P = Gq*Gq'; %
orthogonal projection matrix, to (i+1...m)
        w(:,i) = P*H(:,i); %ZF-BLAST
weights
        w(:,i) = w(:,i)/norm(w(:,i)); %normalize
weights
    end
    out = w;
end
```

B.2. ANALYTICAL AVERAGE AND INSTANTANEOUS ERROR RATES FOR ARBITRARY POWER ALLOCATION

Analytical Instantaneous $P_{ei|Ei-1}$

```
function out = ibpsk(gamma, alpha, H, E, W)
% Analytical instantaneous conditional step BER of BPSK  $P\{ei|Ei-1\}$ 
%
% gamma - average SNR
% H - channel matrix
```

```

% E - error vector of size k-1 which with error amplitudes
sqrt(alpha(i))
% W - V-BLAST weights matrix

k = numel(E)+1;           %current step

w = W(:,k);              %step weight
h = H(:,k);
H1 = H(:,1:k-1);

a = w'*h*sqrt(alpha);
if k==1 || ~any(E)       % 1-st step or E = 0
    out = Q(sqrt(2*gamma)*real(a)); % if 1-st step
else
    S = 0;
    [indices,j,Es] = find(E);           % Indices of nonzero
    elements of E and dissected version of E
    ne = numel(indices);               % Number of errors in E
    for i=1:2^ne                       % Different sign
        combinations in E
            signs = dec2binvec(i-1,ne); % Signs in form {0,1}
            signs = signs' - ~signs';   % Signs in form {-1,1}
            Eis = signs.*Es;           % Dissected error pattern
            Ei = sparse(indices,1,Eis,k-1,1); % Reassembled error pattern
            b = 2*w'*H1*Ei;
            S = S + Q(sqrt(2*gamma)*real(a+b)) + Q(sqrt(2*gamma)*real(a-b));
    end
    out = S/2^(ne+1);
end

end

end

Analytical Average  $P_{e|E_i-1}$ 
function Out = abpsk(n,mu)
% Analytical average BER of BPSK of MRC order n
% n - diversity order
% mu - equivalent SNR

P = 0;

for i = 0:n-1
    P = P + nchoosek(n-1+i,i)*((1+mu)/2)^i;
end

Pea = P*((1-mu)/2)^n; % average BER, order n MRC
Out = Pea;

end

TBER, Instantaneous or Average
function Out = ber(m,n,alpha>ErrorRateHandle,gamma,H,WeightsHandle)
% Exact TBER, instantaneous or average
%
% m - number of Tx antennas
% n - number of Rx antennas
% alpha[m,1] - set of alphas for a given SNR

```

```

% ErrorRateHandle - handle of function defining step error rate P{ei|Ei-
1}
% gamma - average SNR
% H - channel matrix
% WeightsHandle - handle to function calculating V-BLAST weights (ZF or
MRC)

switch func2str(ErrorRateHandle)
    case 'abpsk'
        mu = sqrt(1/(1+1/(alpha(1)*gamma)));
        args = {n-m+1,mu};
    case 'ibpsk'
        W=WeightsHandle(H, gamma);
        args = {gamma, alpha(1), H, [],W};
end

% Computing probability matrix P

P(1,1) = 1-ErrorRateHandle(args{:}); % no error at
step 1
P(1,2) = 1-P(1,1); % BER at step 1

for k = 2:m
    ak = 2^(k-1)+1;
    for i = 1:2^k
        if i < ak
            Eki = dec2binvec(i-1,k-1); % error (row)
vector at step k with ei = {0,1} (binary rep of i-1 with k-1 bits)
            Eki = alpha(1:k-1).*Eki'; % error vector
at step k with ei = {0,alpha(i)}
            switch func2str(ErrorRateHandle)
                case 'abpsk'
                    mu = sqrt(alpha(k)*gamma/(1 + gamma*(
alpha(k)+4*sum(Eki)) ) );
                    args = {n-m+k,mu};
                case 'ibpsk'
                    args = {gamma, alpha(k), H, sqrt(Eki),W};
            end
            P(k,i) = (1-ErrorRateHandle(args{:})) * P(k-1,i); % no
error at step k
        else
            P(k,i) = P(k-1,i-ak+1)-P(k,i-ak+1); % error
at step k
        end
    end
end

% Computing step BER

for k=1:m
    Psk = 0;
    for i = 2^(k-1)+1:2^k
        Psk = Psk+P(k,i);
    end
    Ps(k) = Psk; % step k BER
end

Out = sum(Ps)/m; % total BER

```

end

BLER, Instantaneous or Average

```
function Out = bler(m,n,alpha,ErrorRateHandle,gamma,H,WeightsHandle)
% Exact BLER, instantaneous or average
%
% m - number of Tx antennas
% n - number of Rx antennas
% alpha[m,1] - set of alphas for a given SNR
% ErrorRateHandle - handle of function defining step error rate P{ei|Ei-1}
% gamma - average SNR
% H - channel matrix
% WeightsHandle - handle to function calculating V-BLAST weights (ZF or MRC)

Pc = 1; %Probability of no error in block

switch func2str(ErrorRateHandle)
    case 'abpsk'
        for k = 1:m
            mu = sqrt(alpha(k)*gamma/(1 + gamma*alpha(k)));
            args = {n-m+k,mu};
            Pc = Pc* (1 - ErrorRateHandle(args{:}));
        end
    case 'ibpsk'
        W=WeightsHandle(H, gamma);
        for k = 1:m
            args = {gamma, alpha(k), H, zeros(k-1,1),W};
            Pc = Pc* (1 - ErrorRateHandle(args{:}));
        end
end

Out = 1 - Pc;

end
```

B.3. OPTIMIZATION BASED ON VARIOUS CRITERIA

Average BLER/TBER for Instantaneous Optimization

```
function out = instOpt(m,n,SNR,alpha,ErrorRateHandle, WeightsHandle)
%returns average Error Rate for instantaneously optimized V-BLAST
%if alpha!=NULL returns average Error Rate for this alpha

% m - number of transmit antennas
% n - number of receive antennas
% SNR - vector of SNR(dB)
% ErrorRateHandle - handle of function defining step error rate P{ei|Ei-1}
% WeightsHandle - handle to function calculating V-BLAST weights (ZF or MRC)

SNRw = 10.^(SNR./10); %Convert dB to W, SNR - SNR for 1 antenna in
unoptimized case, SNRw - total SNR
N=length(SNRw);
options = optimset('LargeScale','off','TolCon',1e-015,'TolFun',1e-015,'Display','off'); %optimization options
```

```

fprintf('Instantaneous Optimization\n');
for i=1:N
    tic
    fprintf('SNR = %.0f dB \n', SNR(i));

    out = getAVER(m,n,SNR(i),NaN,ErrorRateHandle,WeightsHandle); %instantaneously
    %optimized

    etime = toc; hours = floor(etime/3600); minutes = floor(etime/60);
    %elapsed time
    fprintf('Elapsed time: %i hours, %i minutes, %i seconds\n', hours,
minutes - hours*60, floor(etime)-60*minutes );
    fprintf('%s\n',datestr(now));
end
end

function out = getAVER(m,n,SNR,alpha,ErrorRateHandle,WeightsHandle)
%returns average Error Rate for instantaneously optimized V-BLAST
%if alpha!=NULL returns average Error Rate for this alpha

%m - number of transmit antennas
%n - number of receive antennas
%SNR - scalar SNR (dB)
%ErrorRateHandle - handle to a function representing error rate
(TBER/BLER)

N = numberOfTrials(SNR); % number of simulations is changed adaptively;
the higher SNR the higher N

gamma = 10.^(SNR./10);
options = optimset('LargeScale','off','TolCon',1e-012,'TolFun',1e-
012,'Display','off');
Pti = 0;
Ptib = 0;
if isnan(alpha)
    for k=1:N
        H = wgn(n,m,1,'linear','complex'); %generate
        %complex MIMO channel matrix each component of which is distributed as
        %Nc(0,1)
        alphaBer = fmincon(@Piber,ones(m,1),[],[],ones(1,m),m,zeros(m,1),m*ones(m,1),[],opt
        %ions); %Finds min Pi(alpha) subject to ones(1,m)*alpha =m, 0<alpha<m
        alphaBler = fmincon(@Pibler,ones(m,1),[],[],ones(1,m),m,zeros(m,1),m*ones(m,1),[],op
        %tions); %Finds min Pi(alpha) subject to ones(1,m)*alpha =m, 0<alpha<m
        Pti = Pti + ErrorRate(alphaBer);
        Ptib = Ptib + ErrorRate(alphaBler);
    end
else
    for k=1:N
        H = wgn(n,m,1,'linear','complex'); %generate
        %complex MIMO channel matrix each component of which is distributed as
        %Nc(0,1)
        Pti = Pti + ErrorRate(alpha);
    end
end
out = [Pti/N Ptib/N]; %average
BER

```

```

function out = ErrorRate(alpha)
    out = ErrorRateHandle(m,n,alpha,@ibpsk,gamma,H,WeightsHandle);
end

function out = Piber(alpha)
    out = ber(m,n,alpha,@ibpsk,gamma,H,WeightsHandle);
end

function out = Pibler(alpha)
    out = bler(m,n,alpha,@ibpsk,gamma,H,WeightsHandle);
end

end

```

Average BLER/TBER for Average Optimization

```

function out = avOpt(m,n,SNR,ErrorRateHandle)
% counts analytical average error rate (BLER/TBER) for optimized and
% unoptimized V-BLAST
% returns [Ptavop, alpha, gain] for each component in SNR vector
%
% m - number of transmit antennas
% n - number of receive antennas
% SNR - vector of SNR (dB)
% ErrorRateHandle - handle to a function representing error rate
% (TBER/BLER)

SNRw = 10.^(SNR./10); %Convert dB to W, SNR - SNR for 1 antenna in
% unoptimized case, SNRw - total SNR
N=length(SNRw);
au=ones(m,1); %unoptimized alpha
options = optimset('LargeScale','off','TolCon',1e-015,'TolFun',1e-
015,'Display','off'); %optimization options

fprintf('Average Optimization\n');
for i=1:N
    tic
    fprintf('SNR = %.0f dB \n', SNR(i));

    Ptun(i) = ErrorRate(au);
%unoptimized Pt

    aBer (1:m,i) =
fmincon(@Pe,au,[],[],au',m,zeros(m,1),m*au,[],options); %Finds min
Pa(alpha) subject to ones(1,m)*alpha =1, 0<alpha<1
    PtaBer(i) = ErrorRate(aBer(:,i));
%optimized numerically by average
    gaBer(i) = gain(PtaBer(i)); %SNR gain

    aApBer(1:m,i) = aapp(SNRw(i),m,n, 'ber'); %closed-
form alpha
    PtaApBer(i) = ErrorRate(aApBer(:,i));
    gaApBer(i) = gain(PtaApBer(i)); %SNR gain

    aBler (1:m,i) =
fmincon(@Pb,au,[],[],au',m,zeros(m,1),m*au,[],options); %Finds min
Pa(alpha) subject to ones(1,m)*alpha =1, 0<alpha<1
    PtaBler(i) = ErrorRate(aBler(:,i));
%optimized numerically by average

```

```

    gaBler(i) = gain(PtaBler(i));                                %SNR gain

    aApBler(1:m,i) = aappSimple(SNRw(i),m,n, 'ber');           %closed-
form alpha
    PtaApBler(i) = ErrorRate(aApBler(:,i));
    gaApBler(i) = gain(PtaApBler(i));                          %SNR
gain

    etime = toc; hours = floor(etime/3600); minutes = floor(etime/60);
%elapsed time
    fprintf('Elapsed time: %i hours, %i minutes, %i seconds\n', hours,
minutes - hours*60, floor(etime)-60*minutes );
    fprintf('%s\n',datestr(now));

end

out = {Ptu' PtaBer' PtaApBer' PtaBler' PtaApBler'...
      aBler' aBer' aApBer' aApBler'...
      10*log10([gaBer' gaApBer' gaBler' gaApBler'])
      }

function out = ErrorRate(alpha)
    out = ErrorRateHandle(m,n,alpha,@abpsk,SNRw(i));
end

function out = Pe(alpha)
    out = ber(m,n,alpha,@abpsk,SNRw(i));
end

function out = Pb(alpha)
    out = bler(m,n,alpha,@abpsk,SNRw(i));
end

function out = gain(ER)
    %SNR gain
    %
    %ER - target error rate (error rate of optimized system)

    out = fsolve(@Pdiff,m,options);

function out = Pdiff(g)
    %Difference in Error Rates between Optimized and Unoptimized
    %systems
    %
    %g (scalar): difference un SNR (W) between Optimized and
Unoptimized
    %systems

    out = log(ErrorRate(ones(m,1)*g)) - log(ER);
end
end

end
end

```

Closed-Form Approximate α^{opt}

```
function alpha = aapp(gamma,m,n,type)
%Closed-form approximate alpha
%Returns [alpha1; alpha2; .. alpham] for given SNR

%gamma - SNR (scalar)
% m - number of Tx antennas
% n - number of Rx antennas
% type - type of approximation ('bler or 'ber')

for k = 1:m
    alpha(k) = b(k)*(4*gamma)^(-d(k))*(1 - b(2)/(m*c(1))*(4*gamma)^(-
d(2)))^c(k)/gamma; %calculate closed-form alpha
% alpha(k) = b(k)*(4*gamma)^(-d(k));
end
%alpha(1)=m-sum(alpha(2:m));
alpha = m*alpha/sum(alpha);

function d = d(k)
    d = (k-1)/(n-m+k+1);
end

function c = c(k)
    c = [1+n-m+1:1+n-m+m];
    c = prod(c)/(1+n-m+k);
end

function b = b(k)
    switch type
        case 'bler'
            b = (nchoosek(2*k-1,k)*(n-m+k)/(n-m+1))^(1/(n-
m+k+1))*m^((n-m+2)/(n-m+k+1));
        case 'ber'
            b = (nchoosek(2*k-1,k)*(n-m+k)*(m-k+2)/(n-
m+1)/(m+1))^(1/(n-m+k+1))*m^((n-m+2)/(n-m+k+1));
    end
end

end
```

Closed-form Approximate SNR Gain of Average Optimization

```
function Out = gainApp(gamma,m,n,type)
%Closed-form expression of gain of power allocation by average versus
SNR
%
%gamma - scalar SNR
%m - number of transmit antennas
%n - number of receive antennas
%type - string representing optimization type ('ber' or 'bler')

Out = gainA(m,n,type);
if (gamma==Inf)
    return;
end
```

```

Out = Out*(1+c()*(4*gamma).^(-1/(n-m+3))).^(-1/(n-m+1));

function Out = c()
    b = b(2);
    switch type
        case 'ber'
            Out = 1/b^(n-m+2)/m/(m+1)*(b^(n-m+3)*(m+1)*(n-
m+1)+3*m^(n-m+3));
        case 'bler'
            Out = 1/b^(n-m+2)/m*(b^(n-m+3)*(n-m+1)+3*m^(n-m+2));
    end
end

function Out = b(k)
    switch type
        case 'ber'
            Out = (nchoosek(2*k-1,k)*(n-m+k)*(m-k+2)/(n-
m+1)/(m+1))^(1/(n-m+k+1))*m^((n-m+2)/(n-m+k+1));
        case 'bler'
            Out = (nchoosek(2*k-1,k)*(n-m+k)/(n-m+1))^(1/(n-
m+k+1))*m^((n-m+2)/(n-m+k+1));
    end
end

function Out = gainA(m,n,type)
%Asymptotic gain of power allocation by average
    switch type
        case 'ber'
            mu = sqrt(1/5);
            for k=2:m
                Ps(k) = abpsk(n-m+k,mu); %Step k BER
            end
            Out = m*((1+sum(Ps))*2/(m+1))^(1/(n-m+1));

        case 'bler'
            Out = m;
    end
end

```

B.4. ERROR RATES THROUGH MONTE-CARLO SIMULATIONS

BPSK Quantizer

```

function out = quantize(val)
% BPSK quantizer
    out = sign(real(val));
end

```

Unordered V-BLAST Decoder for Arbitrary α

```

function out = vblast(z,alpha,gamma,H,WeightsHandle)
%Unordered V-BLAST decoder with arbitrary power allocation, returns
demodulated
%signal
%
% z[m,N] - N received vectors, N - number of Monte-Carlo simulations
% alpha[m,1] - set of alphas
% gamma - average SNR
% H - channel matrix

```

```

% WeightsHandle - handle to function calculating V-BLAST weights (ZF or
MRC)
%

[n,m] = size(H);
A = sqrt(alpha*gamma); %amplitude of
transmitted signals
N = size(z,2); %number of
Monte-Carlo simulations

W = WeightsHandle(H,gamma);
y = z;
G = H; %Allocate
matrix from which we'll be successively deleting columns
[m,n] = size(H);
for i=1:m
    sest(i,1:N) = quantize((W(:,i))'*y); %Detect next
symbol according to signal constellation
    y = y - H(:,i)*A(i)*sest(i,:); %Subtract the
contribution of already detected symbols from y
end
out = sest;
end

```

Numerical Instantaneous TBER for Arbitrary α

```

function out = montecarlo(m,n,N,alpha,gamma,H, WeightsHandle)
%Numerical total instantaneous BER for V-BLAST with arbitrary power
%allocation

% m - Number of transmit antennas
% n - Number of receive antennas
% N - number of Monte-Carlo simulations
% alpha[m,1] - set of alphas
% gamma - SNR
% WeightsHandle - handle to function calculating V-BLAST weights (ZF or
MRC)
% H - channel matrix

s = randsrc(m,N,[-1,1]); %generate
transmit signal vector for BPSK modulation
A = sqrt(alpha*gamma); %amplitude of
transmitted signals

for i=1:m
    st(i,:) = A(i)*s(i,:);
end

v = wgn(n,N,1,'linear','complex'); %generate
received noise vector each component of which is distributed as Nc(0,1)

z = H*st+v; %received vector

sest = vblast(z,alpha,gamma,H,WeightsHandle); %demodulated by
V-BLAST symbol

out = sum(abs(sign(sest-s)),2); %Total Number of
errors
out = sum(out)/m/N; %Total BER

```

end

Numerical Instantaneous TBER for Different V-BLAST Receivers: ZF and MMSE, With and Without Ordering

```
function Pe=compareBLASTs(m,n,N,gamma)
%Numerical total instantaneous BER for different V-BLASTs:
%ZF-BLAST,
%ZF BLAST with ordering at 1st step,
%ZF BLAST with optimal ordering,
%MMSE BLAST,
%MMSE BLAST with optimal ordering
%
%m - number of transmit antennas,
%n - number of receive antennas,
%gamma - SNR (W)

s = randsrc(m,N,[-1,1]); %generate
transmit signal vector for BPSK modulation
H = wgn(n,m,1,'linear','complex'); %generate
complex MIMO channel matrix each component of which is distributed as
Nc(0,1)
v = wgn(n,N,1,'linear','complex'); %generate
received noise vector each component of which is distributed as Nc(0,1)
A = sqrt(gamma/m); %amplitude of
transmitted signals
z = A*H*s + v; %received vector
sest = zeros(m,1); %Initialize
vector of estimates
Pe = zeros(5,1);

%-----ZF BLAST-----
Y = z;
G = H; %Allocate
matrix from which we'll be successively deleting columns
for i=1:m
    G(:,1)=[]; %Delete next
column
    P = eye(m)- G*pinv(G); %Projection
matrix
    sest(i,1:N) = quantize((P*H(:,i))*y/A); %Detect next
symbol according to signal constellation
    y = y - A*H(:,i)*sest(i,:); %Subtract the
contribution of already detected symbols from y
% Null i-th column of G
end
Pe(1) = sum( sum(abs(sign(sest-s)),2)); %Total Number
of errors

%-----Ordered ZF BLAST-----
Y = z;
[B,index]=sortrows(inv(H'*H)); %Ordering
G = H(:,index); %Allocate
matrix from which we'll be successively deleting columns
for i=1:m
    G(:,1)=[]; %Delete next
column
    P = eye(m)- G*pinv(G); %Projection
matrix
```

```

        sest(index(i),1:N) = quantize((P*H(:,index(i)))'*y/A);%Detect
next symbol according to signal constellation
        y = y - A*H(:,index(i))*sest(index(i),:);           %Substract the
contribution of already detected symbols from y
% Null i-th column of G
        end
        Pe(2) = sum( sum(abs(sign(sest-s)),2));               %Total Number
of errors

%-----Optimally ordered ZF BLAST-----
y = z;
G = H;                                                       %Allocate
matrix from which we'll be successively deleting columns
for i=1:m
        maxSNR=0;                                           %Null maxSNR
value
        for k=1:m                                           %Ordering:
Find symbol with max SNR for this stage
                if all(G(:,k)==0) continue;                 %Skip if this
symbol is already detected
                end
                F=G;
                F(:,k)=0;
                P = eye(m)- F*pinv(F);                       %Projection
matrix
                SNRk = abs(H(:,k)'*P*H(:,k));                %SNR
                if (SNRk>maxSNR)
                        maxSNR=SNRk;
                        index(i)=k;
                end
        end
        G(:,index(i))=0;                                     %null next
column
        P = eye(m)- G*pinv(G);                               %Projection
matrix
        sest(index(i),1:N) = quantize((P*H(:,index(i)))'*y/A); %Detect next
symbol according to signal constellation
        y = y - A*H(:,index(i))*sest(index(i),:);           %Substract
the contribution of already detected symbols from y
% Null i-th column of G
        end
        Pe(3) = sum( sum(abs(sign(sest-s)),2));             %Total Number
of errors

%-----MMSE BLAST-----
y = z;
G=H;                                                         %Allocate
matrix from which we'll be successively deleting columns
for i=1:m
        P=inv(m/gamma*eye(m)+ G'*G);                       %MMSE
nulling matrix
        w=G*P;                                             %MMSE
weights
        sest(i,1:N) = quantize(w(:,i))*y;                   %Detect next
symbol according to signal constellation
        y = y - A*H(:,i)*sest(i,:);                         %Substract
the contribution of already detected symbols from y
        G(:,i)=0;                                           %null next
column% Null i-th column of G
        end

```

```

Pe(4) = sum( sum(abs(sign(sest-s)),2)); %Total
Number of errors

%-----Optimally Ordered MMSE BLAST -----
y = z;
G=H; %Allocate
matrix from which we'll be successively deleting columns
for i=1:m
    minEr=inf; %Set min
    error to infinity (just in case)
    P=inv(m/gamma*eye(m)+ G'*G); %MMSE
    nulling matrix
    for k=1:m %Ordering:
        find symbol with min MSE for this stage
        if all(G(:,k)==0) continue; %Skip if the
        symbol has already been detected
        end
        Erk=norm(P(:,k)); %MSE
        if (Erk<minEr)
            minEr=Erk;
            index(i)=k;
        end
    end
    end
    w=G*P; %MMSE
weights
    sest(index(i),1:N) = quantize(w(:,index(i))'*y); %Detect next
    symbol according to signal constellation
    y = y - A*H(:,index(i))*sest(index(i),:); %Substract
    the contribution of already detected symbols from y
    G(:,index(i))=0; %null next
column
end
Pe(5) = sum( sum(abs(sign(sest-s)),2)); %Total
Number of errors

Pe = Pe./m/N; %Total BER

end

```